

Hull Form Optimization for Monohull Ships

by

Justin A. Harper

B.S., Naval Architecture and Marine Engineering
Webb Institute of Naval Architecture, 1997

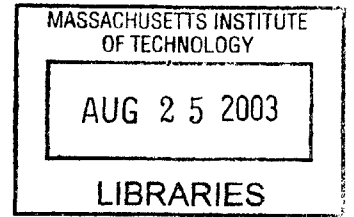
SUBMITTED TO THE DEPARTMENT OF OCEAN ENGINEERING
IN PARTIAL FULFILLMENT OF THE REQUIREMENTS FOR THE DEGREE OF

MASTER OF SCIENCE IN NAVAL ARCHITECTURE
AT THE
MASSACHUSETTS INSTITUTE OF TECHNOLOGY

JUNE 2003

© Justin A. Harper. All rights reserved.

The author hereby grants to MIT permission to reproduce
and to distribute publicly paper and electronic
copies of this thesis document in whole or in part.



Signature of Author..

[Handwritten signature]

.....
Department of Ocean Engineering
May 9, 2003

Certified by.....

.....
Cliff Whitcomb
Senior Lecturer SDM
Thesis Supervisor

Accepted by.....

>.....
Michael Triantafyllou
Chairman, Departmental Committee on Graduate Studies

BARKER



Room 14-0551
77 Massachusetts Avenue
Cambridge, MA 02139
Ph: 617.253.2800
Email: docs@mit.edu
<http://libraries.mit.edu/docs>

DISCLAIMER OF QUALITY

Due to the condition of the original material, there are unavoidable flaws in this reproduction. We have made every effort possible to provide you with the best copy available. If you are dissatisfied with this product and find it unusable, please contact Document Services as soon as possible.

Thank you.

The images contained in this document are of the best quality available.

Hull Form Optimization for Monohull Ships

by

Justin A. Harper

Submitted to the Department of Ocean Engineering
on June, 2003 in Partial Fulfillment of the
Requirements for the Degree of Master of Science in
Naval Architecture

ABSTRACT

A study was carried out to investigate methods and to determine the “optimum” hull form for monohull ships, based upon several weighted criteria. The main product of this study is a hull form optimization program. Propulsion power minimization is the primary focus of the program, although simplified seakeeping and weight/cost issues can also be studied with the existing program. The program uses standard naval architecture methods to simultaneously evaluate many hydrodynamic aspects of hull form design, and provides confidence intervals on the resistance estimate. The result is a flexible tool that allows naval architects to quickly compare the performance of a known hull form with many alternatives, based upon expected operating profiles and expected environments. Reasonable agreement was achieved when comparing program optimization results with real-world hull designs.

Thesis Supervisor: Cliff Whitcomb
Title: Senior Lecturer, SDM

Biographical Note

The author received a B.S. in Naval Architecture and Marine Engineering from Webb Institute of Naval Architecture, Glen Cove, NY in June, 1997. While at Webb, he was awarded the American Society of Naval Engineers (ASNE) Undergraduate Scholarship. The author also presented his undergraduate thesis, "An Evaluation of the Military Effectiveness of Battleships in Modern Naval Warfare," to the New York Metropolitan Section Meeting of SNAME in May, 1997 at Stevens Institute. He took the EIT exam to become a registered intern engineer (Mechanical Engineering-Cert. # 076974) in New York. Upon graduation the author worked as a professional naval architect and marine engineer at Oceanic Systems and also at John J. McMullen Associates, taking part in vehicle design, model testing, and other engineering studies. During this time he wrote: Three White Papers on Underwater Vehicle Concepts, submitted as part of DARPA's Team 2020 Submarine of the Future National Industry Consortium Program, n.p., 1999, n.pag. In the Fall of 2000 he took a ship structural design course from Virginia Polytechnic Institute and State University. The author was also the lead author for the paper: Harper, Justin A., and Scher, Robert M., "Improvements in the Prediction of Maneuvering Characteristics of Ships Using Regression Analysis," Presented at 26th ATTC, July 23-24, 2001, Glen Cove, NY. Before enrolling at MIT the author was awarded the NDSEG Fellowship.

Acknowledgements

This thesis would not be possible without the guidance of Professors Cliff Whitcomb and John Amy. I would also like to thank everyone else who made this work possible, including but not limited to: Siu Fung, U.S. Navy, all of the UROP and graduate student members of the Towing Tank, Fred Cote of the Student Shop and the MIT Central Machine Shop, the faculty and staff of the Ocean Engineering Department for their consultation and advice, and all of the friends and family who allowed me to maintain an even strain in my professional and personal life.

Contents

Abstract	2
Biographical Note	3
Acknowledgements	4
Contents	5
List of Figures	6
List of Tables	7
1 Introduction	8
1.1 Background of the Problem.....	8
1.2 Previous Work in Ship and Hull Design Optimization.....	12
1.3 Focus of Current Work.....	24
1.4 Outline of the Text.....	27
2 Overview of Method	28
2.1 Outline of Methods Used.....	28
2.2 Outline of Program Logic.....	31
3 Detailed Description of Methods	36
3.1 Hull Geometry and Hydrostatics.....	36
3.2 Calm Water Resistance.....	39
3.3 Shallow Water Resistance.....	44
3.4 Air Resistance.....	61
3.5 Steering Resistance.....	62
3.6 Directional Stability, Maneuvering and Appendage Resistance.....	63
3.7 Seakeeping.....	65
3.7.1 Seakeeping Motions.....	65
3.7.2 Added Resistance in Waves.....	72
3.7.3 Derived Responses.....	80
3.8 Propulsion and Power.....	82
3.9 Stability, Weights and Costs.....	84
3.10 Confidence Interval.....	92
3.11 Optimization Methods.....	101
4 Example Optimization Results	104
4.1 Frigate Length-Cost Study.....	104
4.2 Frigate Powering Study.....	108
4.3 Slender Hull Powering Study.....	119
5 Conclusions and Recommendations	124
Bibliography	128
Appendix A Correlation and Limitations of Analysis	133
Appendix B Sample Input Files	177
Appendix C Sample Output	185

List of Figures

Fig. 1.2-1 Notional two-dimensional classification area of ship design methods.....	17
Fig. 1.2-2 Notional three-dimensional classification space of ship design methods.....	23
Fig. 1.3-1 Imported body plan for Taylor Standard Series.....	25
Fig. 3.1-1 Comparison of sectional area curve shift methods.....	38
Fig. 3.3-1 Photograph of a model in shallow water (3 in. depth).....	48
Fig. 3.3-2 Calculated and experimental wavemaking resistance in a canal.....	51
Fig. 3.3-3 Digitized shallow water residuary resistance data.....	53
Fig. 3.3-4 Shallow water resistance data using depth-based Froude number...	53
Fig. 3.3-5 Worm curve factor comparison to the Taylor Standard Series.....	55
Fig. 4.1-1 Test 2. Sample optimization output.....	106
Fig. 4.1-2 Test 1. Sample optimization output.....	106
Fig. 4.1-3 Test 3. Sample optimization output.....	106
Fig. 4.2-1 Test 12. Scatter plot.....	111
Fig. 4.2-2 Test 12. Trend of exponential random search results.....	112
Fig. 4.2-3 Test 32. Plot of average resistance versus speed.....	114
Fig. 4.2-4 Test 33. Plot of resistance versus length.....	116
Fig. 4.2-5 Test 34. Plot of resistance versus length.....	116
Fig. 4.3-1 Body plan.....	120
Fig. 4.3-2 Test 43. Basic bare hull resistance at 9.5 knots versus C_V	121
Fig. 4.3-3 Test 23. Comprehensive resistance at 9.5 knots versus C_V	121

List of Tables

Table 2.1-1 Current program functions and desirable future upgrades..... 28
Table 4.1-1 Files and options used for tests..... 107
Table 4.2-1 Files and options used for tests..... 118
Table 4.3-1 Files and options used for tests..... 123

1 Introduction -

1.1 Background of the Problem

This chapter provides a general description of the ship hull form design optimization problem. The design problem is to determine an optimum hull form for a given figure of merit. This usually requires the achievement of many goals simultaneously. The problem is complex, and sensitive to external factors that are not hydrodynamic. Errors in the hydrodynamic calculations required for hull design can be significant, so it is important to have a method to estimate the magnitude of the errors. This will provide information regarding the validity of the optimization being performed. Additionally, criteria discrimination and communication of results can themselves be difficult problems.

Optimal ship hull form design is a complex, non-linear optimization problem with many interrelated variables. While the topic has been previously researched there is often a gap between the approaches used in optimization papers and those used in actual design practice. Studies often use theoretical methods of limited practical utility or that require hours or days of computation time for large design investigations. In contrast, designers often want to start optimizing from an existing parent hull design whose characteristics are well known, and want to use a method that can yield useful results in minutes or hours.

The design problem is to determine a ship hull form of minimum resistance, or other figure of merit, given a set of expected operating conditions of speed versus time, expected operating environments of wind, wave, and water depth versus time, and other limiting criteria of stability, payload, etc. The design of a ship hull form represents a challenging engineering

optimization problem because of the complexity of calculations involved, and because of the multitude of results that need to be clearly communicated to allow effective decision-making.

Design of a hull form requires achievement of many goals, many conflicting, including desired performance in the areas of:

- Displacement
- Static Stability
- Resistance and Propulsion
- Maneuvering and Directional Stability
- Seakeeping

In addition there is a strong interrelationship between the hull form and other aspects of a total ship design that must be taken into account to achieve an acceptable, if not optimal, design. These other aspects include such items as: arrangements, weights, and producibility, to name a few. Multiple analyses are required in different areas, and the optimal hull form may not be able to be defined by optimizing the objectives independently.

Since these other aspects of ship design influence hull form design, it is customary to try including approximations for them in the hull design process in actual design work. Varying levels of design detail are used depending on the resources available. Even simple regression equations or physical relationships can reflect the first-order effects of these external factors. This allows determination of an approximately optimal hull form design for the entire ship, without requiring detailed calculations for every aspect of design external to the hydrodynamic problem (such as detailed structural calculations). This approach was followed in the present

work, in which simple relationships for items such as weights, yearly costs, and propulsive efficiency were used to influence the main focus on hull form hydrodynamic optimization (when selected by the user). Some comments on these external factors are included in the results and conclusions chapters.

Working in isolation on the hull design alone, or in concert with simplified expressions for extraneous design factors, there are many calculations required to evaluate a hull form. These calculations are not exceptionally accurate or even completely developed in a theoretical sense, and they are often non-linear. Significant empiricism is required to obtain accurate results in some areas, and is especially needed when selecting a resistance-prediction methodology for disparate hull forms.

Errors between calculated and actual results can be large compared with other engineering disciplines, leading to a question as to what level of optimization continues to provide realizable performance benefits – that is, with the given error bands likely in certain calculations, how well can an engineer trust the calculated resistance trends with changes in hull form, even if the absolute values are significantly in error? Therefore it is important to have a method to estimate the magnitude of the errors and therefore the validity of the optimization. For this reason resistance intervals receive some attention in the following chapters, in addition to the more typical material on resistance estimation and optimization.

Though not investigated here, but more important in a business sense than the detailed design work itself, is the job of clearly communicating the tradeoffs involved in design. A hull form can have 10-20 major design variables that are of some significance, more of minor importance. Many of these characteristics are related, and can have varying impacts on overall design performance depending on their value and the value of other characteristics (as well as

depending upon the expected operating conditions and environments). To clearly communicate this information is difficult. It also becomes difficult to discriminate between the desirability of different options when multiple criteria are involved (such as: is it better to have 1% of passenger sea-sickness, or 2.5% passenger sea-sickness and 95% as much operating cost?)

1.2 Previous Work in Ship and Hull Optimization

This chapter provides an overview of some previous work done in ship and hull form optimization.

DESIGN APPROACHES AND PROCESS REDESIGN

Traditional ship design methods dealt with the complexity of naval architecture problems through gross simplification. The conventional design cycle began with an initial point design started within what was believed to be a feasible design region. The design would then be improved in an iterative manner to achieve a reasonably balanced final result. The level of design detail used would be higher for each iteration, though gross simplification would still be made of many aspects of the problem to reduce computational effort. Sometimes known as the “Design Spiral” method (Taggart,1980)(Evans, 1959), iterative or bracketing design methods (Saunders, 1957) are a classic approach used in early ship, airship and airplane design efforts throughout the twentieth century.

Given the complexity and cost of large ship design projects, the marine industry has always tended to favor conservative, modest evolutionary changes in established practices. Traditionally, designs changed slowly and adopted few new features in each ship.

Yet changes in technology, and awareness of potential improvements in design and construction, have led many naval architects to the conclusion that it is no longer necessary to economize on calculation to the extent that was previously done, to grossly simplify design problems – or to rely entirely upon iterative “Design Spiral” methods. Calculations are

(comparatively) free compared to their cost even twenty years ago. Since so many more calculations can be performed for the same design budget, an “optimum” design today can truly be much closer to the optimum than a design performed several decades ago.

The push for improved ship design has led to at least two major areas of change in the way engineering work is performed, in some corporate organizations, since large-scale computerization occurred. These two areas can loosely be described as either: (a) overall process redesign; or (b) changes in design calculations themselves. Process redesign is not the focus of the current work, but is mentioned because of its involvement in some ship design optimization papers.

Briefly, process redesign involves changing the day-to-day functioning of people and groups within an organization. For instance it could involve changing the division of labor in a design office to provide information to the people who need it more easily, or eliminating unnecessary reports from a design process. Process redesign probably provides the largest productivity enhancements in typical organizations. This is because it involves improving the largest cost of operations: the way workers spend their time interacting with each other, with systems, and otherwise performing their jobs.

Most companies have shown much greater productivity improvements through process redesign than through purely stand-alone software or other changes. This is probably because stand-alone software changes represent a small portion of total costs, and are of little benefit when done without the cooperation and input of the many affected parties (Landauer, 1995). Process redesign is primarily a management issue, though engineering must be engaged in a dialogue with management if such efforts are to prove successful. It often includes changes in software as part of the redesign.

In contrast, changes in the way that design calculations are performed are chiefly an engineering issue, a question of how best to pursue design and, more recently, true optimization. Major changes in how ships are designed do affect organizations, and therefore the line between process redesign and changes in design calculations becomes indistinct. Nevertheless, the improvements that can be made in engineering design calculations regard the mechanics of how calculations are performed – not managed. Improvements in optimization and design calculations are the primary focus of thesis study.

CURRENT USE OF OPTIMIZATION IN SHIP DESIGN

Before discussing specific aspects of previous work done in ship design optimization, it may be worthwhile to note the current status of true optimization methods in industry today. The current use of computer optimization methods in ship design today could be described as limited, fragmented, and expensive. Every design organization does not use multi-variable optimization methods, ones that do often use them in limited areas of design with custom software, and the small size of the naval architecture software market means that such software is generally expensive and has limited distribution.

As suggested by Taggart, 1980, there had been little computer ship optimization work done or widely used up to that time, in large part because design is a complex process that is highly customized or personal in nature. While there has been much more work done since that time, thanks in large part to the widespread availability of computers, these optimization methods have not spread to become a tool for general use, let alone a standardized tool that can be shared and interpreted across the industry. As noted by Schneekluth and Bertram, 1998, design programs can become highly customized affairs, with the result that they are rarely used outside

of academic settings where time and labor is available for writing or greatly modifying existing programs.

Recent efforts to use optimization software tend to focus on only one area intensely (such as computational fluid dynamics), or try to cover an entire ship design using simple regression equations (and therefore with poor accuracy in any one particular area of design that is of interest). Overall, ship design and optimization that simultaneously and accurately accounts for most elements of the hydrodynamic design problem is not generally practiced. Multi-element ship optimization that includes non-hydrodynamic elements is even less common.

HISTORICAL PROGRESS IN SHIP DESIGN OPTIMIZATION

A great body of work has been performed in the area of ship design optimization, with much of the work focused on the hull form problem in detail. Only a brief sample can be discussed below.

As mentioned above, the papers written on ship design optimization tend to exist on the extreme ends of the spectrum. Many papers use simple regressions or relational expressions to define ship characteristics, resulting in a generally applicable method with modest accuracy. It would be difficult to know how useful the optimization results were from such a simple method, since only broad trends are described by the regression equations used. It is telling that many of these regression equations are plotted with a logarithmic vertical scale, since such a scale tends to minimize the apparent error (see Watson, 1998 for examples). Other papers focus intensely upon a specific type of ship or element of design, with resulting higher accuracy but a lack of general applicability to design. Designers would like the highest accuracy methods combined with a program of wide applicability.

To illustrate this point a figure could be made, like the one shown in Figure 1.2-1.

This figure plots historical ship design investigations (in a notional or qualitative manner) in a space defined by two axes. The x-axis represents a scale of increasing complexity (and ideally, accuracy) of individual design calculations. The scale starts with virtually no complexity, such as the design of hulls using only half-hull model carving as was done for the 1800's-era Chesapeake schooners, and ends with extreme complexity, such as the CFD and direct numerical simulation of the Navier-Stokes equations. The y-axis represents a scale of increasing number of design elements that are simultaneously considered in the design and optimization calculations. This scale begins with considering a very limited set of elements, such as approximate vessel displacement and dimensions, and ends with all design elements being considered simultaneously, such as arrangements and available machinery sizes.

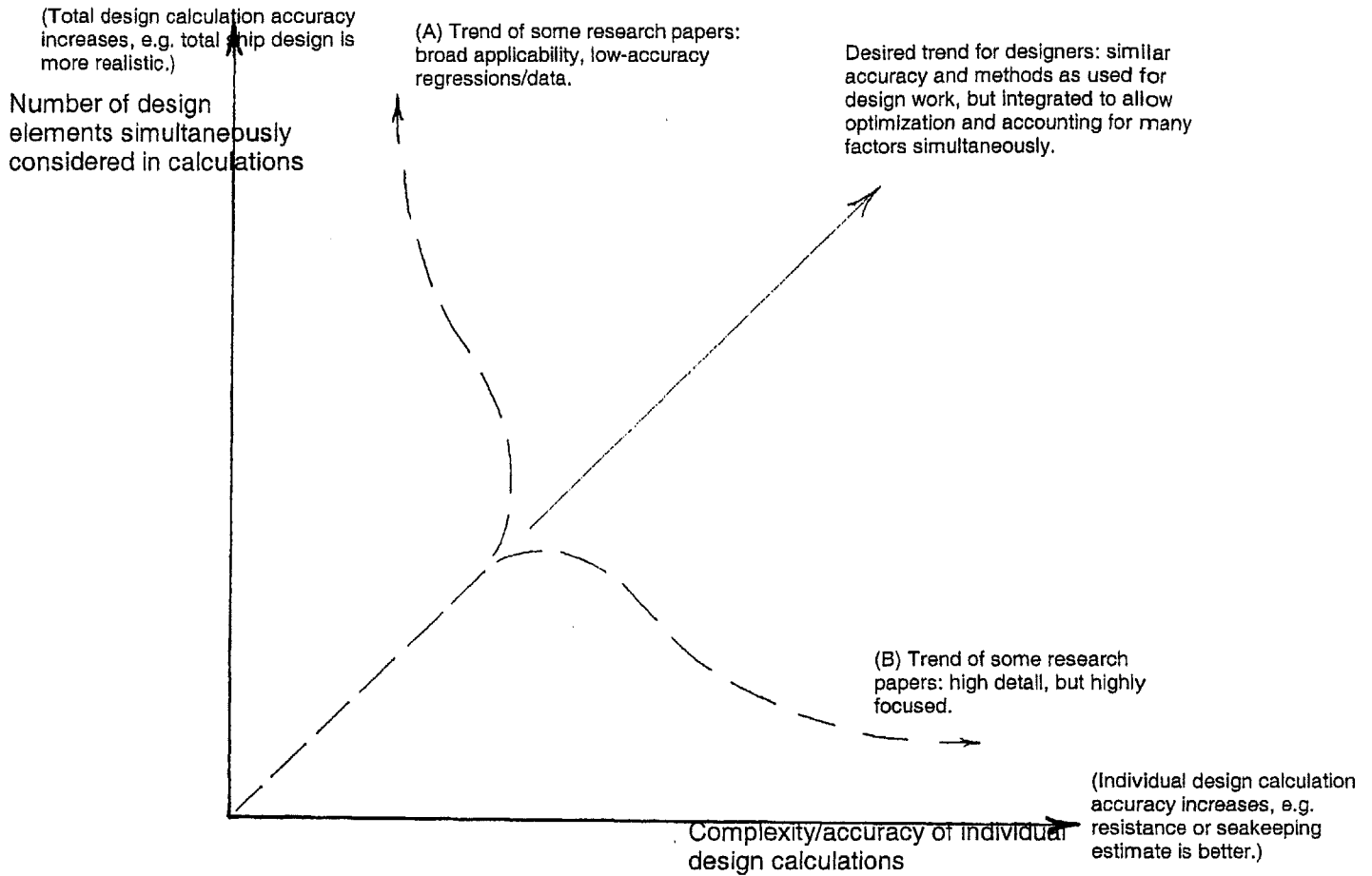


Fig. 1.2-1 Notional two-dimensional classification area of ship design methods.

By notionally plotting the history of ship design investigations some trends become apparent. As individual design calculations became increasingly complex, the effort involved in making total, integrated design and optimization tools (software) became too burdensome for the typical researcher or short-term company project. Also, the types of professionals needed to create the calculation methods (researchers), and to integrate the methods in a reliable and useful way (professional computer programmers), became distinctly different. So by the 1960's the ship design and optimization investigations began to diverge into two (very approximate) classifications.

Broadly speaking, previous research efforts can be classified according to two types of investigation strategies. One set of investigations (a) consists of optimization studies that simultaneously consider many elements, but not necessarily at the level of accuracy desired in engineering practice. The other major branch of investigations (b) consists of the more typical “specialist” investigation that focuses intensely upon one or a very limited number of design elements simultaneously, and advances the state of the art.

What is visible when making a figure such as this is that there have been few or no practical investigations on the upper-right end of a 45-degree slope originating at the origin. This region, consisting of moderate to high complexity and accuracy of calculations, with many design elements simultaneously considered, is of greatest utility and interest to design professionals. The America’s Cup yacht design efforts may come close to rising above the “specialist” zone of the figure towards this region. However, even utilizing a battery of tests and calculations, these design efforts are still prolonged, compartmentalized affairs. They do not directly link state-of-the-art 3-dimensional aerodynamic, hydrodynamic resistance, and seakeeping and added resistance calculation software to achieve true optimization, though they may achieve good approximations by marshalling data from design investigations over a period of months. Also, such designs represent the exception rather than the norm in the field.

Investigations of type (a), representing general optimization studies, began with simple weight equation and relational models in pre-computerization studies, such as the MIT method described in Manning, 1959. One of the first major papers to make use of computer techniques in general ship design optimization was Murphy, et al, 1965. Murphy, et al could be classified as one of the papers that utilize simple regression equations with broad applicability and moderate

or low accuracy. This paper did, however, use Taylor Series resistance data that is more accurate than the resistance routines of some much later papers.

More recent investigations into total ship design optimization include Lavis and Forstell, 1999, and Jiang et al, 2002. Both of these papers made use of a large optimization program based upon regressions and modelling of ships system data. An interesting feature of the method used is that it recreates the “design spiral” method of design for each variant tried. It is broadly applicable, even to multihull designs, and provides guidance to complex problems – but its reliance on crude regression data, such as Holtrop and Mennen resistance prediction methodologies, means that when the optimization is compared to identical “parent” vessels the predictions have less accuracy than would be desired (standard deviation for power prediction of known designs was 7.9%, and the power prediction error for some known ships was over 10-15%). In contrast the current hull assessment program calculates relative changes in resistance between candidate hull forms and a known parent hull, so that there is a high level of confidence in resistance predictions, especially for hull forms that are only slightly modified from the original parent.

Another broad ship design optimization method that was investigated by Parsons, et al, 1999, was the hybrid agent approach using set-based design. This approach is derived from studies of the set-based design methods employed at Toyota for automobile design. In set-based design, design variables for each subsystem or element within a complete design (such as the volume occupied by a subsystem) are initially allowed to fall within wide ranges, or sets, of values. As the design effort proceeds and ongoing tradeoffs reveal the cost and performance impacts over the range of variable sets, the allowed size of the sets is gradually reduced until an optimum design results from the converged final answer.

In the method used by Parsons, et al, 1999, “agents”, whether human or their computer interfaces, represented each subsystem involved in the design effort, and an optimum design was (quickly) achieved by using a “market-based” system which bought and sold various volume, weight, etc. variables among the competing subsystems. The set-based design approach is more of a process redesign than an optimization process, since it provides a rational, human-speed method to allow diverse organizations to optimize a design. Theoretically, the traditional optimization methods would perform the optimization faster without this set-based approach, or at least as fast – and within a single computer – but practical organizational dynamics make the set-based design method useful for real design offices. Parsons, et al, 1999 focused on the method and to a lesser extent upon the detailed analyses – Holtrop and Mennen regressions were used for resistance prediction, with the attendant lack of accuracy expected from this method.

A much more focused general ship design investigation was that of Majumder, et al, 2002. More detail could be used in this paper because it focused on fishing vessels (and vessel motions). However the difference between installed power of a known vessel and a predicted vessel was still as great as 38% in one comparison, revealing a lack of accuracy present in many of these general ship design papers.

Investigations of type (b), representing more focused “specialist” studies include seakeeping and resistance studies.

Many papers have focused more on hull form optimization with regards to seakeeping performance. Walden and Grundman, 1985 used a combined head seas seakeeping program and a Holtrop resistance regression method with an exponential random search method to produce hulls optimized according to weighted seakeeping and resistance criteria. Their program, SKOPT, was one of the very few practical seakeeping optimization programs produced. Work

by Bales, 1980, extended by Bales, 1981 and Walden, 1983 used a series of seakeeping calculations to produce a regression equation of average ship motion response versus hull characteristics. While of limited applicability, some observations from the investigation were of interest, including that the motions of a hull designed for optimum seakeeping may be reduced to the equivalent of an anti-optimum seakeeping hull of three times the displacement.

This research suggested that large improvements in seakeeping performance are possible with limited design constraints. Such a conclusion is a matter of debate between authors. Bhattacharyya, 1978 suggests that only modest changes in seakeeping performance are possible with large changes in ship proportions. Improved seakeeping designs tend to increase calm-water resistance, and hence Maroulis, 1968 found that in most situations a cargo vessel would not derive direct economic benefits from seakeeping optimization. Different economic analyses give different conclusions, though clearly seakeeping motions and therefore operability can be affected at least modestly by small changes in hull form (Lewis, 1988).

A variety of investigations have also been made into detailed ship resistance optimization. Recent investigations include Hollister, 1996, who developed a program based on Holtrop and Mennen resistance regressions to allow up to two variables at a time to be altered during hull form optimization for resistance. Day and Doctors, 1997 used the thin ship analysis of Michell in optimizing the resistance of slender hulls (and found that small changes in speed could require large changes in the optimum hullform). Unfortunately thin ship analysis is not accurate enough for resistance prediction of typical hull forms of interest.

Many computational fluid dynamics (CFD) investigations have been made, including one focused upon practical hull form optimization for resistance by Harries, 2000. CFD will likely become a common optimization tool in the coming decades with the steady increase in computer

processing speed. Currently such analysis is not fast enough for practical optimization on inexpensive desktop computers.

Some work has also focused on shallow water resistance optimization with exciting results, especially for supercritical depth-Froude number speeds where it appears that very low wavemaking resistance can be achieved through proper hull shaping (Chen and Sharma, 1997).

Plotting ship design investigations as before, but with a third dimension representing the number of design variables that can be simultaneously varied, can be done as in Figure 1.2-2. Design investigations that allow many design variables to not only be evaluated, but also allows them to be varied as part of the optimization process, speeds the design effort. This is because fewer trade studies need to be performed, where each trade study can only vary a finite number of design variables.

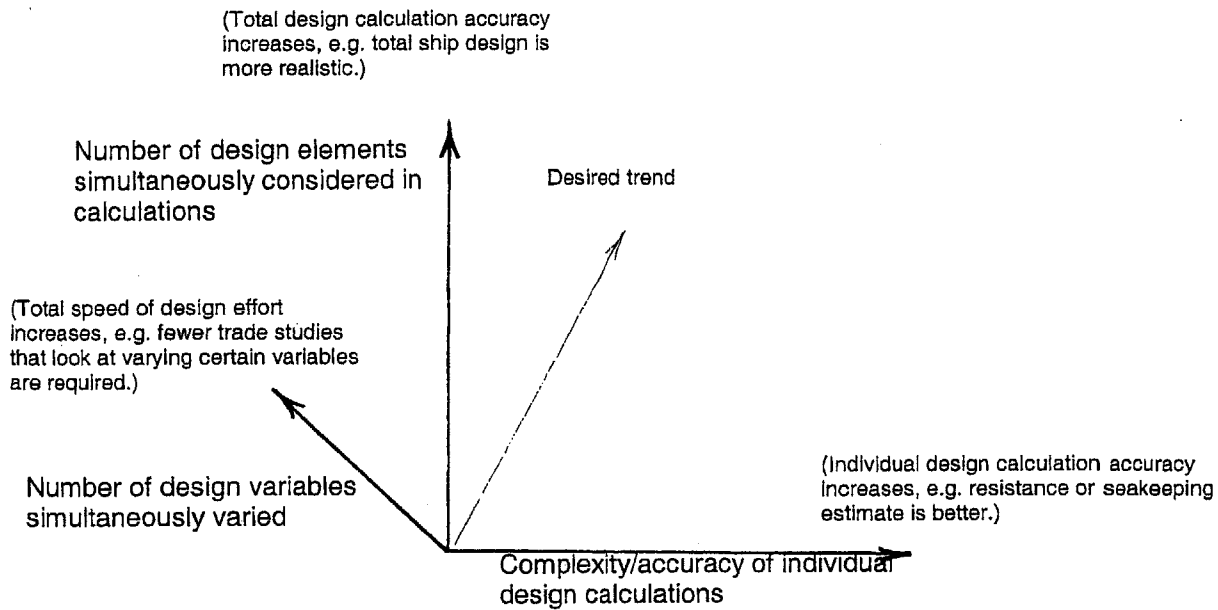


Fig. 1.2-2 Notional three-dimensional classification space of ship design methods.

Clearly, the desired trend would be to push ship design methods to higher values on all three axes. What is notable is that the only axis on this figure that is very difficult to move to higher values on is the x-axis, the scale of individual calculation complexity and accuracy, which is driven by the state-of-the-art in research. All the other scales, using current computer technology, merely require a one-time capital investment of computers and programming to link the various design elements together, and this investment is at least an order of magnitude less than that required to make major progress in many areas of basic research. Yet progress along any of the axes results in more accurate design optimizations in less time. Therefore it makes sense to attempt to bring ship design optimization techniques and tools as far into the desired region as possible.

1.3 Focus of Current Work

EMPHASIS OF CURRENT WORK

As has been shown in the previous chapter, there is often a gap between optimization research and optimization practice in naval architecture design firms. Also, there is a need for more integrated design optimization methods that simultaneously account for many design elements, and allows them to be varied automatically. There is a real gap in design practices between preliminary design, where many elements are considered simultaneously but use is made of crude methods such as stability, wetted surface or resistance estimation charts and gross regressions, and detailed design where more rigorous methods are used but little flexibility is available in the design.

The purpose of the current work is to bridge this design gap, and to use recognized, reasonably accurate ship design methods to provide relatively quick, integrated optimization of hull form design accounting for many factors at once, instead of in the usual manual and piecemeal fashion.

A study was carried out to determine the “optimum” hull form for monohull ships, based upon several weighted criteria. The main product of this study is a hull form optimization program, called the hull assessment program. Propulsion power minimization is the primary focus of the program, although simplified seakeeping and weight/cost issues can also be studied with the existing program. The program uses standard naval architecture methods to simultaneously evaluate many hydrodynamic aspects of hull form design, and provides confidence intervals on the resistance estimate. The result is a flexible tool that allows naval architects to quickly compare the performance of a known hull form with many alternatives,

based upon expected operating profiles and expected environments. Reasonable agreement was achieved when comparing program optimization results with real-world hull designs.

The hull assessment program allows the easy importation of parent hull offsets using a text file (an example of the imported body plan for a Taylor Standard Series hull is shown in Figure 1.3-1). The program interpolates the input hull offsets to a standard system of offsets used throughout the program, thus alleviating a common data entry problem. After the first hull has been evaluated, new hull form parameters are automatically selected by an exponential random search optimization routine. The parent hull form is stretched to the new form, and calculations are performed of the new, true wetted surface with obliquity correction, stability, and other properties. Relative changes in characteristics between the new and parent hull are calculated, instead of producing gross estimates without such correlating points. Confidence intervals of 95%, based upon a normal error distribution, are produced for each component of resistance and summed to provide an estimate of the reliability of the resistance prediction.

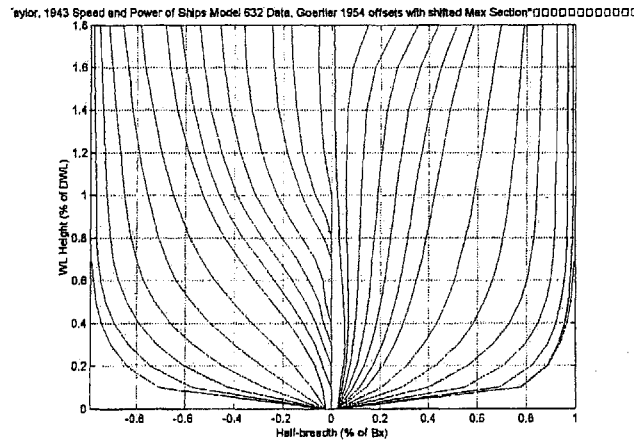


Fig. 1.3-1 Imported body plan for Taylor Standard Series.

Taylor Standard Series resistance data is used (extended to high speed using Graff, et al, 1964), along with the option of using a comparative residuary resistance ratio (worm curve

factor) file for the parent hull. An option also exists to use the high speed transom stern resistance regression of Fung, 1993 and Fung, 1998, which provides detailed error information, features nearly 10,000 data points, and was found to be more accurate than Jin's work, which in turn was found to be "far better than that of Holtrop" for such high-speed vessels (Fung, 1993).

A variety of other options also exist, including shallow water resistance estimation, the ability to let rudder area vary to achieve the same directional stability index of the parent design, and to use a fixed propulsive coefficient, or allow the propulsive coefficient to vary based on disk loading and the relative size constraints set on the propeller. Calculations are currently limited to head seas, and a variety of output options are available for presenting results.

CHANGING MARINE DESIGN PRACTICES

The application of approaches to ship design and optimization, similar to the hull assessment program produced as part of this study, has a real potential to change the way naval architecture design is done. Instead of the manual, approximate design methods pursued in naval architecture today, methods that lock-out major changes to design just as detailed calculations become available in later passes through the design spiral, the same high level of detail can be used to produce preliminary optimized ship designs using more extensive automation of the design process.

1.4 Outline of the Text

The remainder of the text deals with the current investigation into optimum hull form design. Section 2 provides an overview of the calculation methods used in determining hull form performance characteristics, and gives a brief outline of the logic flow of the program used to make the calculations. Section 3 provides a detailed description of the major calculation methods used to calculate hull form performance, and reflects the primary focus of the current study upon hydrodynamic characteristics. Shallow water resistance effects receive a relatively large amount of coverage because it is felt that this topic is rarely given a comprehensive overview in modern literature. Section 4 records the results of several optimum design investigations performed using the current program. This chapter also shows good correlation between optimum hull dimensions calculated by the current program, and a real-world slender hull form design that is primarily driven by hydrodynamic considerations. Section 5 gives some conclusions and recommendations based upon the current investigation. The appendices contain correlation and validation analyses for major calculation routines, describe limits to the use of some of the methods, sample input files and descriptions, and sample output.

2 Overview of Method –

2.1 Outline of Methods Used

The following table summarizes the major calculation methods that were used in the optimization program. Some methods may or may not be used, depending upon the options selected by the user in the input profile file. Also shown in the table are areas where improved capabilities would be helpful in future updates to this work.

Table 2.1-1 Current program functions and desirable future upgrades.

Current Functions	Desirable Upgrades
<p>Geometry and Hydrostatics:</p> <ul style="list-style-type: none"> * Imports parent WL half-breadths, interpolates to a standard system of stations. * Calculates DWL hydrostatics, including wetted surface with obliquity correction. * Calculates SA curve, transom stern parameters for Fung regression. <p>Optimization:</p> <ul style="list-style-type: none"> * Use of batch file to automate calculations. * Allows variation of displacement, Cv, B/T, Cp, LCB. * Automatic selection of new hull form using exponential random search method. * Stretch parent hull form to desired hull form Cp using Lackenby method SA shift. * Evaluation of hull forms using multiple parameter weighting criteria, with user-defined weighting of propulsion power, displ.:payload ratio, seakeeping (Bales rank-factor or strip-theory C.G. heave acceleration), and cost:payload ratio. 	<ul style="list-style-type: none"> * Import parent buttock line heights. * Calculate design-wave hydrostatics for strength purposes, other WL values. * Allow variation of Cm, hull depth, other stern, section shape, appendage, etc. parameters. * Allow optional use of Box-Guin “Complex Method” or Nelder and Mead Simplex search methods for faster local optimization.

- * Rejection of hull forms that violate input limits on maximum or minimum stability, negative payload.
- * Uses even spreading of all conditional probabilities to determine average performance.

Resistance and Propulsion:

- * Imports parent hull residuary resistance vs. Taylor series data (WCF).
- * Uses Taylor series data with WCF, or Fung regression for transom stern hulls, to determine relative change in residuary resistance from parent hull, or thin-ship theory.
- * Uses ITTC 1957 friction line, with roughness correction via C_a based on Townsin.
- * Evaluates rudder resistance and uses a lump sum for other appendages.
- * Fixed user-defined air drag areas and C_d .
- * Shallow water residuary resistance from Graff, et al tests or thin-ship theory.
- * Uses actuator disk-theory, with realistic efficiency reduction and limits on propeller disk size based on user constraints, to determine maximum open-water propeller efficiency.
- * Propulsive coefficients derived from regression equations.

Maneuvering:

- * Directional stability maintained by changing rudder sizing per Jacobs.

Seakeeping:

- * Calculates head seas seakeeping responses using Salvesen, et al method.

- * Rejection of hull forms that violate tactical diameter or directional stability limits.

- * Use matrices of conditional probabilities to determine average performance, and provide transit speed modifications based upon water depth or sea condition.

- * Use more than the limited set of Taylor Series data currently being used, and incorporate other resistance databases.

- * Use more refined roughness evaluations as given in Carlton.
- * Include more detailed appendage resistance.

- * Vary shallow-water residuary resistance augment versus C_v and other dimensions based on model or 3-D panel method data.
- * Use true propeller-matching methods.

- * Use more accurate methods, where available.

- * Use linear theory for large diameter tactical diameter evaluation, or Harper and Scher method for tactical diameter.

- * Correlate seakeeping analysis with model test information.
- * Calculate responses in all headings, use

* Calculates added resistance using Salvesen for long wavelengths and ray-theory where appropriate for shorter wavelengths.

Weights and Costs:

- * Imports parent hull data for several crude weight groups.
- * Uses basic weight ratiocination regressions; and allows users to define what percentage of hull weight change is volume-driven, vice bending moment-driven.
- * Annual costs calculated using basic regressions given in Mandel and Leopold.

appendages.

* Correlate with model test data and allow use of other added resistance methods.

* Use refined weight group data.

* Use more refined weight models.

* Use more refined cost models.

2.2 Outline of Program Logic

The Hull Assessment Program is run from the main MATLAB file, the latest version of which is haprev6.m (March, 2003). This file is called by typing the filename (without extension) in the command window of MATLAB, after setting the current directory that MATLAB is using to the directory that contains all of the HAP files. The logic flow in the main program, haprev6, is as follows.

The display asks the user if the program shall use a batch file to set the run options, options that are otherwise entered manually on the screen as described below. If one is selected, signifying that a batch file is to be used, then the program will run automatically from this point onward. For a description of the batch file see the appendices. It is recommended that a batch file be used for normal operation of the program. The other options described below are generally for debugging or experimental purposes only.

If a batch file is not used to automatically run the program then the following options are available. A display asks the user to select from two options, automatic optimizer mode or manual mode. This selection will set a variable, "manual", to either zero for automatic or one for manual mode. If the variable equals one, then the total number of iterations run will be one, and thus the resulting calculations will only be for the hull defined by the input file. If the variable "manual" is zero, then the program will ask the user for the total number of iterations which will be run un an attempt to optimize the input weighting function (described below). The program running in automatic optimizer mode will adjust all of the variables designated in the input file to produce an "optimum" design.

The user is asked about iteration options in automatic optimizer mode. If the variable “iteration options” is set to one, the hull will be optimized per the operating profile file. If the option is set to two, the hull will be optimized only according to minimum WS by varying the beam-to-draft ratio.

The program `inputprofile.m` is now called, which reads the operating profile text file, an example of which is given in the appendices. The operating profile file contains basic information that is used to produce the optimization, including initial vessel dimensions and coefficients, whether they may be varied, limits on variations, weighting factors for power optimization and other criteria, limits on hull design for GM, conditional frequency distributions of speed (the speed profile), water depth, sea state/wind state, and other miscellaneous items.

Next the program imports the parent hull form using the program `importparent.m`. At the start of this program (or function), the variable “testcount” is set equal to zero. Testcount defines the iteration number that the program is currently evaluating, and when it is zero the program `offsets.m`, which manipulates the hull offsets, will import a parent hull, rather than using offsets stored in MATLAB memory, as for later iterations. The program will request that the user enter a parent hull offset file, such as the example shown in the appendices. It should be noted that the baseline offsets in the offsets file should have a positive, non-zero half-breadth value if the keel extends to the baseline, for calculating local draft.

Next the program archives the original offsets under archive-type variable names, so that the original offsets can be used as a starting point for each iteration when the hull is to be stretched to some new desired form. Use of a fixed archived offset file avoids the drift that is possible if small errors in geometry stretching in each iteration were allowed to add to one another, by stretching hulls that had already been stretched multiple times.

Next the current LWL, B, T and offsets are set to being equal to the original values read from the parent offsets file. Thus when hydrostatics are calculated next, using the function hydrostaticsh.m, the values determined will be those of the original parent. These hydrostatics are also archived so that future hull variations may be stretched from the parent hull based upon the difference between desired and parent hull form characteristics. Parent hull stability and residuary resistance are also calculated.

The main iterative loop in the program now begins, one loop being run for every iteration desired. The “testcount” numbering scheme index counts down for each loop from the maximum equal to the number of iterations to be evaluated, to the final hull evaluated equal to one.

Now the program findhull.m determines the desired dimensions that will be used to stretch a new hull form, and evaluate it for various derivative resistance, etc. properties. If the option “manual” equals one the user is queried for desired dimensions, and some resulting dimensions are calculated for them. If “manual” equals zero, the exponential random search technique is used to determine the desired dimensions for this iteration. The exponential random search makes selections based upon limits in the operating profile file, and also will make only beam-to-draft ratio variations if the appropriate value of 2 is used for the variable “iteration options”. Other details are provided in the following chapters of detailed method descriptions. If this is the first loop then the search uses the initial dimensions listed in the input profile file.

The program now sets the current values of L, B, T to the desired values, in preparation for running the hydrostatics program again. (Note that the hydrostatics program always uses the current variables and non-dimensional offsets for calculations.)

The sectional area shift is run next, in which the stations are shifted to a new, desired C_p sectional area curve. The output of this function is the desired station positions (shifted from the default 40-station system used in this program) and also a warning variable "lackenby limit", which equals one if the absolute limits of shifting have been exceeded for the given C_p desired. Note that currently a warning is only given in manual mode, to the user via screen display – therefore one must carefully chose the limits on the operating profile file if running in automatic optimizer mode. The prior sectional area curve is saved as the "preshift" version, to make a comparison with the new sectional area curve. A comparison graph is shown if the program option is manual.

The offsets function is called again in order to interpolate offsets from the shifted stations. Note that the variable "testcount" is now greater than or equal to one, so the function offsets.h will not refer to the user input option for a parent file, but will use the existing interpolated offsets, with the newly shifted stations, to determine the new interpolated offsets.

The variable "current offsets" is reset to be equal to the newly found offsets, in preparation for use in the hydrostatics program. Also the variable "stations" is reset to the values used by default throughout the main program (a 40-station system), instead of the shifted values used in offsets.m above.

Hydrostatics are run on the new, final stretched hull design for this particular iteration. Other than the option to adjust rudder size to match the directional stability of the initial hull evaluated, the geometry will now remain fixed for this iteration.

At this point in the iteration the many derivative properties of the hull are calculated using the functions that constitute the bulk of the program. These include static and directional

stability, resistance and propulsion, seakeeping, weight and cost, and combinations of data to get overall average operating profile performance statistics and resistance and powering uncertainty.

A limits evaluation is made to determine which limits on performance goals are exceeded for each hull. These include minimum and maximum static stability, Lackenby limits, and negative payload if weights are evaluated. The function `checklimitsrevj.m` produces a variable “sum of exceeded limits” which if greater than one, means that a limit has been exceeded.

Next the multiple parameter weighting criteria are evaluated, for iterations option 1, automatic optimizer mode. Weighting functions are defined in the profile file entered by the user. The end result of the weighting criteria is a variable “factor” which describes the desirability of the solution hull just evaluated. If any limits are exceeded then the factor is weighted by the program with such a large weighting that it will be rejected, in favor of a hull that does not exceed any limits. For iterative runs the main program checks if any limits have been exceeded (that is, if the value of “sum of exceeded limits” is greater than zero). If so, the program multiplies the variable “factor” calculated by one million, as a simple way to disqualify it from future consideration as a best hull for further iterative designs to be based around.

The resulting data is recorded for each iteration in a matrix “testdata”, and several other variables. As part of this record, the factor is set to zero for the case of single iteration manual runs. The final part of the main iterative loop is to determine the best testcount hull of all prior runs, based upon the “factor”. Now the iterative loop ends and is repeated as desired.

At the completion of all runs the program terminates with a text display of results, primarily focusing on geometry, resistance and powering, with many graphs displayed depending upon the calculations selected in the input file.

3 Detailed Description of Methods –

3.1 Hull Geometry and Hydrostatics

Geometry and hydrostatics information are fundamental to any hull form optimization program. Therefore the current program features basic geometry stretching and hydrostatics calculation routines. The hull assessment program, haprev6.m, requires the entry of parent hull offsets data to allow resistance and hydrostatics calculations to be performed. Several basic offsets files are currently available to the user if other data is not available.

The offsets of a desired parent hull are entered into a text file, or entered into Excel spreadsheets and then saved as a text file. A portion of a sample file is shown in the appendices. The salient feature of the required file format is that a specific set of offsets at particular stations and waterlines is not required. Instead the program will perform a cubic spline interpolation between the offsets provided to determine the regularly-spaced offsets needed for calculations. Input file offsets can be used that are based on any system of waterlines and stations, with the only limitation being that the waterlines used must be the same for each station.

Also, it is recommended that offsets be provided extending well above the waterline, so that the underwater hull form, which is the only information used in the optimization calculations, is properly represented. Sharp chines may cause visible unfairness in the body plan interpolated by the program, which uses cubic splines. In cases where this is noted, the program could be adjusted to make use of linear interpolation instead.

Some basic parent hull dimensional information needs to be provided in the offsets file in metric units, as shown in the example in the appendices. The wetted surface coefficient is not

required and is for informational purposes only. The number of rows of data in the offsets chart, and the number of columns, must be listed. Also the centerline offsets, all with a half-breadth of zero, must also be provided for proper wetted surface calculation. The breadths and heights are presented as percentages of half-beam and DWL height, respectively.

Hydrostatics and wetted surface calculations are made according to methods given in Lewis, 1988. Wetted surface is determined both with and without obliquity correction, although the value with the obliquity correction is what is used by the remainder of the program. For making these calculations two “virtual” stations ahead of the bow and behind the stern are extrapolated, in order to facilitate calculation of local waterline slopes at the ship ends. The half-siding of the keel is included in the wetted surface calculation if shown in the offset file. Cutaway at the stern or bow is determined by assuming that all areas with a zero half-breadth, or areas below them, have no wetted surface contribution.

The Lackenby (Lackenby, 1950) method of sectional area curve shifting is used to vary C_p . This differs from other methods, such as that of the Taylor Series. A comparison of sectional area curves for the actual Taylor Series hull form at $C_p=0.60$, and the Lackenby shift (of both C_p and LCB) from the Taylor Series parent hull to a C_p of 0.60 is shown in Figure 3.1-1. The agreement is close, but not perfect. An investigation of what types of sectional area curve shifting is most beneficial has not yet been made. It is difficult to know what the full impacts on frictional, form, and residuary resistance would be for different sectional area curve shifting techniques, for various hull proportions.

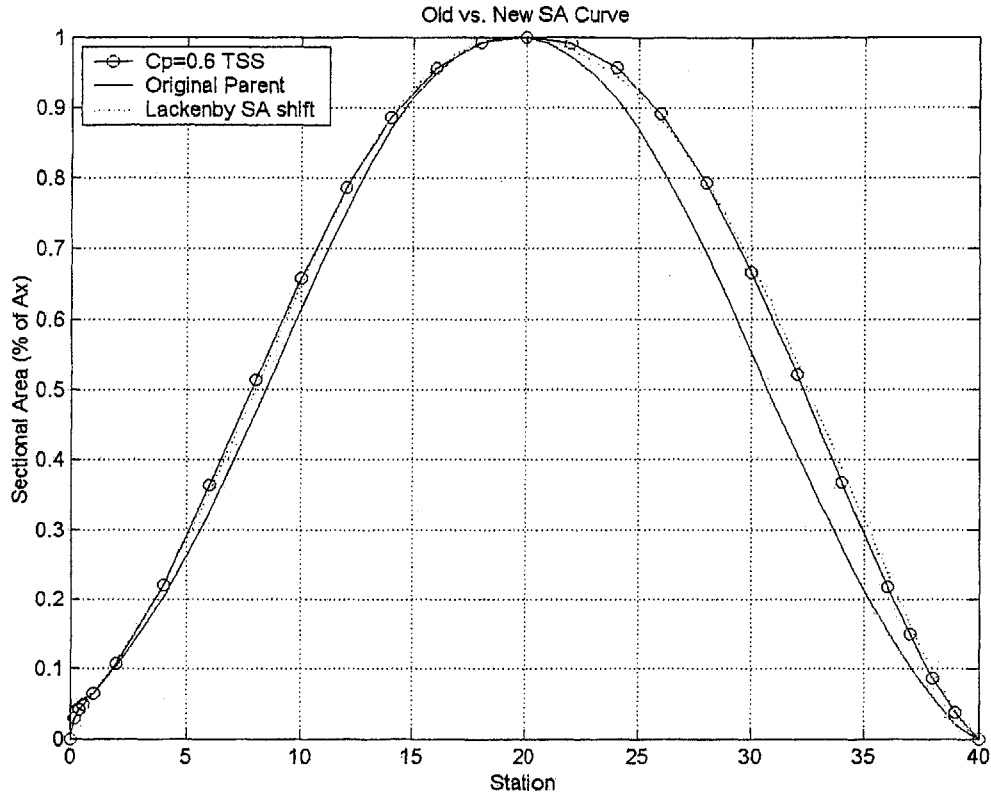


Fig. 3.1-1 Comparison of the sectional area curve of a $C_p = 0.60$ Taylor Standard Series hull form, the parent hull with a $C_p = 0.555$, and the Lackenby method shift from the parent hull to achieve a $C_p = 0.60$ hull form. Note that the Lackenby shift is shown as a light dotted line lying nearly on top of the Taylor Standard Series sectional area curve.

3.2 Calm Water Resistance

FRICTIONAL RESISTANCE

Frictional resistance is calculated using the standard ITTC 1957 ship-model correlation friction line, and the wetted surface (with obliquity correction) calculated within the program's hydrostatics calculation routine.

Correlation allowance (including roughness and non-roughness effects) is accounted for if selected as an option in the input profile file, for an assumed average hull roughness. The correlation allowance, C_A , to be added to the frictional resistance coefficient is given in Lewis, 1988 Vol. II as: $C_A \times 10^3 = 105 (K_S / L_{WL})^{1/3} - 0.64$, where K_S is the mean apparent amplitude of surface roughness over a 50 mm wavelength, in microns (note that the equation must have consistent units used for both roughness and length, and that a micron is 1×10^{-6} meter). Only 69% of this C_A value is used, per the empirical findings of Townsin et al, 1981. For more detailed discussions of correlation allowance and roughness, see Townsin et al, 1981, Lewis, 1988 Vol. II, Harvald, 1991, and Carlton, 1994.

RESIDUARY RESISTANCE

The following procedure is used to determine residuary resistance in the program: a) a worm curve factor for the parent hull (the ratio of residuary resistance of the parent hull to the equivalent Taylor Standard Series hull) is entered into the program for a range of speeds using an input file; b) the Taylor Standard Series and its extensions are used to estimate the residuary resistance of the newly devised hulls in the program (the hulls which have been stretched from the original parent hull form) making use of the parent hull worm curve factor; and if desired and

applicable, c) other regression equations are used to estimate the residuary resistance, albeit with higher probability of error.

These other regression equations are used to determine the relative residuary resistance change between the original parent hull and the newly devised hulls, thus superceding the worm curve factor and Taylor Series prediction method for newly devised hulls that are far removed from the original parent hull form. The method that is used is to determine the residuary resistance per displacement of the parent hull using the Taylor Series and the known parent worm curve factor. Then the Fung, 1998 regression method residuary resistance per displacement is calculated for the original parent hull and the newly modified hull form. The differential between the Fung 1998 residuary resistance per displacement for the parent and new hull is applied to the known parent hull resistance per displacement, to determine the relative change in residuary resistance per displacement.

Use of the regressions with good accuracy for transom stern ships at moderate speed (Fung, 1991) and high speed (Fung, 1998, 1993, 1986) allows us estimation of changes to the residuary resistance that a stationary worm curve factor cannot provide. For example, there is a possibility that residuary resistance is influenced by the effective aspect ratio of the transom stern area, and thus a fixed worm curve factor will not provide accurate results for hull forms with widely varying proportions. Also, taken to the extreme, some of the high C_V , or “fatter” Taylor Series hull forms have large run angles in the stern that obviously lead to flow separation, thus radically changing the nature of flow around the stern and thereby the residuary resistance characteristics as well.

It should be noted that there are some errors in the Fung and Leibman, 1998 paper. Firstly, the regression coefficients listed as x_1 through x_9 are actually the coefficients c_1 through

c₉. Second, the expression for wavemaking length, λ , is missing a constant and the entire term should read:

$$\lambda = [a_1 * C_P + a_2 * 0.034977 * \Delta / (L_{WL} / 100)^3]$$

A correlation analysis was done to check for discrepancies or errors between the implementation in this work and that of Fung and Leibman, 1998. Comparison with an example given in the paper confirms that using the corrections above produces exactly matching resistance estimates.

All other terms in the paper by Fung and Leibman, 1998 are correct and use standard English-system naval architecture units of feet and long tons. The residuary resistance coefficient at any given speed is:

$$C_R = \exp \left\{ \sum_{i=0}^n \left[B_i \prod_{j=1}^9 x_j^{c_{ij}} \right] \right\}$$

and the other terms (except for the extensive list of coefficients, to which the reader is referred to the original paper or the text file, fung98regression.txt, used in the present program) are:

$$x_1 = F_N^d$$

$$x_2 = \cos(\lambda * F_N^e) * \exp(a/F_N^2)$$

$$x_3 = \{0.034977 * [\Delta / (L_{WL} / 100)^3]\}^{0.5}$$

$$x_4 = A_{20}/A_x$$

$$x_5 = C_P^2$$

$$x_6 = B_{20}/B_x$$

$$x_7 = B_x/T_x$$

$$x_8 = \ln(90-I_E)$$

$$x_9 = C_x$$

Use of these regression equations for determining *relative* residuary resistance changes between transom stern hulls, as opposed to determining *total* residuary resistance using regression equations, substantially reduces the error in the resistance estimate. Also, when the hull form lies close to the original parent entered by the user, or the regression equations are not applicable, the user can rely on the Taylor Series resistance data through use of run options in the program.

Data files used for the Taylor Standard Series resistance interpolation calculation include the following:

Graffspeed.txt – R_R ratios for speeds above $F_n=0.6$ from Graff et al.

Exp1.txt – SNAME R&D sheets for high C_V hulls, $DLR = 300,400$ $B/T = 2.25$, $C_P = 0.5$, .6, .7.

Exp2.txt – Goertler p.3-20, $C_P = 0.48$, $B/T = 2.25$.

Exp3.txt – Zero C_V file with zero R_R for a range of speeds for $C_P = .48, .86$, $B/T = 2.25$, 3.75. Not used because interpolation routines are used instead, and this data creates problems with the interpolation scheme.

Exp4.txt – Goertler, p.3-84, $C_P = 0.80$, $B/T = 2.25$.

Exp5.txt – A deleted file was removed, and two zero- C_V placeholder values were entered to keep the file indexing sequence intact. Not used because of problems with the interpolation scheme.

Exp6.txt – Goertler p. 5-162, $C_P = 0.48$, $B/T = 3.75$.

Exp7.txt – Goertler p.5-203, $C_P = 0.68$, $B/T = 3.75$.

Exp8.txt – Goertler p.3-22, $C_P = 0.49$, $B/T = 2.25$.

Exp9.txt – Goertler p.3-24, $C_P = 0.50$, $B/T = 2.25$.

Exp10-18.txt – Goertler p. 3-28 – 3-60, $C_p = 0.52 - 0.68$ in 0.02 increments, $B/T = 2.25$.

Exp19-27.txt – Goertler p. 5-166 – 5-198, $C_p = 0.50 - 0.66$ in 0.02 increments, $B/T = 3.75$.

Exp28 - 37.txt – Goertler p.5-203 – 5-167, $C_p = 0.68 - 0.5$ in 0.02 increments , $C_v = 2.5$ addition to data $B/T = 3.75$.

Exp38 - 46.txt – Goertler p.3-61 – 3-25, $C_p = 0.68 - 0.5$ in 0.02 increments , $C_v = 2.5$ addition to data $B/T = 2.25$.

Exp47.txt - Graff et al, p.383 fig. 7, $C_v = 1, 1.5, 1.7, 2$, $C_p = 0.64$, $B/T = 3$. Not yet used because not enough other $B/T = 3$ data has been incorporated yet.

There are also many other series and regression estimation techniques available, a good overview of which is presented in Schneekluth and Bertram. Some good data on hull form design, and a non-dimensionalized set of Taylor series residuary resistance data for lower speeds is presented in Henschke, 1957, in contour plots similar to the original work by Taylor, which facilitates optimization of residuary resistance for a specific speed.

3.3 Shallow Water Resistance

SHALLOW WATER EFFECTS: BACKGROUND

When a ship is travelling in water that is not infinitely deep (the shallow water case) or not broad in extent (the case of a channel or canal), the flow around the vessel is changed compared with motion in an ocean of infinite extent. These changes in flow cause many effects, such as sinkage or squat, trim, changes in maneuvering performance and directional stability, etc. For current purposes our interest is the change in the resistance of a ship due to shallow water. This case is of broad interest in many applications, and therefore is the most profitable one to investigate. Resistance in shallow water can be affected by two basic mechanisms, described below.

The first mechanism that changes resistance in shallow water is best understood as the blockage effect: as the ship travels in water that is increasingly restricted, the potential flow around the ship must change. The velocity of water passing the ship must increase compared with the deep water case because of flow constriction, and therefore viscous (and possibly form) drag are increased. This becomes especially important in canals or channels, where the blockage effect is more pronounced (Saunders, 1957)(Lewis, 1988). The increase in local water velocity around the hull because of shallow water is quite small (10% or less) until the water becomes very shallow, on the order of ship draft or shallower. This effect is small at normal ship operating water depths in comparison with the wavemaking effects described below. Because of this, blockage effect was not included in the current program methods in adjusting the frictional resistance of the vessel in shallow water cases. Future upgrades to the program may wish to include this method, especially in light of the results of this study that suggest that even minor

forms of miscellaneous resistance can have a significant effect upon the hull form optimization. This viscous effect should be investigated in the future, although it is small, because it represents another “antagonistic” effect of hull proportions on resistance: a slender hull has lower blockage effects and therefore a smaller increase in viscous resistance in shallow water; but long, slender hulls have a larger increase in wavemaking resistance in shallow water, and more wetted surface, proportional to their displacement.

The second mechanism that changes resistance in shallow water is the change in wave resistance. Energy is required to generate the wave pattern typical of ships in deep water, the Kelvin wave pattern. Changes to the deep water Kelvin wave pattern therefore suggest changes in the wavemaking resistance.

As water depth decreases, the phase velocity of waves decrease, in the limit of shallow water being approximately equal to $\sqrt{g H}$ (Neman, 1977). Thus speeds below a depth-Froude number $= V/\sqrt{g H}$ of 1 are termed subcritical, because they are below the maximum speed of waves at that water depth, speeds at $F_h = 1$ are termed critical, and above that value are termed supercritical.

An interesting change occurs to the angle of the Kelvin wave pattern according to linear theory. As critical speed is approached the angle formed by the waves increases, for speeds above a F_h of about 0.40, from the standard half-angle value of $19^\circ 28'$ to a limit of 90° at critical speed, forming a single crest called a wave of translation. At supercritical speeds the transverse waves are no longer present, and all of the diverging waves are contained within an angle, α , given by: $\sin^2 \alpha = gH/V^2$ (Lewis, 1988). Results of recent numerical investigations into nonlinear effects at supercritical speed, communicated to the author while at MIT, suggest that linear theory is not entirely correct near critical speed.

Thews and Landweber, 1935, provide the best description found in print of the actual observed behavior of ship models in shallow water. They are paraphrased as follows: At some relatively low F_h frictional resistance increases because of blockage effects. During this phase there is a modest increase in resistance over deep water values.

As water depth decreases at subcritical speed, the water depth in front of the model increases and that behind the model decreases, due to flow constriction effects. The increased height of water in front of the bow is equal to the height of a wave of translation, h_{trans} , given by the expression $V = \sqrt{g(H + h_{trans})}$, where H is the water depth. The deep water bow wave system diminishes, and some waves run ahead of the model while speed is well below critical. During this phase, the resistance increases dramatically over deep water values because of the large increasing bow wave and the fact that the stern waves are moving out from under the stern, heading aft. Neither the start nor ending speed of this phase are at the critical speed. Maximum trim occurs at the end of this phase.

At higher speeds, the next phase of shallow water resistance begins. The stern wave has moved aft completely away from the stern of the model and can no longer influence the model resistance. Therefore the resistance, which had been increasing dramatically over the shallow water values, shows a great reduction in the rate of increase of resistance. This is because the stern waves moving aft can no longer serve to increase resistance, since the model had previously stopped recovering any energy from them. The resistance curve shows almost a plateau in some cases. Approaching critical velocity only a single wave of translation forms ahead of the model and the deep water bow wave system diminishes. Increased resistance is caused by viscous blockage effects and the increase in the height of the bow wave of translation. The bow wave of translation and the stern wave system approach an angle of 90° with the model centerline as

critical speed is approached. As a result the normal wave-cancellation effect between bow and stern wave systems is no longer present, and the wave of translation at forward and the stern wave system act in relative independence of one another. The stern wave system ceases being generated before the critical speed is attained, because of wave breaking in the reduced depth and increased velocity water behind the stern. At critical speed or above the bow wave of translation has a speed greater than the critical velocity by a factor $= \sqrt{((H + h_{\text{trans}})/H)}$.

In the next phase of shallow water resistance the vessel moves through the critical speed and faster. The height of the wave of translation and its speed also increases, but not as fast as the speed of the model. Eventually a speed equal to $\sqrt{g(H + h_{\text{trans}})}$ is reached at which point the model can begin to pass the bow wave at higher speeds. Resistance then drops dramatically, ending the resistance plateau. The width of this plateau increases as depth decreases, since the effect of the height of the wave of translation on the velocity of the wave of translation becomes more important in the velocity equation given above. At some maximum speed for each depth the bow wave of translation can no longer form.

At high supercritical speeds shallow water resistance can be less than deep water because the normal wave system formation is restricted. There is a partial formation of deep water bow waves and an attitude that is increasingly planing in nature.

One of the photographs demonstrating these observations for a model in shallow water is shown in figure 3.3-1.

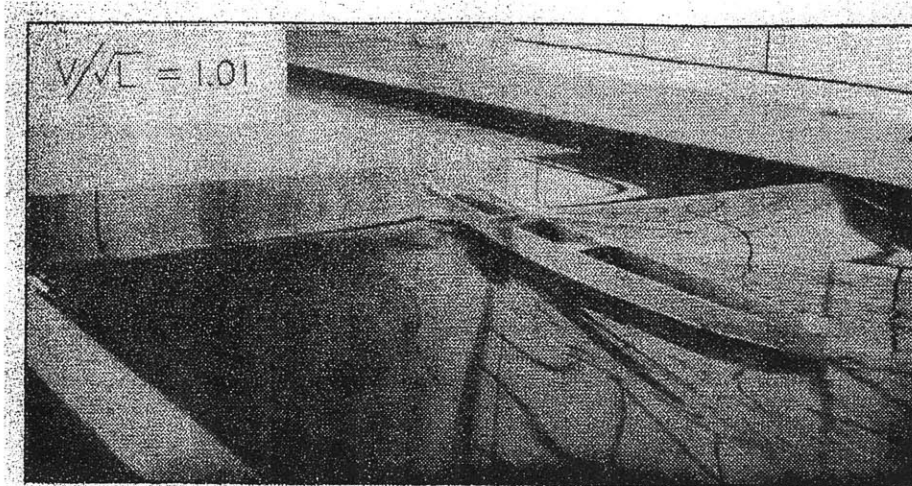


Fig. 3.3-1 One of a series of photographs of the wave pattern about a 48 in.-long model in shallow water (3 in. depth) transitioning from subcritical to supercritical depth-Froude number (Thews and Landweber, 1935).

Thews and Landweber, 1935 make one other interesting observation that is generally not mentioned in literature on shallow water resistance effects. They point out that in deep water ships have a characteristic hump in the resistance curve, which is often given as a maximum at a specific speed V_1 at a given F_N (or speed-length ratio in English units). Now the speed of a wave of translation, in units of knots and feet, is the speed $V_2 = 3.36 \sqrt{(H + h_{trans})}$. “For the condition where V_1 equals V_2 , it is reasonable to expect a maximum in the envelope of the shallow water resistance curves. It would be a condition similar to resonance in forced vibrations.” They go on to set the two velocities, V_1 and V_2 , equal to one another (ignoring the small effect of h_{trans}), and arrive at a critical value of water depth for their particular model of 20% of length, which matches well with their experimental results. Thus an important observation that can be drawn from their results is that not only is there a critical speed for any water depth, but that there is also a critical water depth which exhibits a markedly greater peak shallow water wavemaking resistance effect than other depths. The naval architect can therefore add another speed-depth condition to shallow water operation that is to be avoided if at all possible.

Investigations of both a theoretical and empirical nature have shown that wavemaking resistance is affected by water even twice as deep as ship length, and that wavemaking resistance can be more than doubled at normal operating drafts that are large fractions of ship length (Havelock, 1922)(Taylor, 1943). Also, shallow water wavemaking resistance can be less than that in deep water at supercritical speed, thereby offering an attractive possibility for improving performance if shallow water conditions can be expected. Therefore shallow water wavemaking effects are important much of the time in determining ship resistance.

Shallow water wavemaking resistance can be determined either empirically or theoretically. Schlichting pursued a semi-theoretical, semi-empirical study using both model test data and physical reasoning to estimate shallow water effects. Schlichting reasoned that the wavemaking resistance would be equal for a ship in deep and shallow water if the wavelength of the waves generated by the ship were the same. Since the same wavelength is generated at a lower speed in shallow water, there is some lower shallow water speed with the same wavemaking resistance as in deep water (Lewis, 1988). Detailed model test data have shown that wave nonlinearities invalidate Schlichting's approach for ships of normal form at water depth-to-length ratios of less than 0.333 (Graff, et al, 1964).

Graff, et al, 1964 performed detailed tests on a cruiser stern and a transom stern model. The quality of their data is good, though there is some question as to how reliable it is at very shallow water depth, as viscous effects do not appear to have been subtracted out of the data to arrive at the true residuary resistance changes. Taylor, 1943 provides some model test data but little supporting information, so the value of the data is limited. Some excellent shallow water investigations were performed on two small models by Thews and Landweber, 1935 and 1936.

Tuck, 1966 provided a first-order theory that can predict sinkage and trim well when compared with the data of Graff, et al 1964, but unfortunately predicts zero wavemaking resistance at subcritical speeds. Therefore Tuck's method cannot be used for shallow water wavemaking resistance estimation. Kirsch, 1966 and Hofman and Kozarski, 2000, use thin-ship theory to determine shallow water wavemaking resistance effects. Kirsch also provides a method to evaluate channel wavemaking resistance effects, which are significant.

The thin-ship theory approach is useful for determining approximate resistance ratios between deep and shallow water, but the accuracy of the method has never been shown to be very good. Figure 3.3-2 shows the comparison between calculated wavemaking resistance in a canal and experimental results, revealing moderate agreement. Millward, 1988 also shows very rough agreement between shallow water measured and thin-ship calculated resistance, especially at high values of F_h . Thin-ship theory is probably the best approximate theoretical method available to quickly determine shallow-water wavemaking effects. Care must be taken to remember that thin-ship theory does not account for deviation from wall-sidedness – a fact which is not emphasized in enough papers using thin-ship theory (Michell, 1898).

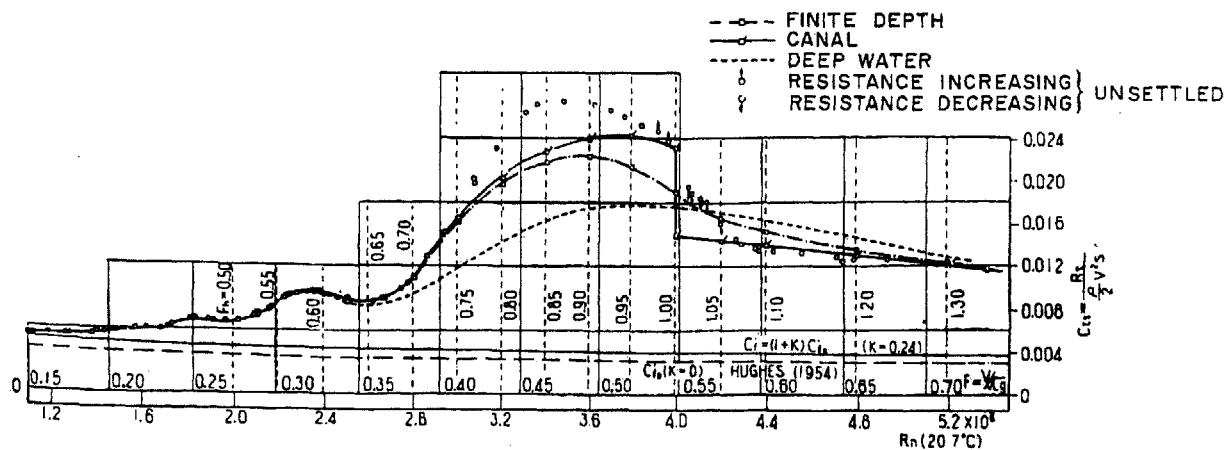


Fig. 3.3-2 Calculated thin-ship theory wavemaking resistance calculated in a canal (solid line with squares) and experimental results (points), along with other data (Inui results published in Wehausen, 1973).

The best theoretical calculations methods available for shallow-water resistance estimation appear to be those of Chen and Sharma, 1995 and 1997. These are complex, time-intensive three-dimensional panel method calculation routines that show good general agreement with results from Graff et al 1964, among others. Interestingly, they find that at supercritical speed a ship operating in a channel can be designed to have zero wavemaking resistance – what they term a superconducting channel. Their methods are too time-consuming to include in a quick optimization routine at present.

GENERAL APPROACH USED

The approach used here to calculate shallow water resistance effects was to focus upon wavemaking effects, assuming that viscous effects were of minor importance in comparison. This simplification is justifiable because the current hull assessment program is oriented towards moderate to high-speed vessels, vessels that tend to be slender, operate at high speed and at moderate to deep water depths. Changes in wavemaking effects are quite important for such

vessels, but viscous effects and blockage considerations do not become important except in very shallow water or confined channels. Cases that require investigation into viscous effects and blockage should probably receive special attention, since they are likely to involve specific port or channel situation where maneuvering, squat, and speed limits for safety become dominant concerns.

METHODS USED: EMPIRICAL

Two methods are available to the user of the current hull assessment program: an empirical method based upon model test data that is quick and reliable in the region of the test data; or a theoretical method that is slower and less reliable in absolute values, but probably more reliable in capturing the trends of shallow water resistance versus dimensional changes. Users can decide which method they would prefer to use by selecting the appropriate options in the input file.

The empirical method used here to calculate the shallow water increased wavemaking resistance was to use the Graff, et al 1964 model test data. Deep and shallow water residuary resistance data was read from the plots given in the paper. An example of the raw data provided is given in Figure 3.3-3.

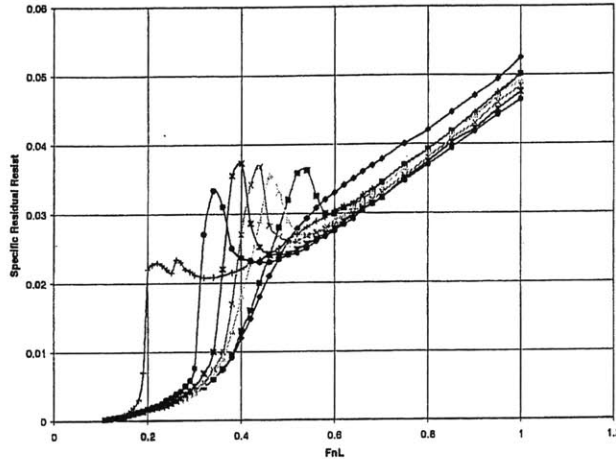


Fig. 3.3-3 Digitized deep water, and increasingly shallow water (draft/ L_{WL} from 0.333 to 0.05), residuary resistance data, from the transom stern destroyer model of Graff, et al, 1964.

The raw model test data was then re-plotted as a percent increase of residuary resistance over deep water values, against the depth-based Froude number, F_{h1} , as shown in Figure 3.3-4.

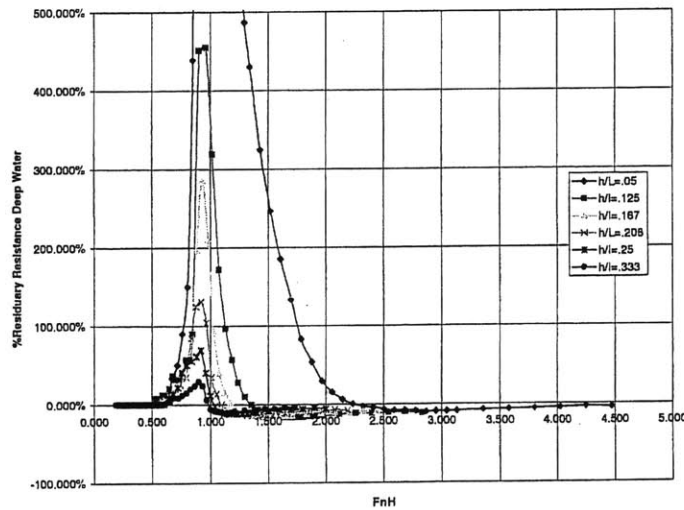


Fig. 3.3-4 Shallow water resistance data converted to a depth-based Froude number presentation, from the transom stern destroyer model of Graff, et al, 1964.

Values of the percentage increase in residuary resistance were then interpolated for both the cruiser stern and transom stern model data, at any particular speed and water depth of interest.

A linear interpolation was made between the data from the two types of models based upon the transom DWL beam. The transom beam at DWL was approximately zero for the cruiser stern and 55% of maximum DWL beam for the transom stern model. It was found that the differences between percentage increase in residuary resistance for the two different stern types tested was about 10% or less in most cases, so that a linear interpolation appeared to be a reasonable simplification. The transom stern model generally had a larger increase in resistance due to shallow water, probably because the resistance benefits of the transom stern are derived from dynamic effects (such as lift) that are affected by shallow water effects (such as the Bernoulli effect).

Note that the proportions of the transom-stern model tested, and the worm curve factor comparison to the equivalent Taylor Standard Series model, are quite similar to standard destroyer designs of interest for naval design investigations. The worm curve factor for the hull is shown below in Figure 3.3-5.

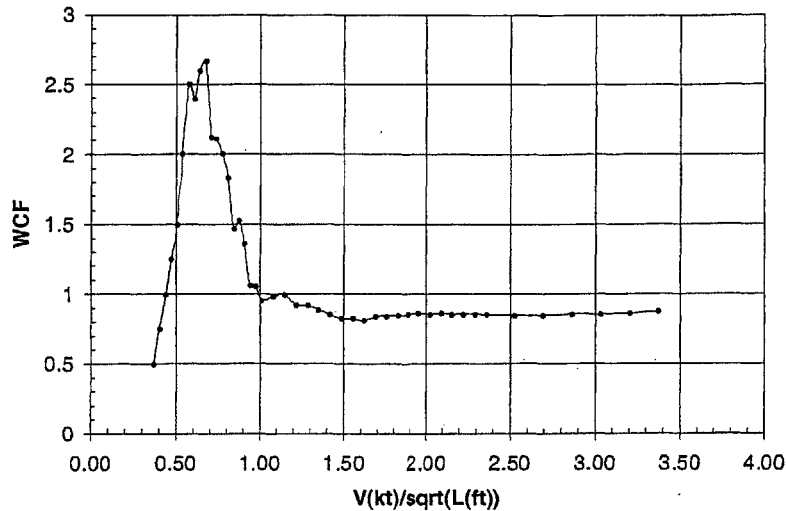


Fig. 3.3-5 Worm curve factor comparison to the Taylor Standard Series, from the transom-stern destroyer model of Graff, et al, 1964.

For the purposes of setting a lower bound on the interpolation routine, limits were added to the raw data. For speed limits, a F_h of 0.10 was set as the lower limit, and a F_h of 6.0 was set as the upper limit, at which point the effect of shallow water on residuary resistance was set to zero. Additionally, the program itself was set to assume that shallow effects are negligible for F_h of less than 0.30. This was confirmed by the model test data. This approach is also supported by the work of Schlichting, who reasoned that since wave speed and length is little affected compared to deep water values by F_h values of 0.40 or less, the effect of shallow water is unimportant below that F_h value (Lewis, 1988, Vol. II). For depth limits, the shallowest depth data available is for a draft-to-length ratio of 0.05, and the program added false data to zero the influence of shallow water upon resistance at a draft-to-length ratio of two or greater.

No corrections were made to this method to account for changes in volumetric coefficient or other changes in hull proportions other than transom stern beam. In fact, the shallow water resistance impact of changes in hull proportions seems to be an area of research that has received comparatively little attention. No model test investigations were found that would provide

reliable guidance in how shallow water wavemaking resistance changes in response to hull form proportions. What little comparative model test data exists is difficult to compare.

Hofman and Kozarski, 2000, suggest that thin-ship theory investigations show little change in the percentage increase in wavemaking resistance in shallow water from changes in hull form proportions. However they do not provide limits on the dimensions investigated. Comments in Graff, et al, 1964 p.398 suggest that at very large B/T ratios there is an increasingly strong effect of B/T on resistance that is nonlinear. It appears justifiable to ignore this effect at normal B/T ratios and water depths of interest for ships, however, since even at a depth-to-length ratio of 0.04 the B/T effect is modest for ships of normal proportions. Tuck, 1966, has provides a useful first-order shallow water theory that predicts sinkage and trim effects quite well considering the simplicity of the method. By using Tuck's expression for resistance at supercritical speeds one can deduce that the percentage change in wavemaking resistance is proportional to the inverse of vessel length scaling, so that finer vessels will experience less shallow water effect than fatter vessels. However Tuck's theory predicts zero resistance at subcritical speeds, so it is difficult to know how to confidently apply his resistance approach to actual problems.

This lack of information on the effects of hull proportions also makes it difficult to set a criterion for the water depth at which shallow water effects become significant. Many criteria, such as given in Carlton, 1994, or Taylor, 1943, rely upon one ratio, such as draft-to-depth or length-to-depth, that are not valid over wide ranges of ship proportions. In fact it appears that for fine vessels in relatively deep water the length-to-depth ratio dominates because wavemaking concerns dominate, but that at some critical point blockage begins to dominate. This would

explain the great variety of relationships used to relate resistance changes to water depth (some including waterplane coefficient).

Overall, shallow water effects can be present even at depth-to-length ratios of greater than two (Havelock, 1922), and at depth-to-draft ratios of greater than 16 (Lewis, 1988 Vol. II). Also it should be added that channel walls that are 40 times as wide as ship beam can have appreciable effects upon wavemaking resistance at speeds anywhere in the neighborhood of critical shallow water speed ($F_h = 1$) (Kirsch, 1966). The implication is that model test investigations that are performed within tanks of normal proportions tend, for many reasons, to exaggerate the effects of shallow water upon resistance (Lewis, 1988 Vol. II).

The best that can be done, as in the current empirical shallow water resistance estimation method used here, is to set approximate limits at which shallow water effects are no longer present. Thankfully the resistance effects of shallow water are modest until relatively shallow water depths are approached, at which point reliable model test data is available. Therefore the error in resistance estimates made by setting arbitrary limits on shallow water resistance effects will be small.

METHODS USED: THEORETICAL

The theoretical method used here to calculate the shallow water increased wavemaking resistance was thin-ship theory as given in Kirsch, 1966. Wavemaking resistance was calculated for both the deep water case (using the basic thin-ship theory approach) and for the shallow water case (using the Sretenski integral extension of thin-ship theory to shallow water). A ratio between shallow water and deep water wavemaking resistance was then determined, and this ratio was applied to the *entire* residuary resistance of the ship being evaluated. The use of a ratio

avoids using absolute resistance magnitudes from thin-ship theory, which are far too inaccurate for most engineering applications. A ratio can reflect the trends in wavemaking resistance which, broadly speaking, are well represented by thin-ship theory. Note, however, that there is some error inherent in this method because the *wavemaking* resistance ratio is being applied to the *residuary* resistance ratio determined by other means.

Details of the theoretical method will be discussed below because of the numerous errors or omissions found in the literature regarding the mechanics of calculating an actual ship resistance. Correlation was made with the published results, as described in the appendices.

All of the following expressions only need to be evaluated over one half (port or starboard) of a vessel to determine the total wavemaking resistance, since the equations used account for this by doubling the final results.

In deep water the thin-ship resistance is given by the integral derived by Michell, 1898:

$$R_{W\infty} = \frac{4\rho g^2}{\pi v^2} \int_1^{\infty} (I_{\infty}^2 + J_{\infty}^2) \frac{\gamma^2 d\gamma}{\sqrt{\gamma^2 - 1}}$$

where $R_{W\text{deep}}$ is the deep water wavemaking resistance, v is the speed, γ , is the integration variable, and J and I are integrals over the surface of the ship which account for the symmetric and asymmetric portions. For ships with fore-aft symmetry, the expression I is equal to zero when the usual coordinate system is used: origin at midships, x positive forward and z positive down, y representing the half-breadths. The expressions I_{∞} and J_{∞} for the deep water case are:

$$I_{\infty}(\gamma) = \int_{-LWL/2}^{+LWL/2} \int_0^T \frac{dy}{dx} e^{\frac{-\gamma^2 gz}{v^2}} \cos\left(\frac{gx}{v^2} \gamma\right) dz dx$$

$$J_{\infty}(\gamma) = \int_{-LWL/2}^{+LWL/2} \int_0^T \frac{dy}{dx} e^{\frac{-\gamma^2 gz}{v^2}} \sin\left(\frac{gx}{v^2} \gamma\right) dz dx$$

where dy/dx represents the slope of the half-breadths with respect to the length fore-aft. The total solution for the deep water case requires many calculations to evaluate the above triple-integral expression over many values of the integration variable.

For the shallow water case, the lower value of the integration variable must be determined for the specific case being evaluated. This value, γ_0 , is equal to zero if the depth-Froude number, F_h , is supercritical (greater than one). If the speed is critical, $F_h = 1$, then the following expressions are not valid and there is a singularity to be avoided (the hull assessment program assumes that $F_h = 0.999$ in this case). If F_h is subcritical (less than one), the value of γ_0 is the solution of the equation:

$$\frac{\tanh(\gamma_0 H)}{\gamma_0 H} = \frac{v^2}{gH} = F_h^2$$

In shallow water the wavemaking resistance, R_h , according to the Sretenski integral is:

$$R_h = \frac{2\rho g}{\pi h} \int_{\gamma_0}^{\infty} \frac{(I_h^2 + J_h^2)}{\sqrt{\gamma - \frac{g\gamma}{v^2} \tanh(\gamma H)}} \frac{\gamma d\gamma}{\cosh^2(\gamma H)}$$

where H is the water depth. The expressions I_h and J_h for the shallow water case are:

$$I_h(\gamma) = \int_{-LWL/2}^{+LWL/2} \int_0^T \frac{dy}{dx} \frac{v}{2\pi} \cosh[\gamma(H-z)] \cos\left[x \sqrt{\frac{g\gamma}{v^2} \tanh(\gamma H)}\right] dz dx$$

$$J_h(\gamma) = \int_{-LWL/2}^{+LWL/2} \int_0^T \frac{dy}{dx} \frac{v}{2\pi} \cosh[\gamma(H-z)] \sin\left[x \sqrt{\frac{g\gamma}{v^2} \tanh(\gamma H)}\right] dz dx$$

Some of the integral expressions involved are infinite. In reality only a finite upper value of the integration variable can be evaluated, so the upper limit was determined by automatically

running a convergence check on each speed and depth condition calculated. Numerical integration was performed in 0.01 increments for the integration variable gamma, γ , and for the convergence study the number of gamma terms evaluated was increased by 100 for each test until convergence within 2% of the preceding value was achieved. A convergence limit of 2% was selected because investigations showed that convergence was quite rapid after this point. In any case, the goal was to find the ratio of shallow to deep water resistance, not the absolute values. Also it was important to terminate the convergence test for each case quickly. This was important not only to save time but also to avoid divergence, which could occur in some extreme cases where the convergence study was run to large gamma values. At that point the ratios of very small values contained within the expressions would approach the computer's numeric tolerance limits, and resistance values could begin to (incorrectly) grow.

3.4 Air Resistance

There is a great deal of data available on the air and wind resistance (and center of pressure) of specific ship types. Some notable references include a U.S. Navy Memorandum, Apr. 23, 1984, that concludes that the best estimates are made when a drag coefficient of 0.91 is used for the superstructure in head winds, and 0.36 is used for the hull in head winds, all based on a variety of U.S. Navy ships. This data is only applicable to head wind conditions, but it is reasonably accurate. This data is also more useful for accurate air drag and head wind resistance estimates than the other references listed below, because it very rationally uses separate drag coefficients for the hull and superstructure. Several of the references mentioned below can provide good estimates for side force and yaw moments, which the Navy method does not determine. The Navy air resistance method for determining still air drag coefficient, C_{AA} , as well as head wind resistance, is used.

Currently a fixed superstructure area is entered into the input file, as well as a fixed ratio of hull freeboard versus draft. The areas used in the calculation can easily be changed to other parametric or fixed values if desired by future users, with minor modifications to the program.

Isherwood, 1972 has a good regression equation method for commercial ships for forces and moments. Saunders, 1957, and of course Principles of Naval Architecture, 1989 also contain a good mix of data on forces and moments. Schneekluth and Bertram, 1998 also have quoted a variety of data for modern ship forms (p.202).

3.5 Steering Resistance

Basic steering resistance of large ships in calm water is given by Harvald, 1991 as being:

$$C_{AS} = 0.04 \times 10^{-3}$$

This quantity is often ignored, and varies greatly depending upon directional stability, as well as wind forces and moments resulting from superstructure arrangement. This value is used as a basic estimate in the program, for calm-water steering resistance.

The increase of steering resistance of a ship in head seas and winds based upon at-sea observations is presented on p.244 of Korvin-Kroukovsky, 1961. The data are for a low-powered ship, and probably provide a conservative estimate of steering resistance. The resistance is related to wind speed, and is used in this program to increase the calm water hydrodynamic hull resistance in proportion to the steering resistance given in this example. The estimate for steering resistance is therefore approximate, being based upon a single observation. It is felt that separating this poorly known quantity from the somewhat more directly predictable added resistance of a hull in waves is important. Regressions for added resistance in waves may or may not take steering resistance into account, and it is therefore better to calculate steering and added resistance separately as accurately as possible instead of guessing what is included in a regression equation method.

3.6 Directional Stability, Maneuvering and Appendage Resistance

DIRECTIONAL STABILITY

The directional stability of the hulls generated in the hull assessment program can be evaluated if selected as an option by the user. Using basic hull section, rudder and skeg geometry, the directional stability of the parent hull form was estimated using the method of Jacobs, 1966. For later hulls that were stretched versions of the parent hull, the rudder area could be automatically adjusted, if desired, to achieve the same directional stability as the parent hull. In this way the resistance effects of fixed rudder area or alternately of fixed directional stability could be compared.

Comparison of Jacobs, 1966 to Lewis, 1988 and Prohaska, 1947 reveals that the Jacobs paper has an error in Figure 3. The x-axis label of that figure needs to be changed to read “4 times draft over beam”, not “beam over draft” as printed. When this change is made the results calculated for correlation and validation of this program agree well with the published results, as shown in the appendices.

The Jacobs, 1966 method is valid at speeds where wavemaking effects are not dominant. For more detailed information see the appendices.

MANEUVERING

Time did not allow the inclusion of tactical diameter estimation methods in the current program. Inclusion of tactical diameter estimation methods would be a straightforward affair. For estimation methods see Lewis, 1988 or Harper and Scher, 2001.

APPENDAGE RESISTANCE

Appendage resistance is determined, if desired, for the rudder using the methods given in Lewis, 1988 for both direct rudder drag and for interference drag. Reynolds-number and thickness-dependent drag coefficients as reported by Kirkman and Kloetzli, 1980 were used. A blanket allocation of additional appendage resistance can be selected by the user, in the input profile file. This percentage allocation will be used to increase the bare hull frictional and residuary resistance to account for other appendages, such as bilge keels or skegs, that are not evaluated in detail in the current program.

3.7 Seakeeping

3.7.1 Seakeeping Motions

PROGRAM FLOW

Seakeeping calculations within the main program, hap.m, are handled by the overall seakeeping program seas.m. At the beginning of the program the Bales seakeeping Rank-factor is calculated for the hull for comparison purposes, if selected as an option in the input file. Next, an option is included to allow a debugging feature to be used. If this debugging feature is used ($B_{test} = 1$), then variables used in the seakeeping calculations will be those of the example Series 60 hull given in Bhattacharyya, 1978 in english units. If running normally, the program will use normal variables for seakeeping derived from the rest of the program, such as: speed, constants, number of stations to use (hard-coded for a reduced, 21-station system only for seakeeping, to reduce seakeeping calculation time), lcg from amidships (positive fwd.), length, beam, draft, k_{33} , and wave amplitude (set for convenience = 1).

Within the main seakeeping program seas.m, data preparation is performed by the program preseakeeping.m. The range of wave frequencies used for the seakeeping analysis must be hard-coded in this file. Typically designers would be interested in wave frequencies that corresponded to wavelength-to-ship waterline length ratios of from 0.50 to 2 or more. Products of this program include the a_{33} and b_{33} section coefficients for the Bhattacharyya test (and placeholders otherwise until these values are determined in the later program seakeeping4.m when the program is normally run), local section beam, draft, and section area, LCB and LCF, the wave frequencies of interest, waterplane area, displacement, and the DWL offsets (for use in later added resistance ray-theory calculations). The calculations used herein make use of a

coordinate system located at the waterplane, at the LCG, assumed to be synonymous with the LCB. When located ahead of amidships, the location, x_c , of the LCG is considered positive.

The motion solution program `seakeeping4.m` determines the matrix elements and solves the coupled heave-pitch equations of motion for the ship in regular waves.

`Seakeeping4.m` begins by incorporating input speeds, headings, current LWL and constants such as seawater density (ρ) and the acceleration of gravity (g). I_{55} is found from the relationship $I = k^2 m$. Also incorporated into the start of the program is the list of desired wave frequencies (ww), and the size of this column vector, ($lengthww$). Note that `seakeeping5.m` was a test case version of this file that is not used in the final version of the program.

Nested calculation loops through all speeds of interest are made. A separate set of nested loop calculations is made for each discrete heading of interest, to avoid confusion between head seas and other heading cases. Currently only head seas results are calculated. For each speed and heading, calculations are made through a loop of all regular wave frequencies of interest. It is these regular wave results that will be post-processed to determine vessel responses in an irregular seaway.

Many calculations are performed for each specific wave frequency. A specific encounter frequency must be calculated:

$$\omega_e = \omega_w - (\omega_w^2 / g) U \cos(\beta)$$

where:

ω_e = encounter frequency

ω_w = wave frequency (actual frequency of wave)

g = acceleration of gravity

U = vessel velocity

β = heading angle of ship with respect to waves (180° = head seas, heading directly into incoming waves.)

It is important to remember that various calculations will require use of terms involving exponentials of kz , etc., and that the wave number, k , used should derive from the original ambient wave frequency, not the frequency of encounter (Sclavounos, 2002) (For non-head seas case, refer to p. 88,89 of Lewis, 1989 Vol. III for frequency and spectrum transformations at various headings.)

The first set of significant calculations are made to determine the added mass and damping coefficients for the vessel. This calculation is broken into discrete parts. First the program sectioncalc.m is called to determine the coefficients a_{33} and b_{33} for the stations along the hull. These coefficients are found using Lewis-form data tabulated in Bhattacharyya, 1978, and Grim, 1960. In the future it would be desirable to incorporate a Rankine panel method calculation for actual hull sections (such a method does not suffer from irregular, or natural, frequency problems as some other methods do.) These are the only added mass and damping coefficients that need to be directly determined for the head seas case; all other coefficients need for head seas calculations can be derived from the sectional a_{33} and b_{33} terms. These derivative calculations are performed in the program addedmass.m.

The program addedmass.m calculates the coefficients for the following two degree of freedom system of equations presented in matrix form, which itself is a reduced form of the six degree of freedom system that can be solved in future upgrades of this program (from Lewis, 1988 Vol. II p. 47, and Salvesen, et al, 1970 among others):

$$|m_{33} = \Delta \quad -\Delta x_c \parallel \eta_3'' \quad | + | A_{33} \quad A_{35} \parallel \eta_3'' \quad | + | B_{33} \quad B_{35} \parallel \eta_3' \quad | + | C_{33} \quad C_{35} \parallel \eta_3 \quad | = \zeta |F_{I3} + F_{D3}| e^{i\omega t}$$

$$| -\Delta x_c \quad I_{55} \parallel \eta_5'' \quad | \quad | A_{53} \quad A_{55} \parallel \eta_5'' \quad | \quad | B_{53} \quad B_{55} \parallel \eta_5' \quad | \quad | C_{53} \quad C_{55} \parallel \eta_5 \quad | \quad | F_{I5} + F_{D5} \quad | \quad .$$

where F_I represents the incident and F_D the diffracted forces and moments on the ship.

The added mass, damping, and restoring coefficients, and the exciting force and moment, are determined according to the approach presented in Bhattacharyya, 1978.

There is a degree of judgement involved in the selection of the terms used to calculate the various coefficients. Since linear strip theory consists of a set of simplifications, no one set of equations can truly be called the "correct" method. The equations presented in Lewis, 1988 Vol. III p.44 are established as being reasonably accurate. However, there are damping terms not present in these equations that are used in Bhattacharyya, 1978, and further damping terms in Salvesen, et al 1970 (with corrections to typographical errors given on pages 284 and 287) that have been used with some success. Also there are stern-dependent terms added in Salvesen, et al 1970 for purely empirical reasons that have generally been removed since that time. Lloyd, 1998 also has differences with the other references in the equations he presents.

Interestingly, the correlation and validation analyses presented in the appendices shown that using the Bhattacharyya, 1978 method, the added resistance results were quite reasonable considering all of the simplifications made here. The Bhattacharyya, 1978 approach uses older forms of the strip theory exciting force and moment expressions that include the rate of change of added mass along the body length (Newman, 1977). These terms were derived from slender-body theory, and are also present in Lloyd, 1998. Perhaps the redeeming feature of these approaches is that they are less sensitive to the use of approximate sectional added mass and damping values as used in this study. The use of Lewis, 1988 exciting force and moment equations resulted in less satisfactory agreement, as shown in the appendices.

The inertia matrix elements must be determined in forceandmoment.m, as well as the exciting forces and moments. Exciting forces and moments can be calculated according to a procedure like that shown on p.196 of Bhattacharyya, 1978. (In the 6 D.O.F. case an effective wavelength is used in place of the wavelength for heave and pitch exciting forces and moments: $\lambda' = \lambda/\cos(\beta)$. See p. 191 of Bhattacharyya, 1978.)

The magnitude of the exciting forces and moments is the square root of the sum of the real and imaginary components each squared, such as for heave:

$$|F_{EX3}| = \sqrt{(F_{EX3I}^2 + F_{EX3R}^2)}$$

The phase angle is the inverse tangent of the imaginary divided by the real component, placed in the appropriate quadrant, (such as for phase angle of heave exciting force, σ_3):

$$\sigma_3 = \tan^{-1} (F_{EX3I} / F_{EX3R})$$

In this case a negative imaginary component means that the phase angle is negative (lagging), and a positive imaginary component means that the phase angle is positive (leading).

Bhattacharyya has a definition of the real (F1) and imaginary (F2) force components that appear may be switched, because of switched phase angle conventions using a sine wave instead of a cosine wave excitation as is done in many papers.

The equations of motions are solved using the programs motion.m to solve using the Bhattacharyya, 1978 approach, and matrixmotion.m to solve using standard matrix-inversion techniques (as a check on the accuracy of the calculations. The matrix solution method is used for the final results).

Solution of the coupled equations of motion in the head seas case can be approached using an impedance matrix ($[Z(i\omega)]$) like those used for general vibration analysis (Rao, 1995).

This matrix is assembled with elements:

$$Z_{ij}(i\omega) = -\omega^2 m_{ij} + i\omega b_{ij} + c_{ij}$$

yielding the traditional head seas coupled heave and pitch solution in Lewis, 1989 and in Bhattacharyya, 1978, with elements:

$$P = -\omega_e^2 (\Delta + A_{33}) + i\omega_e B_{33} + C_{33}$$

$$Q = -\omega_e^2 (A_{35}) + i\omega_e B_{35} + C_{35}$$

$$R = -\omega_e^2 (A_{53}) + i\omega_e B_{53} + C_{53}$$

$$S = -\omega_e^2 (I_{55} + A_{33}) + i\omega_e B_{55} + C_{55}$$

and complex response amplitude in heave, (index $j = 3$) and pitch (index $j = 5$):

$$\bar{\eta}_3 = \frac{F_{EX3}S - F_{EX5}Q}{PS - QR}$$

$$\bar{\eta}_5 = \frac{F_{EX5}P - F_{EX3}R}{PS - QR}$$

Another equivalent method for solving the equations of motion, useful for systems with more degrees of freedom, is the more general matrix solution:

$$X = \{ -(M + A) \omega_e^2 + i\omega_e B + C \}^{-1} F$$

In this expression, only real terms of each matrix are used in the evaluation, except for the force matrix which contains phase information in the complex numbers.

Importantly, the non-diagonal elements of the inertia matrix M are non-zero if the LCG is not located on the coordinate origin.

BALES R-FACTOR

The seakeeping rank factor concept suggested by Bales, 1980 and extended by Walden, 1983, can be used to evaluate the seakeeping performance of a hull in the current program if

selected in the input profile file. The seakeeping rank factor represents an approximate estimate of the seakeeping performance of a monohull ship based upon several critical hull characteristics. A higher rank factor equates to better seakeeping motions performance. The original Bales investigation was extended by Walden, 1983, to include the effects of displacement over the range from 3000 – 9000 long tons (it turns out that the effect is nearly linear over this range). While approximate, the rank factor concept can be a fast, useful tool for gross hull form seakeeping optimization. The estimated rank factor is given by:

$$R = 8.422 + 45.104 C_{WPF} + 10.078 C_{WPA} - 378.465 T/L_{WL} + 1.273 c/L_{WL} - 23.501 C_{VPF} - 15.875 C_{VPA} + 12.9 (\Delta(LT) - 4300)/4300$$

where c/L_{WL} represents the distance from the forward perpendicular to the point where the keel begins to rise appreciably above the baseline, divided by the waterline length.

Optimization of the rank factor is not as straightforward as for resistance or power, since the goal is to maximize the rank factor, which itself can be negative at times. When optimizing any given factor, the approach taken was to non-dimensionalize the value for the current hull by the value for the first hull evaluated. This was changed slightly for the rank factor concept. The absolute value of the rank factor for the first hull evaluated was multiplied by two, and added to all the rank factor values used in the evaluation process. In this way, the rank factors were simply shifted as a group towards larger positive values, and the rank factors were sure to be positive at all times. Then the inverse of the non-dimensionalized rank-factor ratio was taken as the factor to be minimized (thus maximizing the rank factor).

3.7.2 Added Resistance in Waves

GENERAL

The added resistance that a ship encounters in waves is difficult to predict for a specific hull form with anything approaching the accuracy of calm water resistance prediction methodologies. Regression equations or theoretical methods may be used to make predictions of added resistance in a given sea state.

Regression equations exist to predict added resistance in waves, based upon full-scale ship data and, more typically, based upon model tests or theoretical investigations. These regression were usually developed several decades ago when ships were operating at slower Froude numbers than many ship operate at today, and the hull forms investigated were of older styles (cruiser-sterns). Typical is the data on the added resistance of a large set of typical commercial vessels that cover a wide set of principal characteristics is provided by Moor and Murdey, 1970, also given in Bhattacharyya, 1978. Therefore the applicability of the existing regression equations is limited.

Some of the more useful data includes that given in Carlton, 1994, which has some regression and experiential graphs on trial allowances in rough weather starting on p.292. Leibman, et al, 1990 has a limited regression equation for corvette-sized vessels operating at speed-length ratios of 0.8-1.2. This regression is based on a detailed theoretical calculation of added resistance for a parametrically-varied set of hull forms. Added resistance data on some destroyer hull forms, among many, is given in SNAJ, 1963, Vol. 8, p.112 onwards, and in Strom-Tejsen, et al, 1973. Sclavounos and Nakos, 1993, performed an investigation of the added resistance of canoe-body yacht hull forms that were parametrically varied. This provides valuable insight into the causes of added resistance – the leading contributor seeming to be large

longitudinal gyradii, and on LCF placement. Heading sensitivity is also briefly reviewed in a graph for one speed. Data on a slender, destroyer-like hull, and some unusual and doubtfully reliable methods to extrapolate this to other proportions, are provided by Pershin and Voznessensky, 1957.

Overall, the information available from some regression method papers does provide the ability to make a quick order-of-magnitude check, such as the Series 60 seakeeping series investigation information provided in Loukakis and Chryssostomidis, 1975. A reference that is reported to correct this series with empirical corrections is Shintani and Inoue, 1984, although this reference could not be located in time for the completion of this study.

Over certain speed regimes, such as below that of synchronous pitching (short wavelength versus ship waterline length), there are added resistance formulas based upon a combination of experience and theory that can be used (see p. 239-240 of Korvin-Kroukovzky and p.145 of Faltinsen, 1990). In the region of large motions and synchronous pitching, when wavelength approaches ship length, the added resistance becomes quite sensitive to specific hull form and mass distribution characteristics, and can vary by 100% because of changes in one of the characteristics. Luckily for design purposes, motions around the synchronous pitching region generally prohibit ships from operating for any length of time in such conditions. Therefore it may be possible to use existing added resistance data or theories for hull design purposes, since the ship will probably not be expected to operate in significant seas around the difficult-to-predict wavelength/shiplength ratio of one.

Common theoretical methods (2-D strip theory) do not provide reliable prediction of added resistance around the synchronous pitching region, and can have errors of 10's% from experimental results. However these methods are the most accurate theoretical added resistance

methods available at this time that can be calculated relatively quickly. While not yet available to many students and requiring significant resources, newer and computationally intensive calculations using three-dimensional panel methods to solve the unsteady potential flow problem have better accuracy.

LIMITING MOTIONS

It must be emphasized that the added resistance of a vessel is one of two major factors that limit its speed in a seaway. The second factor that limits ship speed is the voluntary speed reductions made to avoid excessive motions. Speed reductions are also made to avoid undesirable hull stresses, wetness and slamming. Coverage of these topics is given in Lewis, Vol. III, 1989, and in Korvin-Kroukovzky, 1961, and Saunders, 1957, among others. Speed reductions are not calculated in the current program. The approach taken to account for speed reductions was to evaluate a hull form only at moderate sea states and below where speed reductions would not be expected to have much effect on ship operability. Future upgrades to this program can take seakeeping motion limits into account.

THEORETICAL METHODS

Some detailed overviews of theory by Maruo is given in SNAJ, 1963. Strom-Tejsen, et al, 1973 covers theory in this area. Beck, 1967 also has good coverage of theoretical considerations and lists a basic computer program for added resistance calculation. A very good overall modern reference on seakeeping is provided by Lloyd, 1998, and Lewis, 1988. Salvesen, 1978 provides the best strip-theory method to calculating added resistance in long-wavelength conditions.

EFFECT OF HEADING UPON ADDED RESISTANCE

A simplified formula to approximate the speed loss in waves for tankers or containerships is given on p. 203-204 of Schneekluth and Bertram, 1998. The valuable contribution of this method is that it provides an estimation technique for the added resistance at different headings. Such data is rarely available from tank tests. Another estimate of the effect of heading on speed loss is provided by a figure on p.238 of Bhattacharyya, 1978. Sclavounos and Nakos, 1993, provide a graph at one speed for the effect of heading on added resistance.

MISCELLANEOUS RESISTANCE IN WAVES: STEERING, ROLLING

A good investigation into the large increase in resistance due to rolling and bilge keel vortex-shedding is presented in Bridges, et al, 1964. SNAJ, 1963 p.161 also has some information on added resistance due to model ship rolling, but the low resistance reported is possibly a result of a bare hull without bilge keels. Also unexplained is why wavemaking resistance can be reduced by either a fixed angle of heel or by rolling, at F_n 's of .22-.28. The increase of steering resistance of a ship in seas based upon at-sea observations is presented on p.244 of Korvin-Kroukovsky, 1961.

CALCULATION FLOW

Added resistance is determined within the seas.m program, under the seakeeping.m subprogram, in addedresist.m. The calculation of added resistance in waves is divided for convenience into two wavelength regimes: the regime of short wavelengths that do not cause

significant vessel motions; and the regime of long wavelengths that cause large or synchronous ship motions.

When the wavelength-to-waterline length ratio is less than about 0.5, we can assume that vessel motions are small. Under such conditions incident and diffracted wave forces dominate and radiated wave effects can be ignored, as they represent a small portion of the total added resistance (Korvin-Kroukovzky, 1961, and Faltinsen, 1990). Below a wavelength-to-ship beam ratio of about 0.5, some useful added resistance theories are at the limit of the assumptions used to derive them, and thus should probably not be used for shorter wavelengths (Salvesen, 1978). We therefore have an intermediate region of from three quarters wavelength-to-waterline length ratio, down to one half wavelength-to-waterline length ratio, over which we should blend the added resistance calculation between the two methods used for long wavelength and short wavelength added resistance. A suitable blending function is given by Hughes and Caldwell, 1991:

$$A \tanh^2(8 r^3) + B \operatorname{sech}^2(8 r^3)$$

where:

A = the function that is increasing in weighting at higher values of wavelength-to-waterline length ratio, λ/L_{WL} ,

B = the function that is decreasing in weighting at higher values of wavelength-to-waterline length ratio, λ/L_{WL} ,

r = a value from 0 to 1 which describes where on the spectrum of blending between the two functions the value is to be evaluated at.

Calculations for the long wavelength condition follow the methods of Salvesen, 1978. This method has been found to give the most realistic head seas added resistance results for a

wide variety of hull types and speeds (Salvesen, 1978, Lewis, 1988). Correlation and validation analyses provided in the Appendices bear this out, where even using approximations for sectional added mass and damping characteristics, the calculated added resistances compared well with published results. The mean added resistance is given in terms of the quantities \hat{F}_3 , \hat{F}_5 , and R_7 , taken as the real part of:

$$\langle \delta R \rangle = \frac{i}{2} k (\bar{\eta}_3 \hat{F}_3 + \bar{\eta}_5 \hat{F}_5) + R_7$$

$$\hat{F}_3 = \bar{\zeta} \int_{LWL} e^{-ikx} e^{-kds} \{ \rho g b - \omega_w (\omega_e a_{33} - i b_{33}) \} dx$$

$$\hat{F}_5 = -\bar{\zeta} \int_{LWL} e^{-ikx} e^{-kds} \left\{ \rho g b - \omega_w \left(x + \frac{iU}{\omega_e} \right) (\omega_e a_{33} - i b_{33}) \right\} dx$$

$$R_7 = \frac{1}{2} \bar{\zeta}^2 k \frac{\omega_w^2}{\omega_e} \int_{LWL} e^{-2kds} b_{33} dx$$

Where:

$\langle \delta R \rangle$ = mean added resistance at a given ship speed, wave frequency, and ship heading,

\hat{F}_3 = a combination of the conjugate of the Froude-Krylov (incident) exciting force, and a term which is closely related to the diffraction force,

\hat{F}_5 = a combination of the conjugate of the Froude-Krylov (incident) exciting moment, and a term which is closely related to the diffraction moment,

R_7 = a term related to the diffraction potential,

k = wavenumber = ω_w^2 / g ,

g = acceleration of gravity,

ω_w = wave frequency,

ω_e = encounter frequency

x = station distance from coordinate origin for seakeeping calculations, usually taken as the midships position at the design waterline (D_{WL}),

U = ship velocity,

d = draft of the station being evaluated,

s = local sectional area coefficient of the station being evaluated, = area / (local beam times local draft),

b = local beam at the station,

ζ = incident wave amplitude, (normally the bar denotes complex, but in this case we will use the real amplitude for calculation.),

a_{33} = local station 2-D sectional added mass,

b_{33} = local station sectional damping,

$\bar{\eta}_3$ = complex response amplitude of heave (a complex response),

$\bar{\eta}_5$ = complex response amplitude of pitch (a complex response).

It should be noted that Bhattacharyya, 1978 uses a seaway based upon a sine form, while Lewis, 1988 appears to use a seaway based on a cosine form. The phase angles should therefore be expected to differ by 90-degrees, and so when using the added resistance formulation of Salvesen, 1978 in combination with motions calculated using the Bhattacharyya, 1978 method, the imaginary part was used.

Calculations for the short wavelength follow the methods of (Korvin-Kroukovzky, 1961 p.238) and (Faltinsen, 1990 p.145), sometimes known as “ray-theory”. In general the results for

Faltinsen were found to be more realistic, and therefore the added resistance in this case was found using:

$$\langle \delta R \rangle = \zeta^2 \frac{1}{2} \rho g \left(1 + \frac{2\omega_w U}{g} \right) \int_{LWL} \sin^2(\theta + |\beta - 180^\circ|) \sin \theta dx$$

Where:

β = wave heading, 180° being head seas. For this case only the “non-shadow” portion of the design waterline seen by the incoming waves is integrated. The first \sin^2 term represents the pressure of the incident/diffracted wave action on the hull surface. The last sine term represents the normal of the local surface area relative to the ship axis, which is the direction we wish to calculate forces in. The assumptions for this equation break down at higher speeds, at a Froude number above about 0.20. However no other method is readily available to replace this theory, other than resorting to regression equations of uncertain reliability. Therefore the “ray-theory” was still used at higher speeds in the current program.

The total estimated added resistance is found by blending the two contributors to added resistance, as mentioned above.

The derived added resistance response for an irregular sea is now determined using the subprogram derived.m. This program uses the regular wave response data calculated for each wave frequency and ship speed to evaluate the expected added resistance in an irregular seaway.

• More details are provided in the section on derived responses.

3.7.3 Derived Responses

GENERAL

Mean added resistance and significant heave acceleration amplitude are calculated in the program function `derived.m`, for every combination of head seas case sea state and ship speed. Bretschneider wave spectra are assumed for each case. The individual cases are also summed, weighted by their probability of occurrence as given in the input operating profile file, to produce an overall mean operating profile value of mean added resistance and significant heave acceleration.

ADDED RESISTANCE

The normalized mean value of added resistance, in regular waves of a given encounter frequency, is the value of mean added resistance divided by wave amplitude squared. This relationship holds because added resistance is proportional to wave amplitude squared. The mean added resistance for each long-crested (unidirectional) irregular head seas sea state and speed combination is determined by integrating the normalized mean value of added resistance determined for each individual regular wave encounter frequency, times the encountered variance spectrum of wave elevation at that wave encounter frequency:

$$\langle \delta R_w \rangle = 2 \int \left[\frac{\delta R(\omega_e)}{\bar{\xi}^2} \right] S_{\xi}(\omega_e) d\omega_e$$

HEAVE ACCELERATION

Heave spectral moments m_0 , m_2 , and m_4 are calculated using trapezoidal integration (which Lewis, 1988 describes as sufficiently accurate for these types of calculations). The

response amplitude operator for heave (RAO), given as m of heave per m of wave amplitude, is squared when used in the equations as shown below (Lewis, 1988):

$$m_n = \int \text{RAO}^2 \omega_e^n S_\zeta(\omega_w) d\omega$$

The significant amplitude of heave acceleration is then found to be:

$$H_{1/3} = 2 \sqrt{m_4}$$

3.8 Propulsion and Power

Brake power estimates are necessary to determine the relative propulsion plant weight differences between hull form alternatives, and to provide information on relative fuel consumption. Therefore some form of propulsive coefficient estimation routine is required to translate the bare or appended hull resistance, with its effective power, $P_E = V R$, to brake power, P_B .

Only very crude approximations are made for the propulsive coefficients for the method used here, using regression equations for the hull coefficients and actuator disk efficiency (with realistic adjustment) for the propellers. This very simplified treatment was selected because: a) even a crude estimate of the relative effect of hull form on propulsive efficiency provides second order effects that are generally ignored in classical literature on hull form optimization; b) the detailed determination of propulsive coefficients is not feasible without very involved calculations or test results; and c) a full propeller optimization and matching routine is itself a subject worthy of much study, and could be coupled with current work at some future time. Also, propulsive coefficients were determined for at a single average resistance for each speed, based on the operating time profiles. Ideally a very detailed calculation would be made to include every conceivable combination of loading conditions, and changes in propulsive coefficients with overloading, to be evaluated in tandem with a propeller design and engine-matching routine. The lack of information available for our method does not warrant such an approach.

The wake fraction, w , thrust-deduction fraction, t , and relative rotative efficiency, η_r , are determined using the results of Holtrop, 1982 and 1984, reported in Lewis, 1988, Vol. II, where

D is the propeller diameter, P is the pitch, B is the beam, T is the draft, and %LCB is the percent of L_{WL} of the LCB from amidships:

single screw, transom-stern or open sterns:

$$w = 0.3 C_B + 10 C_V C_B - 0.1$$

$$t = 0.10$$

$$\eta_r = 0.98$$

twin-screw:

$$w = 0.3095 C_B + 10 C_V C_B - 0.23 D/\sqrt{(B T)}$$

$$t = 0.325 C_B - 0.1885 D/\sqrt{(B T)}$$

$$\eta_r = 0.9737 + 0.111 (C_P - 0.0225 \%LCB) - 0.06325 P/D$$

Open-water propeller efficiency, η_o , is taken as the efficiency of an ideal actuator disk, η_i , multiplied by the real efficiency expected, η_{real} , assumed to be 80%. Momentum losses are accounted for using actuator disk theory, and rotational and frictional losses usually amount to about 20% more (Harvald, 1991)(Saunders, 1957). Rotational losses can also be determined directly with the aid of figures presented in Saunders, 1957 Vol. II.

Total propulsive efficiency, η_{total} , is given by the following relationships:

$$\eta_{total} = \eta_{hull} \eta_o \eta_r \eta_{shaft} \eta_{gear}$$

$$\text{OR: } \eta_{total} = \eta_{hull} \eta_{behind} \eta_{shaft} \eta_{gear}$$

$$\text{OR: } \frac{EHP}{BHP} = \frac{EHP}{THP} \frac{THP}{DHP} \frac{DHP}{SHP} \frac{SHP}{BHP}$$

where $\eta_{hull} = (1-t) / (1-w)$. Shaft efficiency and gear efficiency were taken as 0.98 and 0.99, respectively.

3.9 Stability, Weights and Costs

STABILITY CALCULATION

Basic hydrostatic calculations are made to determine the metacentric height. The minimum allowable GM/B ratio is set in the input file, as well as the shortest allowable roll period (corresponding to a maximum allowable value of GM). The maximum GM value at the given minimum roll period is derived from the following expression:

$$T_{roll} = \frac{2\pi \cdot k_{roll}}{\sqrt{g \cdot GM}}$$

and k_{roll} , the gyradius or roll, was assumed equal to 38% of beam, per Cimino and Redmond, 1991, yielding $GM_{max} = (2.39 B / T_{roll})^2 / g$.

VERTICAL CENTER OF GRAVITY

The intent of the weight and stability calculations is to provide a first order of magnitude estimate of the impact of changes in hull form characteristics upon weight and stability. The intent was not to provide a detailed weight estimation method, to which an entire thesis could easily be devoted. Therefore relatively simple relational methods are used to estimate the change in the vertical center of gravity (VCG) of newly stretched hull forms compared to the parent hull.

The method used here involves using the original KG/depth ratio (or VCG/depth ratio) of the parent hull, and using this ratio for the new hull with one modification. The modification involves taking the relative difference between steel hull weight KG estimated from Schneekluth and Bertram, 1998, for the parent and new hull. While this is a gross approximation of the shift of the total ship KG, the major influence of hull form on the center of gravity is at least estimated. The relationships used are:

$$KG_{\text{hull}} / D_s = [58.3 - 0.157 (0.824 - C_{BD}) (L/D)^2] 0.01$$

$$\text{Adjust for } L/B \neq 6.5 \text{ by } 0.008 (L/B - 6.5)$$

$$C_{BD} = C_{bDWL} + (1 - C_{bDWL}) (D - T) / 3T$$

where D_s is the hull depth increased to account for the sheer and hatchway volume, which in our case was set equal to the hull depth, C_{BD} is the block coefficient as evaluated at the deck, and a simple expression for this is given by Watson, 1998 without needing to resort to an additional hydrostatic calculation.

Note that the hull depth used throughout the program is based upon the ratio of hull depth to draft entered into the input file. Some optimization investigations have evaluated the effect of varying this parameter, but it was felt that depth is a weaker contributor to optimization of the hull hydrodynamics that were of primary interest here, and thus would not be varied in the optimizations. Depth appears as a second-order contributor to hydrodynamics through weight, stability, and freeboard issues.

WEIGHT RATIOCINATION

Changing the hull form of a ship design will have a major effect on the weight groups: hull weight, propulsion machinery weight, fuel weight, and the like will all be affected. While detailed weight estimation could itself be a topic worthy of major study, a rough weight estimation method is adequate to show the general impact of weight on the optimization problem. Therefore a simple weight ratiocination method was adopted to estimate the effect of hull form changes upon ship displacement and available payload.

Basic weight group information for a parent hull can be entered into the program via the operating profile file. Maximum speed (for estimating propulsion machinery weights) and cruise

speed (for estimating fuel consumption) are also input. Finally, the full load displacement at which this parent hull weight group data was taken is included.

The first hull evaluated as part of the optimization routine is treated as the parent hull for all further designs evaluated for purposes of weight ratiocination and estimation. Ideally, the full load displacement at which the parent hull weight data was given would match the displacement of the first hull evaluated in the input profile file. If this is not exactly true then adjustments are made to ratio the available parent hull weight group data, to values appropriate to the dimensions of the first hull evaluated as part of the optimization routine. These adjustments are based on simplified displacement ratios: hull, electric and auxiliary system, and outfit weight being linearly scaled by displacement (with electric and auxiliary system and outfit weight being scaled by the square root of length as well); fuel, propulsion machinery, and armor weight being scaled by $\Delta^{2/3}$. It is recommended that the proportions and characteristics of the first hull evaluated in the profile file be set as similar as possible to the parent hull, in order that the weight estimates are as accurate as possible. This is because the simplified corrections made to the weight groups of the first hull, as described above, do not take as many factors into account as the detailed weight ratiocination routines used for the optimization routine, described below.

An example reference from which weight group data was taken for the FFG-7 class vessels is given in Garzke and Kerr, 1981.

The procedure for estimating weights of various weight groups, for each hull form evaluated as part of the optimization routine, is loosely based upon procedures given in Manning, 1959 and other references. The change in weight of each group is estimated based upon ratiocination methods, using the first hull evaluated as the baseline from which all weight group changes are made. Necessary weight groups are summed, and the difference between the total

displacement and the summed weights represents the available payload. A negative payload is treated as zero payload for purposes of the optimization calculation. Optimization is made upon a minimization of the ratio of displacement/payload.

Weight groups are scaled for all later hulls from the first hull form evaluated in the following way: Armor weight is assumed to be proportional to displacement to the 2/3 power. Fuel and propulsion machinery weight is assumed to be proportional to the power required at cruise speed. Electric and auxiliary system are assumed to be proportional to the square root of length, since increased length has an effect upon these systems through increased runs of infrastructure and some increased loads (heating, deck equipment, etc.). Outfit weight is assumed to be proportional to the value of the following relationship, from Mandel and Leopold, 1966:

$$\text{outfit weight} \propto 0.15 \left[\frac{(L \cdot B)^{0.986}}{100} \right]^{1.6}$$

The method used to scale the hull weight group is more involved than that used to scale the other weight groups. The greater attention given to accurate estimation of hull weight is due to the fact that hull weight represents a large percentage of total displacement, and has much greater sensitivity to changes in hull proportion than other weight groups.

There is substantial uncertainty in estimating the variation of hull weight with dimensions for a variety of reasons. Global hull girder bending moment requirements differ depending upon the analysis or rules used, and are sensitive to varying degrees to both hull form and length. Also, panel loading dominates the sizing of some hulls, while at larger sizes the global hull girder bending moment loads begin to dominate. Even if bending moment loads are well established, the change in hull weight for most ships falls somewhere between being hull girder-based and volume-based (Watson, 1998). This is because there are major elements of hull

structure that are sized nearly independent of hull girder loads, such as internal bulkheads and decks. It is important not to rely entirely on volume-based hull weight estimation techniques, such as cubic number calculations ($L \times B \times D$), because the results are only reasonable for limited changes in hull proportions (Munro-Smith, 1975). This is apparent when looking at the hull girder bending moment, which is very sensitive to hull proportions and how they are related to one another as each is changed. Depending upon the relationships between length, beam and depth, hull weight can vary almost linearly or highly non-linearly with length. Close examination of texts that cover this topic, such as Manning, 1959, shows that gross simplifications are often used in the example cases presented, in order to avoid these complicating issues.

The current program uses a blend of hull girder-related (section modulus) and hull volume-related (cubic number) terms to define changes in the hull weight group. The user inputs what proportion of changes in hull weight are related to volume changes in the profile file, and the two contributions are determined and summed.

Use of the hull girder-related (section modulus) ratio method assumes that the bending moment induced stress is equal for all hulls evaluated:

$$\sigma_{BM} = \frac{My}{I}$$

It is assumed that the proportions of the parent hull for which hull weight data is provided, and the first hull evaluated are similar, and that therefore the bending moment ratio between the two is only a function of displacement, since M is proportional to ΔL_{WL} per Manning, 1959. For determining the relative change in bending moment, M , between hulls evaluated during the optimization routine and the first hull evaluated, the bending moment is assumed to be proportional to $L_{WL}^2 B C_B$. This is the basic proportionality relationship for wave induced

bending moments per Rawson and Tupper, 1994. Although there are further modifications to the wave induced bending moment used in various Classification Society rules, these details do not materially improve the results of the present study for general ship optimization. To perform a more accurate structural analysis would require more detail than desired for this program, which is intended to have broad applicability and physical rationale, and not become sensitive to discontinuities in existing rules. Steps or kinks in the functions inherent in existing rules could artificially constrain the resulting optimizations.

The ratio between current and prior hull girder bending ratios is known, and now it only remains to determine the section modulus of the midship section, I/y , that is required to produce the same bending moment induced stress as in the first hull evaluated. For present purposes it is assumed that the midship section consists of a thin rectangular beam or tube. Assuming that the beam is $2b$ wide and $2d$ deep, with a uniform internal wall thickness of t , and applying the parallel-axis theorem, we find that the moment of inertia of this section for wave induced bending moment calculations is:

$$I = \frac{4bt^3}{12} + 4btd^2 + \frac{4td^3}{3}$$

and y is $2d/d = d$. Dividing I/y to get the section modulus, we arrive at a section modulus of:

$$Z = \frac{4bt^3}{12d} + 4btd + \frac{4td^2}{3}$$

where the first term's contribution to the answer is usually so small as to be disregarded (as it is in Lewis, 1988 Vol. I.), but it will be retained here. The procedure is to solve for a value of t that will produce the same bending moment induced stress as for the first hull evaluated.

The hull girder-related weight is found by multiplying the ratio of new/old plating thickness by the ratio of new/old plating area. The plating area ratio is taken as the ratio of the

new rectangular box area $2(B + D)L$ times the old area. Use of this box area is a simplification that could be improved upon in future revisions.

The total change in hull weight must use the proportions entered in the input profile file for hull weight changes sensitive to hull girder-related effects and weight changes sensitive to cubic number-related effects.

COSTS

A crude cost model was incorporated in the program used here. Clearly, it would be advantageous for purposes of design to incorporate the most detailed cost model available for specific applications. Such improvements can be made in the future.

The sole purpose of the cost model used here was to demonstrate the influence of life-cycle cost considerations on hull form design. Resistance considerations tend to dictate longer length hulls, for reduced residuary resistance, reduced added resistance in waves, and reduced frontal area for lessened air resistance. Displacement and initial cost considerations tend to dictate shorter hulls because hull weight, which is such a large proportion of lightship weight, is quite sensitive to changes in length. Thus we have some of what Manning, 1959, describes as the "antagonistic" effects of changes in dimensions. Life-cycle cost estimates provide one way to explore the tradeoffs in the compromise space between the conflicting demands of minimum displacement or initial cost, and minimum resistance. Because propulsion machinery is much more expensive per pound than hull structure, and because fuel consumption is a recurring cost over the life of a vessel, cost analyses inevitably strike a balance between a least-initial cost vessel and a lowest-resistance hull form.

The life-cycle cost of hull structure, propulsion machinery, outfit, and fuel was estimated using the expressions given on p.501 and p.502 of Mandel and Leopold, 1966. This method determines the costs per year over the life-cycle of a ship using "cost points" instead of absolute dollars. The one change made to the methods of the cited reference was that fuel cost was computed by assuming that the amount of fuel consumed each year could be taken as: $0.40 \text{ lb/hp hr} \times \text{average power of operating profile} \times 1 \text{ LT}/2240 \text{ lb} \times 2920 \text{ hr/yr}$, which assumes continuous operation for one third of the year.

3.10 Confidence Interval

GENERAL ERROR ESTIMATION

Ninety-five percent confidence intervals were estimated for all of the major resistance components calculated in the hull assessment program. Each +/-value corresponding to a 95% confidence interval for every resistance component was summed to provide a total resistance 95% confidence interval at each speed. This allowed a comparison to be made between the optimization improvement achieved and the estimated confidence interval. If the optimization improvement was large compared with the confidence interval, then the naval architect could have a high level of confidence that the optimum hull form found represented a true improvement. On the other hand, if the optimization improvement were quite small compared with the confidence interval then the merit of the optimization would be questionable. Major assumptions that were made calculating the confidence intervals are described below.

Critical to the implementation of any engineering method is an understanding of its range of validity and its probable accuracy. Most naval architecture papers outline the range of validity of the work presented, but few papers address the absolute accuracy or confidence in the resulting calculations that can be expected from various methods. Statistical analysis is now commonplace in mechanical engineering design, helped by the breadth of the field and the vast amount of data available. In naval architecture, the lack of available data and the poor accuracy of prediction methods have probably contributed to the lack of attention on stating confidence intervals. It may be considered embarrassing to present results to customers that show possible error bands of plus or minus twenty percent, especially if the customer is not educated about the technical uncertainties beforehand!

Estimating the expected error of answers from various prediction methods is very helpful to the design engineer. Error estimates provide guidance on the usefulness of continuing to optimize a design, and guidance on where problems may arise as the design progresses.

The approach taken here is to estimate as well as possible the plus or minus error band for a 95% confidence interval, by assuming that the prediction errors for any form of resistance would follow a normal distribution. The normal distribution is a good estimate of the error distribution likely to be found with naval architecture methods, as evidenced by comparisons shown in Harvald, 1991, between Taylor Series and NSMB method resistance predictions and comparisons with model tests of actual ship forms. In these cases the data roughly follow a normal distribution that is close to being centered about the zero error point.

Some papers and reports provide detailed statistical error information that can be extrapolated to a 95% confidence interval using the normal distribution, such as Fung, 1998. These papers provide either the standard deviation of results, or provide the value of the results at some given confidence interval. Using standard normal distribution tables, one can then determine the equivalent value at a 95% confidence interval. Other papers only provide a few sample errors or worst-case errors noted in comparisons, such as added resistance papers. In such cases where little or no statistical error information is provided, reported worst-case errors are assumed to be equal to the value of the 95% confidence interval.

OVERALL SHIP RESISTANCE CONFIDENCE INTERVAL

The likely error of various ship resistance prediction methods will be determined in the following sections. Before presenting this material it is important to put the magnitudes of the errors in perspective. One way to do this is to compare the errors for each individual calculation

to the errors expected in the “best case” of the field. Data is presented below on the best predictions to be expected for calm water ship resistance, which is a well-developed area that can be expected to represent the “best case” of naval architecture prediction methodologies, methodologies that have had decades of testing and refinement.

Ship resistance in calm water can be estimated closely using models that are approximately 3.6 m long or longer, though at high speeds the viscous effects that create errors extrapolating results from small model tests are insignificant, and Hadler, et al, 2001, showed good correlation between 5 foot and 20 foot long model test results. Kirkman and Pedrick, 1974 showed large model tests as being able to predict clam water resistance of sailing yachts to within 2-3% error bands. Scott, 1970 showed in a detailed paper on correlation and tank testing that the best available extrapolation methods could predict calm water resistance to within a 3% error band at slow to moderate speeds. The ITTC 1978 work reported in Harvald, 1991 found that model test resistance prediction errors had a standard deviation of 1-2% compared with actual ships. Other errors are of course also present in actual trials conditions, such as measurement errors and errors accounting for local environmental conditions, which add up to give a standard deviation in power prediction of 6-7% according to Harvald, 1991.

According to the information reviewed above, calm water ship resistance extrapolated from model tests have a 95% confidence interval of approximately plus or minus 3.92%, and a power prediction in sea trials 95% confidence interval of plus or minus 13.72%. The discussion to follow suggests that actual errors can be larger in practice, even in calm water conditions - and that these errors probably work to cancel each other out or are accounted for through engineering judgment and correction “factors” based upon experience at the practicing level.

From these results it can be concluded that, compared with some other engineering disciplines, naval architecture calculations have a large amount of uncertainty. That this is true is highlighted even more clearly when reviewing the errors in more complex naval architecture calculations, such as maneuvering. In maneuvering investigations discrepancies between model test and ship can be an order of magnitude larger than for the total resistance prediction error bands described above (Harper and Scher, 2001).

FRICIONAL RESISTANCE CONFIDENCE INTERVAL

The +/-95% confidence interval used for frictional resistance calculated according to the 1957 ITTC ship-model correlation line was 6.0%, with another 0.5% added to account for possible errors in wetted surface calculations. A frictional resistance error band was chosen based upon the comparative results reported in Watson, 1998 by Grigson, 1993, and also in Lewis, Vol. II, 1988, Harvald, 1991, and Scott, 1970. The error in roughness estimation and correlation allowance is roughly lumped together into a 50% error, based on graphs of trials data in Towsin et al, 1981.

The wetted surface error was included not because the obliquity correction method error was this large, but because for simplicity of implementation, the wetted surface calculation method used involved a coarse sampling of 40 stations and 20 waterlines, and assumed a straight-line profile between points where the half-breadth was first zero below the design waterline. This simplified method therefore may prematurely discount regions as having no wetted surface area. Importantly, the wetted surface area of the half-siding at the keel was included. It may be of interest to note here that of several wetted surface estimation formulas compared in Watson, 1998, the maximum difference between any of the formulas was about 2%.

The entire subject of ship frictional resistance and form factor correction is simply rife with controversy. Because of the present state of the art, which is confused at best, form factor methods such as the ITTC 1978 method were not used. The author cautiously addresses the frictional resistance issue below.

An argument could be presented that the neglect of the form factor method adds additional error to the frictional resistance calculation. The form factor methods tend to use different friction line formulas that take out some of the “average form factor” effect built into the ITTC 1957 ship-model correlation line. Also, for fine hull forms the form factor is generally small (see Harvald, 1991 and Scragg and Nelson, 1993.) The overall result balances out to a large extent, on average, for fine hull forms. Correlation allowances take care of most remaining discrepancies.

The three-dimensional (form factor) methods with the best correlation and extrapolation to real test data appear to be those of Grigson, 1993 and, proven more rigorously than any other frictional resistance paper reviewed by the author, Scott, 1970. Neither of these methods received the attention of the bulk of the naval architecture community that they should have.

The weakness of form factor methods is that the form factor necessary for their use really should be calculated for specific ship geometry at many speeds using a suitable theory, but the theoretical and computational methods are not yet up to the task (Carlton, 1994). Instead researchers are forced to make a difficult measurement of form factors at very low speed, and apply it at all speeds. The form factor measured is not a true form factor when the hull has an immersed transom or other discontinuities, such as chines, that would cause vortices or pressure drag effects. Thus the whole application of form factors to ships of common geometry is in error. Form factors (or other effects present in towing tanks) have also been shown to be highly

speed dependent for conventional hull forms, in sign as well as in magnitude, by various researchers working with very different data over very different time periods (Eggert, 1939)(Scott, 1970)(Holtrop, 1988). Therefore the practical application of form factor methods over wide speed ranges is fraught with supposition and difficulty. Currently the best calculation methods would make use of Scott, 1970 or Grigson, 1993 over moderate or slow speeds. But the fundamental flaws of weak theory, and even weaker experimental methodology, leave little incentive for the entire industry to switch to these methods.

The bottom line for ship frictional resistance calculation methods is that: a) much of the naval architecture community feels comfortable with the error band of the ITTC 1957 method and the substantial experience built up using it; b) is confused when academics and researchers debate about the esoteric aspects of frictional resistance; c) and have difficulty justifying the switch to form factor methods when they have not been developed to properly handle high speeds or many conventional hull forms that have immersed transoms or chines, and the theory is weakly developed.

TAYLOR STANDARD SERIES RESIDUARY RESISTANCE CONFIDENCE INTERVAL

The +/-95% confidence interval used for interpolation of Taylor Standard Series data was 5%. Two models were tested in the 1950's using various means of turbulence stimulation that had Taylor Series forms, but did not exactly match any of the originally tested Taylor Series models in terms of coefficients of form. Results for these two models were mixed, basically showing at least a 3-5% error in residuary resistance estimation using the Goertler interpolation method for higher speeds, and greater error for one of the models at very low speeds, below a speed-length ratio of 0.85 (Goertler, 1954 and Todd and Forest, 1951). Given that most ships of

interest will operate at higher speeds, and that residuary resistance plays such a relatively minor role in the total resistance at low speeds, and given the lack of other correlation data and the fact that the low-speed correlation was excellent for one model and poor for the other, an average error value of +/-5% was judged to be a reasonable compromise. This level of error is reasonable when compared to more modern resistance investigations using turbulence stimulation and wire probes. For instance, experimental data derived from wave probe measurements of a transom-stern hull form suggest that wavemaking resistance errors are 2-3% at the 95% confidence interval at moderate to high F_N (above about 0.30)(Ratcliffe and Wilson, 1989).

WORM CURVE FACTOR CONFIDENCE INTERVAL

The +/-95% confidence interval used for the residuary resistance differential between the Taylor Series data and that suggested by the parent hull worm curve factor was +/-2.5% above a speed-length ratio of 1.4, and +/-8% below that speed, based upon an example which potentially represented the "worst-case" scenario of a small model, as presented in the discussion of Ackers, et al, 1997.

FUNG RESIDUARY RESISTANCE CONFIDENCE INTERVAL

The +/-95% confidence interval used for Fung's regression is listed in the program input files versus speed. Fung's many papers provide error comparisons between regression predictions and actual model test data versus speed. A good estimate of the error versus speed could be made for the residuary resistance predicted by this method. Because of the large database used, it was assumed that the errors were representative of those to be expected when

other hulls of similar transom-stern design were evaluated (some of Fung's papers utilize data for over 700 ships and 10 000 data points).

SHALLOW WATER RESISTANCE INCREASE CONFIDENCE INTERVAL

Little data was available on the error to be expected between model tests, extrapolation of model tests to other hull forms, and full-scale ship shallow water resistance. Therefore a generous +/-95% confidence interval of +/- 25% was applied to all shallow water resistance data. State-of-the art shallow water resistance prediction methodologies appear to have better accuracy (Chen and Sharma, 1997)(Chen and Sharma, 1994).

AIR RESISTANCE CONFIDENCE INTERVAL

The +/-95% confidence interval used for air resistance was +/-8.6% of the coefficient of drag on the superstructure, and +/-22% on the hull, as given in U.S. Navy Memorandum, 1984. Error distributions for air and wind forces are also given in Isherwood, 1972.

STEERING RESISTANCE CONFIDENCE INTERVAL

The +/-95% confidence interval used for steering resistance was +/-50%, since there was a dearth of data available (only Harvald, 1991, and Korvin-Kroukovzky, 1961). It is also known that the steering resistance varies tremendously as a function of directional stability, control systems, and the location of centers of pressure of wave and wind forces acting on the ship. Therefore we can only attempt an order of magnitude calculation for steering resistance without more detailed calculations of very specific conditions.

APPENDAGE RESISTANCE CONFIDENCE INTERVAL

A blanket +/-20% confidence interval was applied to the appendage resistances. This applied to both the fixed appendage resistance as a fraction of bare hull resistance assigned in the input file (to account for bilge keels, struts and the like), and also to the rudder/fin resistance calculated for specific directional stability requirements. This value represents a compromise between low errors where the appendage geometry is simple and cases where there is more complexity or extrapolation from model test data is used.

To demonstrate the variability of model test appendage data, consider the case of the very detailed *Lucy Ashton* experiments. Detailed model and full-scale investigations of the *Lucy Ashton* showed that models at low and moderate speed doubled the 7% actual vessel shaft/brackets resistance augmentation, and almost quadrupled it at high speeds (Phillips-Birt, 1970). In some cases rudders actually reduced overall ship resistance (Kirkman and Kloetzli, 1980). There is also a great deal of uncertainty regarding the interference drag of the rudder-hull interface, as values can vary dramatically with fairing or changes in rudder leading-edge geometry (Hoerner, 1965). Overall, it is difficult to assign a single confidence interval to such a multi-faceted problem as appendage resistance.

ADDED RESISTANCE (IN WAVES) CONFIDENCE INTERVAL

A +/-30% confidence interval was applied to all added resistance values, as this was the common maximum range of predictions noted in Salvesen, 1978. However, it cannot be overemphasized that the calculation of added resistance is difficult and prone to great inaccuracy using any method. Some methods have disagreed by 100% with each other or with test data. Therefore any added resistance estimation technique should be used with extreme caution.

3.11 Optimization Methods

One of the first major papers to make use of computer techniques in general ship design optimization was Murphy, et al, 1965. The basic approach of that paper was to perform a coarse random search among all the variables (an even spacing was used for each variable evaluated), and then an optimum design was determined using 2-dimensional plots of the resulting design performance. Work was also begun in Europe around this time according to Schneekluth and Bertram, 1998. Murphy, et al could be classified as one of the papers that utilize simple regression equations with broad applicability and moderate or low accuracy.

Random searches as used by Murphy, et al have the disadvantage of requiring a large number of alternatives to be evaluated; for a uniform grid of alternatives along each of n variables, n raised to the n power alternatives must be evaluated. Since even a basic optimization could require 5 or 10 variables to be varied, computational effort becomes prohibitive!

Leopold, 1965, and Mandel and Leopold, 1966, described a more directed search strategy for determining optimum ship characteristics using an exponential random search technique. (In other respects their work was substantially similar to Murphy, et al, 1965.) This basically involves a smooth transition occurring as the optimization calculations are made, from using a completely random search of variables, towards an increasingly focused search made about the best resulting points (designs) of prior searches. The desirable features of this method are that: it is somewhat faster than a random search, since it increases the sampling of points in the region of optima while not wasting this level of resolution on regions that are clearly suboptimal; it is universal (rather than local), in that a random search technique is likely to find the global optimum; and it is robust, because it is a nongradient search (not relying on local partial

derivatives) it is applicable to cases where the function being evaluated is not smooth, not continuous, or is poorly resolved by sparse data points. The exponential random search technique is the first technique being applied to the current hull assessment program.

The downside of using an approach like that of Mandel and Leopold, 1966, is that it is not highly directed – it simply forms a more tightly constrained random search about the best points, without regard for the direction of improvement. (For poorly behaved functions or spotty data this may be a positive aspect of the method.) Simplex searches are faster because they have a directional influence based upon prior data points, and can therefore find optima roughly an order of magnitude faster than exponential random searches. It is planned for the hull assessment program to have the option of utilizing a simplex search in the future, as a future upgrade.

Two optimization techniques that have proven effective and efficient are the Nelder and Mead Simplex Search (Parsons, 1975), and the modified Box-Guin “Complex Method” as used by Parsons, 1972. Both methods are non-gradient search methods (methods not relying on local partial derivatives). They work by initially distributing a group of points in the n-dimensional search space that is being evaluated (this group being known as a simplex or complex). Using suitable rules the worst points (in terms of the optimization criteria) are continually removed from the group under consideration, and new points in the n-dimensional variable space are tried according to directional rules based on the group of remaining points. The volume of n-dimensional space occupied by the group is continually reduced until some search stopping criteria is reached.

Simplex searches and most faster or more “efficient” search techniques can only effectively determine the local optimum, and thus may require starting with another method to ensure that a global optimum has been achieved. An excellent concise overview of optimization

methods applicable to ship design, with comparisons of performance, is provided in Parsons, 1975. Optimization methods themselves represent a large field of research. More sophisticated methods, such as design of experiments based response surface models, are available that can attempt to further reduce the total number of points which need to be evaluated to find the optimum.

4 Example Optimization Results

There are many options available for use in the current hull assessment program. This great flexibility also means that there are innumerable combinations of options that can be investigated (e.g., basic bare hull or appended hull hydrodynamic resistance, fixed or variable propulsive efficiency). To investigate all of these combinations would not be practical within the scope of a limited study such as this, nor is it necessary to demonstrate the flexibility and potential of the current approach. Therefore only a few representative sample investigations will be presented below to demonstrate the capabilities of a program like the one developed here.

4.1 Frigate Length-Cost Study

Economic and weight considerations were not the primary focus of the current work, as described in the previous sections. However, for purposes of illustration an investigation was made into the top-level cost and weight impacts of hull form variation. The purpose of these tests was to demonstrate the order-of-magnitude effects of hull form variation on the weight and cost of a representative ship, including the effects of changing resistance upon fuel and propulsion machinery requirements. These tests also served as a contrast to the results of later tests that focused purely on hydrodynamic aspects.

A brief study was made of the impact of volumetric coefficient, C_v (or equivalently, length) variation upon total yearly life-cycle cost including acquisition and operation expenses. Volumetric coefficient, C_v , was varied with all other variables held fixed (displacement, B/T , C_p , hull depth, etc.). The figure of merit used during the optimization was the payload carried per

yearly operating cost of the vessel, an indication of the “efficiency” of the vessel at carrying cargo or in the case of a frigate, combat systems. Since the displacement was fixed in this basic example, the payload that could be carried was determined by the difference between total displacement and the weight requirements of the other weight groups, including the hull weight, that comprise the required ship weight before any cargo can be carried.

The example used was a pseudo-FFG-7 frigate operating environment, with a speed-time profile for naval surface combatants as reported in Cusanelli and Hundley, 1999. Weight data was derived from Garzke and Kerr, 1981, and cost estimates were based upon Mandel and Leopold, 1966 and Murphy et al, 1965. Added resistance in waves was not included in this analysis.

As described in Watson, 1998, hull weight is partially hull girder bending-moment driven, and partially volume driven. The extent to which the hull weight is volume driven or not depends upon a variety of factors such as the extent of deck and bulkhead plating versus shell plating. To some extent the hull weight could also be strongly driven by the extent of wetted surface, in cases where shell plating thickness is driven by available stock sizes or local ruggedness rather than by global hull girder loads.

Overall, there is a degree of uncertainty as to how much of the hull weight is driven by volume. Therefore several test runs were made of the hull assessment program optimizing on payload per yearly cost. Optimization calculations were made assuming that hull weight was 0%, 50%, and 100% volume-driven, with the rest being driven by hull girder bending-moment considerations.

The results are shown in Figures 4.1-1, 4.1-2, and 4.1-3, and present the ratio of payload carried per yearly operating cost, for varying length and fixed displacement.

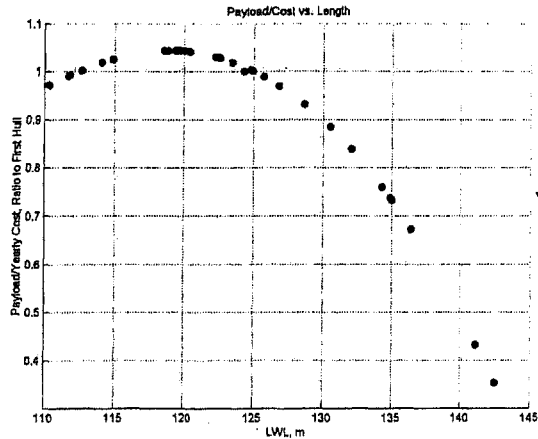


Fig. 4.1-1 Test 2. Sample optimization output showing the payload carried per yearly operating cost, for an operating profile typical of an FFG-7 frigate with 0% of hull weight being volume-driven.

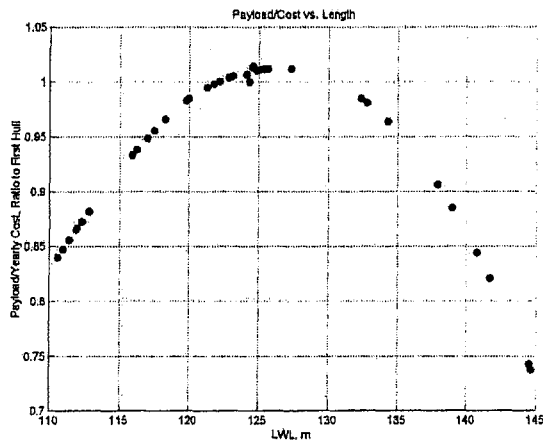


Fig. 4.1-2 Test 1. Same constraints as in the previous figure, except that the hull weight was set as being 50% volume-driven.

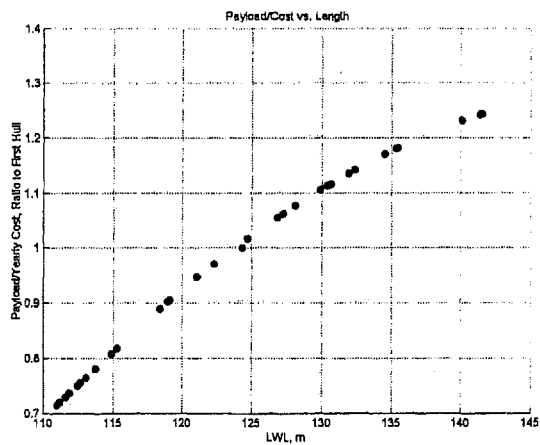


Fig. 4.1-3 Test 3. Same constraints as in the previous figure, except that the hull weight was set as being 100% volume-driven.

An interesting observation that can be made from these plots is that for hull weights which range from being at least 0%-50% volume driven, the length on waterline could range anywhere from 120 m to 125 m and be within a few percentage points of the minimum cost per payload. If hull weight is 100% volume driven then other considerations, such as total resistance, appear to dominate the optimization and drive the hull to be unrealistically long. While the present cost model is quite simple, as discussed above, this simple optimization does appear to justify the length of the actual FFG-7 of approximately 124 m from a payload per cost point of view. It is reasonable to assume that large, slender frigate-type vessels have much of their structural design dominated by hull girder-bending moment considerations, and that the percentage of hull weight that is driven by volume considerations is not dominant.

Some scatter from the mean line of points can be detected on the plots. This is an artifact of some of the iteration procedures used in the optimization program, in which certain aspects of design are iteratively adjusted until they fall within preset limits. Slight differences in iteratively-achieved values can multiply throughout the design, leading to the slight scatter noticeable for some points.

The files and batch file options that were used for these test cases are listed in table 4.1-1.

Table 4.1-1 Files and options used for tests.

Test	Profile File	Offset File	WCF File	Iterations	Fung Used ?	Description
1	profile4.txt	ffg7.txt	ffg7wcf.txt	40	Yes	50% Vol.-driven wt.
2	profile6.txt	ffg7.txt	ffg7wcf.txt	40	Yes	0% Vol.-driven wt.
3	profile7.txt	ffg7.txt	ffg7wcf.txt	40	Yes	100% Vol.-driven wt.

4.2 Frigate Powering Study

An interesting ship design question is: what is the difference in average powering requirements between a “good” and “bad” hull form design, for realistic ship operations. If this value is known then it is much easier to judge the merit of varying levels of hull form optimization. To answer this question, a series of optimization tests were made to demonstrate the differences between the average power consumption of a Taylor Standard Series (TSS) hull form, typical of old cruiser stern-style vessels, and a FFG-7 transom stern-style vessel. These vessels were chosen as representative of extreme solutions to high-speed displacement vessel design – one hull being known as generally “good” for a high-speed displacement ship role, the other as being inappropriate.

The comparisons were made for a fixed vessel displacement representative of an FFG-7 frigate, and by beginning the optimization with the approximate dimensions of that class. Some of the tests to be described below only evaluated bare hull resistance and powering (frictional and residuary resistance only), and some evaluated much more comprehensive ship resistance and powering (including miscellaneous forms of resistance such as appendages and rudder areas sized for constant directional stability, roughness allowances and shallow water effects, propulsive efficiency dependent upon propeller disk area, air and head seas wind and, when noted, added resistance in waves).

The example used was a pseudo-FFG-7 frigate operating environment. Tests were made optimizing for either 30 knots minimum average power consumption, or with a speed-time profile for naval surface combatants as reported in Cusanelli and Hundley, 1999. Bretschneider sea spectra were used, with sea state wind and wave data and occurrence probabilities as given in

Bales, 1983. Because the current program does not incorporate speed limits based upon seakeeping motions, it was felt that a more realistic environment description to use for optimization, followed here, would be to lump all of the sea state occurrence probabilities greater than sea state 5 in with the sea state 5 probability. This removal of sea state occurrences greater than sea state 5 therefore avoided adding many unrealistic results to the optimization that might unduly influence the results. Water depth probabilities were estimated by the author, and can be reviewed in the appendices.

Tests 38 and 39 compared the basic resistance and power of an FFG-7 and TSS hull at identical hull coefficients, at 30 knots. As would be expected from the lower residuary resistance of a transom stern-style vessel at higher Froude numbers, F_n , the FFG-7 hull had about 11% less power consumption than the TSS hull. When both hull forms were fixed in C_v but allowed to vary in C_p and B/T to minimize power, the optimized results (for basic power) given in test 40 and 41 revealed little change in the relative resistance between the hulls. Therefore a partial answer to the question of what is the difference in powering performance between such widely different hull forms is: at one high speed when C_v is fixed, whether from weight, machinery, cost or political constraints, then the difference in powering performance between "good" and "bad" hull forms is on the order of 11%.

The comparisons become more complicated when other aspects are investigated. For example, test 35 and 37 optimized power consumption at one speed (30 knots), allowing all dimensions to vary (at fixed displacement, as for all of this section's tests). In this case the TSS hull had 0.7% *less* power consumption than the FFG-7 hull. The contrast with previous tests occurred because in this case ship length grew markedly, bringing the FFG-7 hull form into a F_n range in which its performance was poor. Also the TSS hull had less wetted surface per

displacement than the FFG-7 hull, and could therefore achieve an even longer length, and therefore lower F_N , than the FFG-7 at optimum proportions.

This example, and the cost study in the preceding section, demonstrate a pair of under-emphasized aspects of naval architecture: (a) the optimum choice of basic hull form depends to a great extent upon hull length limits; and (b) hull length is rarely driven solely by resistance, and is generally driven by complex external factors (e.g., hull structural weight, propulsion, cost, arrangements, politics). Hull length rarely achieves that required for minimum single-speed hydrodynamic resistance, because of these external factors. Manning, 1959, points out another important factor: minimum basic hull resistance versus length tends to form a very flat region, since residuary resistance does not vary greatly at long lengths and low F_N . In such a case, if the vessel operates at lower speeds than the designed optimum speed, there will be a resistance penalty from the extensive wetted surface at the lower speeds.

Tests 12, 14 and 15 optimized the average basic power consumption of a FFG-7 and TSS hull form for a typical speed-time operating profile, allowing all dimensions to vary. The comparative optimization showed that for the broad speed-time operating profile, there was no substantial difference in *average* power consumption between the two different optimized hull forms. The ratio between the average power consumption of the optimized Taylor Series hull and the FFG-7 hull was 100.8% or 99.77%, depending upon whether the FFG-7 hull resistance was calculated based upon Fung, 1998 or a constant Taylor Series worm curve factor, respectively. Since the molded volume and other hull characteristics calculated by the program could have an error of roughly 0.3%, as a result of the many stretching operations performed on the parent hull form during optimization, and the resistance error bands were much larger, the average power consumption differences calculated here are insignificant.

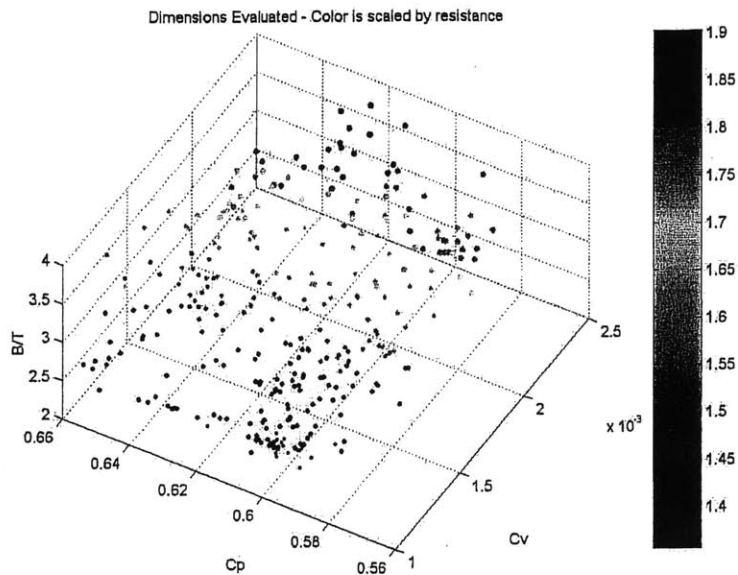


Fig. 4.2-1 Test 12. Scatter plot showing the dimensions of the hulls that were evaluated, and the resistance in $N \times 10^{-5}$.

A convergence study was also made using the basic tests run above. Tests revealed that convergence to an answer within 0.1% of the optimum power was achieved within about 320 hull iterations, with no appreciable improvement for up to 1280 hull iterations. Of course highly focused optimizations of one speed or seakeeping condition could show somewhat slower convergence than the example used here, which featured a broad speed-time operating profile that tended to reduce the impact of hull form changes on overall performance.

As a recommendation for future work, a Box-Guin “Complex Method” or Nelder and Mead Simplex search method could be used in the future to speed the convergence. Use of such directed search methods would vastly increase the speed of the search, at the cost of occasionally requiring multiple searches to be performed to guarantee finding the global optimum. Figure 4.2-2 shows that the current exponential random search method converges at a modest pace.

Adjustments in the m exponent that controls the search technique could improve the method, but not as dramatically as use of a directed search technique would do.

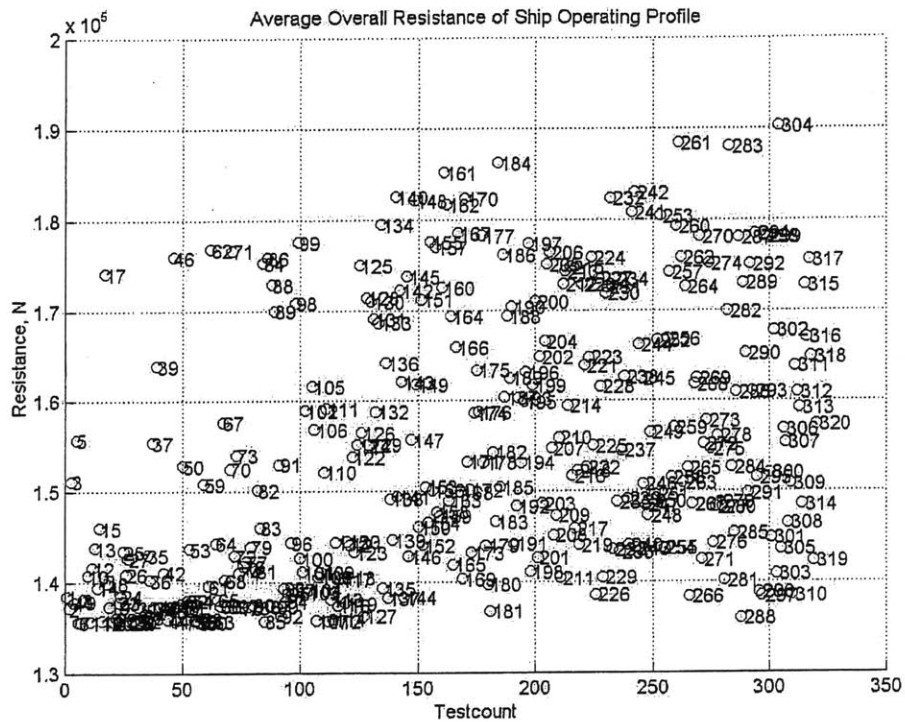


Fig. 4.2-2 Test 12. Plot shows the trend of exponential random search resistance results as the number of hull iterations remaining to be tried decreases (the chronological order of the tests is from right to left). As the test proceeds the search becomes more focused about the hulls with lowest resistance.

Of course most commercial vessels do not have as broad a speed-time operating profile as the frigate example given above. Nevertheless this analysis demonstrates the need to take factors other than bare hull average power consumption into account in order to arrive at a reasonable design. Optimization relying solely upon limited constraints and figures of merit, as done for the bare hull analysis above, can lead to erroneous conclusions as to ships of least cost or displacement, and lead to unrealistic ship lengths when other factors are ignored. Taking other factors into account can lead to widely different conclusions as to optimum designs, as shown in the preceding least-cost length optimization.

Examples of the magnitudes of miscellaneous forms of resistance for a frigate-type vessel were calculated in test 32. Using the FFG-7 example, head seas responses and added resistance in waves were calculated. Added resistance in waves represented about 5-8% of total comprehensive resistance over the middle and high-speed range (later tests 33 and 34 show that unusually long hull lengths can reduce added resistance to 1% or less of total resistance). Shallow water wavemaking resistance was calculated using data from cruiser stern and transom stern model tests by Graff et al, 1964. As mentioned in the correlation section of the appendices, thin-ship theory was investigated for use in estimating shallow water resistance for hull forms of different proportions than those tested by Graff, et al 1964. However, the FFG-7 hull form is close to the general characteristics of the models tested by Graff, et al, 1964, and the moderate accuracy and large time requirement of the thin-ship method did not warrant its use in this test. Shallow water wavemaking resistance (ignoring very shallow water viscous resistance increases that were not calculated) represented about 5% of comprehensive resistance, at most. Head seas air and wind resistance represented less than 10% of comprehensive resistance, although this is quite sensitive to superstructure design and sizing relative to the vessel.

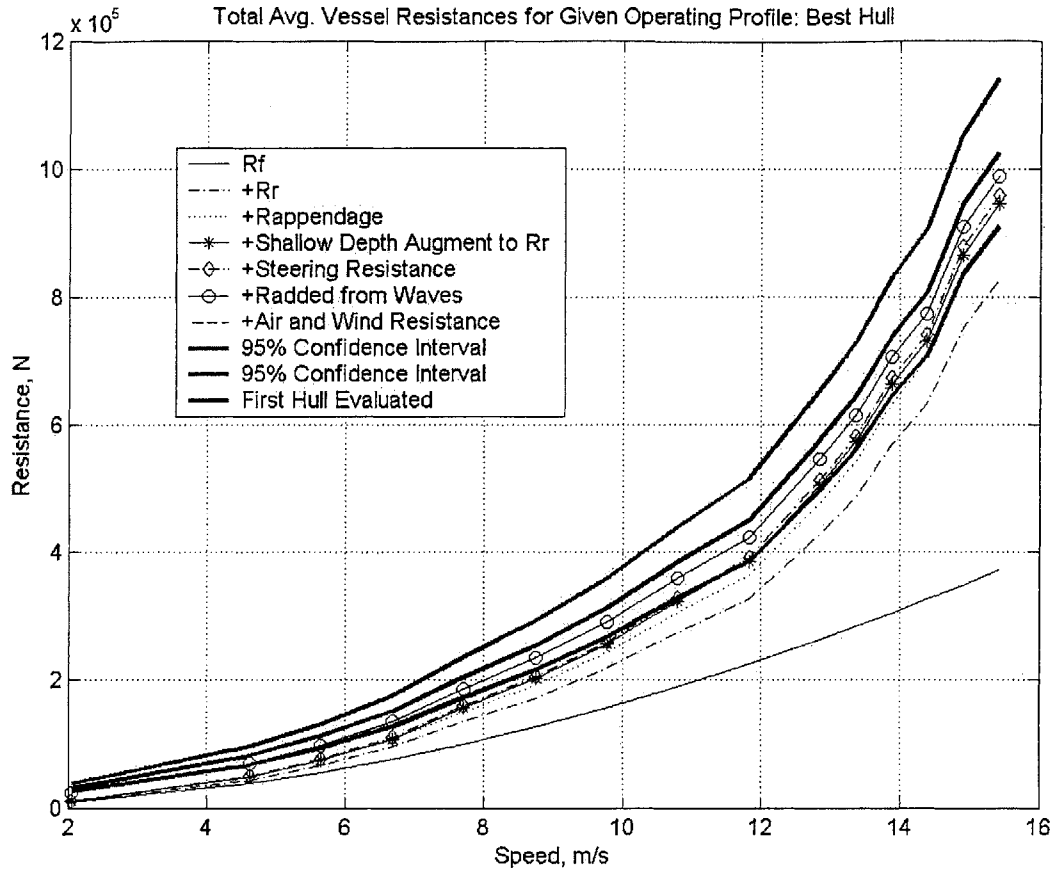


Fig. 4.2-3 Test 32. Plot of average resistance versus speed for all major forms of resistance. Only one hull was evaluated for this test, so the “first hull” and the final resistance component “air and wind resistance” of the best hull are plotted on the same bold blue line. Note that the appendage resistance includes a fixed allocation of 10% of bare hull hydrodynamic resistance, plus a rudder resistance that depends upon rudder size.

Note that the various miscellaneous resistances can form over 20% of total average resistance at mid-to-high speeds, without including appendage resistance. Also note that these forms of resistance are often poorly estimated if at all, and that they may be reduced significantly through reasonable design changes (heavily streamlining the superstructure can reduce air resistance by 50%, reducing pitch gyradius or moving LCF aft can reduce added resistance in waves by 30-50%, Sclavounos and Nakos, 1993). Clearly much work can be profitably done to reduce miscellaneous forms of resistance. As some of the prior tests have shown, changes of

even a few percentage points in overall power consumption are significant in terms of the total optimization problem.

Tests 33 and 34 were power optimizations of an FFG-7 frigate example hull for one speed (30 knots), varying C_v only. These tests show that, logically, the optimum length hull is longer when factoring-in comprehensive resistance than when calculating only basic bare hull resistance. Added resistance considerations, and the skeg/rudder area required for constant directional stability both favor longer ship lengths for lowering resistance. These components of resistance therefore contribute on the side of residuary resistance in what Manning, 1959, describes as the "antagonistic" effects of increasing hull length (increasing frictional and decreasing residuary resistance).

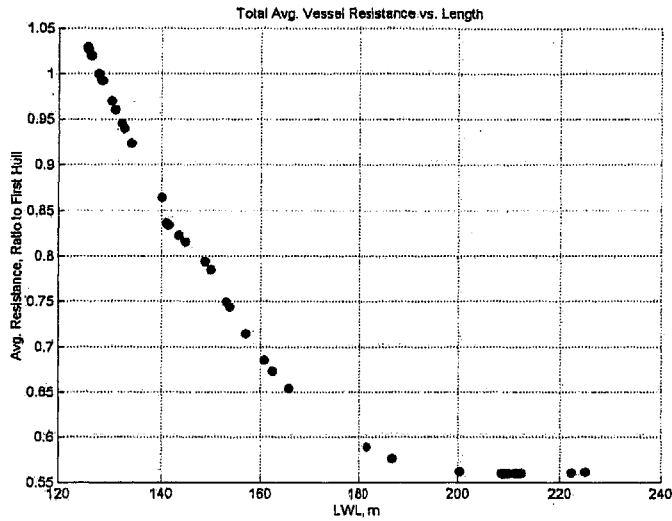


Fig. 4.2-4 Test 33. Plot of resistance versus length, for a test including bare hull resistance only. Optimum length ~212 m.

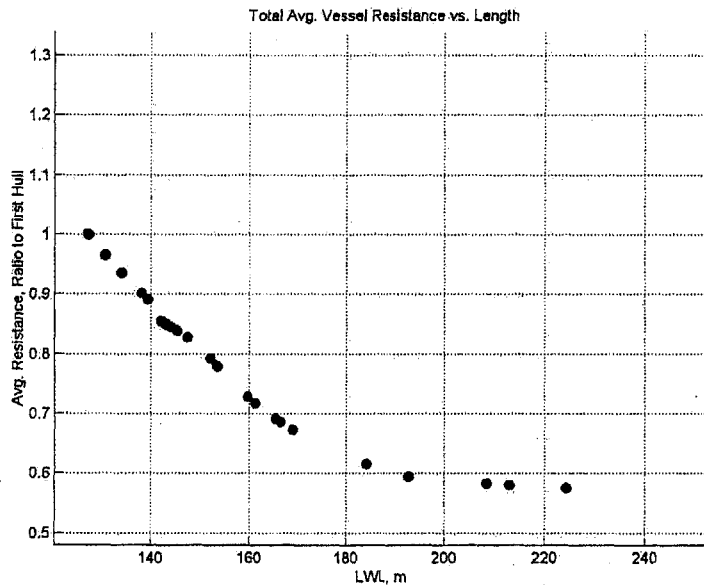


Fig. 4.2-5 Test 34. Plot of resistance versus length, for a test including comprehensive resistance calculation. Optimum length ~224+ m.

Overall, these frigate powering optimization tests highlight the following points: (a) the resistance or powering difference between optimum and non-optimum hull forms can be small, on the order of 10% or much less in many cases; (b) improvements sought during optimization

are the same size as or much smaller than comprehensive powering confidence intervals at the 95% confidence level; (c) miscellaneous resistances that are poorly defined, and somewhat complicated to predict, need to be included in the optimization process to realize further resistance reductions.

To summarize and add to the preceding points, optimizing actual ship powering requirements represents an effort to make small gains, on the order of magnitude of the naval architect's level of uncertainty (or ignorance) in many areas. The 95% confidence interval of total resistance can be seen as a pair of heavy red bounding lines on the resistance versus speed plots, and the width of this band is from 20-30% at moderate to high speeds. Also, length is a major factor in choice of hull form and optimum proportions, and it is usually driven by complex factors external to the hydrodynamic design process. Inclusion of miscellaneous forms of resistance in calculations tends to favor longer hull lengths than when these forms of resistance are ignored.

Midship coefficient was not evaluated in this study, and could have a significant effect upon the results. That is because the wetted surface area of hull forms is strongly influenced by midship coefficient, and the optimum differs for different hull forms.

Finally, significant improvements in ship resistance optimization could be made in the future, but they depend upon an understanding of miscellaneous forms of resistance and the computational ability to estimate them in a fairly automatic manner. In light of this, it is recommended that future investigations seek to integrate even more thorough calculation routines into future optimization software. The U.S. Navy's Ship Motions Program, for example, could be integrated into the optimization program, along with three-dimensional panel method programs for more accurate shallow water resistance estimates.

The files and batch file options that were used for these test cases are listed in table 4.1-1.

Table 4.2-1 Files and options used for tests.

Test	Profile File	Offset File	WCF File	Iterations	Fung Used ?	Min. Power (kW)/ Description
38	prof20.txt	ffg7.txt	ffg7wcf.txt	1	No	16.68E3 / One hull FFG-7 evaluation, 30kt
39	prof21.txt	tss3.txt	flatwcf.txt	1	No	18.61E3 / One hull TSS evaluation, 30kt
40	prof20.txt	ffg7.txt	ffg7wcf.txt	160	No	16.68E3 / FFG-7 varied Cp, B/T, 30kt
41	prof21.txt	tss3.txt	flatwcf.txt	160	No	18.61E3 / TSS varied Cp, B/T, 30kt
35	prof15.txt	ffg7.txt	ffg7wcf.txt	320	No	8596 / FFG-7 all varied, 30kt
37	prof17.txt	tss3.txt	flatwcf.txt	320	No	8530 / TSS all varied, 30kt
12	profile9.txt	ffg7.txt	ffg7wcf.txt	320	Yes	1899 / FFG-7 all varied, speed range
14	input10.txt	tss3.txt	flatwcf.txt	320	No	1914 / TSS all varied, speed range
15	profile9.txt	ffg7.txt	ffg7wcf.txt	320	No	1918 / FFG-7 all varied, speed range
32	prof14.txt	ffg7.txt	ffg7wcf.txt	1	No	FFG-7 one hull evaluation
33	prof18.txt	ffg7.txt	ffg7wcf.txt	40	No	8907 / FFG-7 C _v varied, 30kt
34	prof14.txt	ffg7.txt	ffg7wcf.txt	40	No	13.17E3 / FFG-7 C _v varied, 30kt

4.3 Slender Hull Powering Study

The previous sections described test optimizations of typical frigate hull designs. Some complications were noted, including the great sensitivity of the problem to the choice of length, and that length was sensitive to many external factors that can be difficult to fully estimate. In order to demonstrate another practical use of the current work another optimization study was made. The goal of this study was to focus upon a hull design problem that was less affected by external factors, and more amenable to purely hydrodynamic optimization considerations. A single-person rowing shell was chosen for this problem because rowing shells are generally desired for their single (top) speed performance, and their structural weight is fixed by racing regulation (and owners are often willing to sacrifice structural life for meeting minimum required weight). Shells also often race over shallow water courses where shallow water wave resistance concerns become significant, especially for the longer 8-person rowing shells. The races generally occur in moderate wave and wind environments. In general, the problem is well defined and amenable to the approach used in the hull assessment program developed here.

All of these tests were simple optimizations of top speed power (equivalent to resistance in this case) at a fixed propulsive efficiency of 70%, at a fixed displacement of 220 lb (Note that the hull assessment program uses metric values for all internal calculation routines, except for minor unit conversions and displays of velocity in knots as well as in meters per second). The top speed chosen was 9.5 knots, which is just below the top Olympic racing speeds listed on p.115 of Paduda, 1992 for a 2000 meter race course. The rowing shell offsets were scaled off of body plans for a heavyweight 8-person rowing shell in United States Patent No. 5,474,008, "Eight Man Rowing Shell," Vespoli et al, 1994. While the patent was for an 8-person shell, the

hull sections are quite similar to those of modern single shells. The body plan as used by the hull assessment program is shown in Figure 4.3-1.

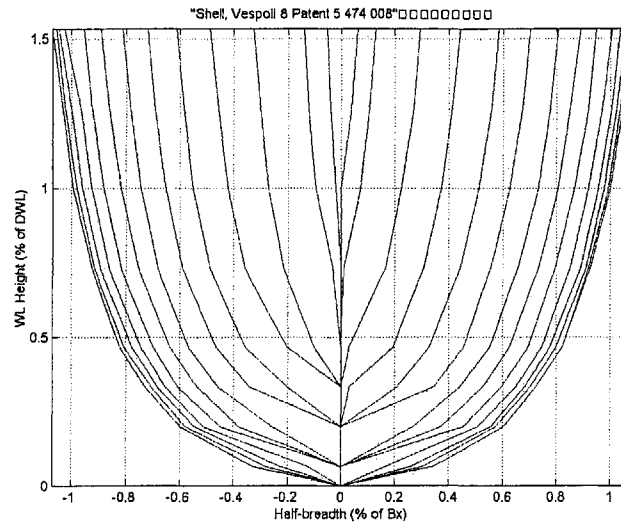


Fig. 4.3-1 Body plan of the example shell used for tests. The irregularities near the centerline could be reduced by using profile/buttock line data, or greater resolution in waterline spacing in future versions of the hull assessment program.

Added resistance in waves was not included in the comprehensive resistance evaluations of the shells. Previous tests had shown that added resistance for a shell, in wave conditions typical of short fetch and low wind environments, was exceedingly small because of the extreme slenderness of the hulls. The wavelengths typically are much shorter than the length of a shell, meaning that diffraction/ray-theory resistance dominates over relative motion resistance. The extremely fine entrance angles of shells means that diffraction/ray-theory resistance is vanishingly small for such hulls, since it is proportional to the sine of the entrance angle cubed.

Tests 43 and 23 investigated the optimum length (C_V) of a conventional shell for top speed for both bare hull and comprehensive resistance. This was for a fixed B/T and C_P which is not necessarily identical to that of actual shells. The results are shown in Figures 4.3-2 and 4.3-3.

The optimum length for basic bare hull resistance optimization was calculated to about 27.5 feet, and for comprehensive resistance was about 28.7 feet.

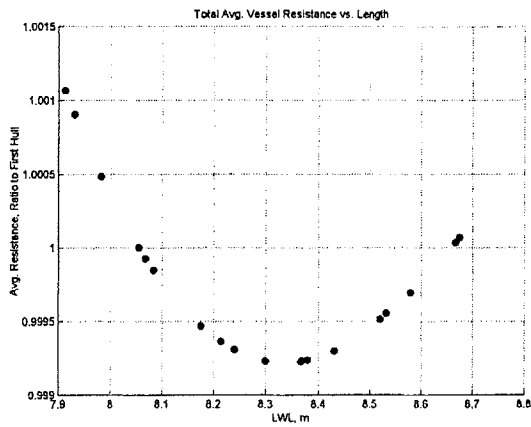


Fig. 4.3-2 Test 43. Basic bare hull resistance at 9.5 knots versus C_V .

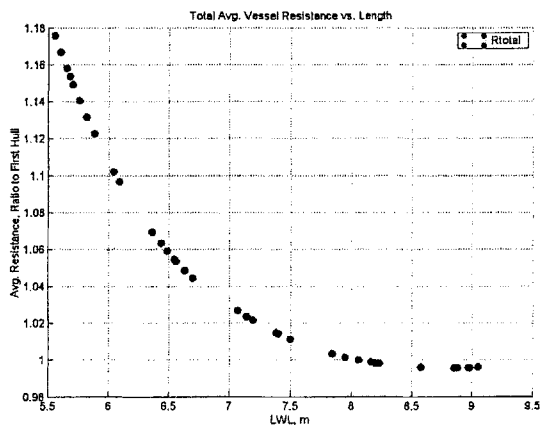


Fig. 4.3-3 Test 23. Comprehensive resistance at 9.5 knots versus C_V .

Tests 28, 44 and 30 investigated the optimum dimensions for both a conventional shell (comprehensive and basic resistance) and a transom-stern hull (the FFG-7 hull) for comprehensive resistance at 9.5 knots. The optimum length for the shell in these tests, which varied all dimensions, was 27.3 feet for comprehensive resistance and 26.7 feet for basic bare hull resistance. As in the earlier frigate tests, these tests showed that the transom-stern hull had

higher optimized resistance than the cruiser-stern style rowing shell hull form, for the comprehensive resistance case that was compared.

Typical modern shell waterline lengths are 26 feet for an Empacher, 26.2 for a VanDusen, and 26.5 for a King (<http://www.maths.adelaide.edu.au/Ap.zausk/hydro/rowing/real/realrow.htm>, July 28th, 2001), and length overall (slightly greater than waterline length) 26.5 feet for a VanDusen (<http://www.composite-eng.com/shells.htm> July 5th, 2001). Considering all the uncertainties in this analysis and the flatness of the resistance curve, the reasonably close agreement between the calculated basic bare hull optimum length (26.7 feet) and the actual shell lengths (up to around 26.5 feet) is gratifying.

The author has not read of any designers having accounted for all of the miscellaneous forms of resistance included in the current study's comprehensive resistance calculation, especially not the optimization of fin/skeg area for consistent directional stability. Therefore it is not likely that many hulls would be sized for the slightly longer length that this study suggests. Also it must be remembered that actual shell designers may not be optimizing their designs for only 9.5 knot top speed, nor for 220 lb displacement, but may have other factors in mind. These other factors include longer and slower races, racers that are less powerful, and building a shell that is slightly shorter because it is less expensive and more rigid for the same weight and practically identical resistance. Finally it should be pointed out that historically, shells as long as 30 feet have been built and raced in large numbers by professionals. This was especially true in earlier time periods when less durable shells had wide acceptance because of their short-term performance advantages (at that time high-stakes gambling was part of professional rowing). Therefore the current analysis, suggesting that shells up to 27.3 feet long are best for high speed comprehensive resistance, may not be inaccurate.

The files and batch file options that were used for these test cases are listed in table 4.3-1.

Table 4.3-1 Files and options used for tests.

Test	Profile File	Offset File	WCF File	Iterations	Fung Used ?	Min. Resist. (N) / Description
43	shellp3.txt	vespoli8.txt	highwcf.txt	20	No	70.3 / varied C_v , basic resist. 9.5kt
23	shellp4.txt	vespoli8.txt	highwcf.txt	40	No	82.6 / varied C_v , full resist. 9.5kt
28	shellp6.txt	vespoli8.txt	midwcf.txt	320	No	80.9 / shell varied all dims., full resist. 9.5kt
44	shell6pb.txt	vespoli8.txt	midwcf.txt	160	No	68.6 / shell varied all dims., basic resist. 9.5kt
30	trans4.txt	ffg7.txt	ffg7wcf.txt	320	No	81.9 / transom stern varied all dims., full resist. 9.5kt

5 Conclusions and Recommendations

OBSERVATIONS

The results of the present hull form optimization study include the following observations:

- An example of a practical naval architecture design tool has been demonstrated. The hull assessment program performs many of the basic design calculations that are essential for true hydrodynamic hull form optimization for medium-to-fast displacement vessels in realistic operating scenarios. As opposed to more traditional design methods, the current program is truly integrated, automatic, and avoids some of the historic gross simplifications or omissions in the area of hydrodynamic optimization (though cost and other non-hydrodynamic calculations are gross simplifications). It also allows rapid use of existing parent hull geometry and resistance data (manual offsets and resistance entry within minutes or an hour) to serve as a design investigation starting point, or to serve as a comparison with another candidate hull form.

- Technical literature in the field of naval architecture comes from a variety of industry and academic authors and is not nearly as concentrated or as easy to locate as, for example, aerospace references from NACA/NASA. The literature is replete with substantial typographical errors that are time-consuming and potentially dangerous for the practicing engineer.

- Hull form optimization is quite sensitive to the expected operating profile, and to the forms of resistance included in the calculations. A large number of calculations are required to provide optimum hull form characteristics. Therefore, automatic evaluation routines are essential when exploring realistic combinations of conditions, resistances, goals and constraints.

- Miscellaneous resistance components (items other than bare hull residuary and frictional resistance) represent a significant portion of the resistance of actual frigate-size vessels in realistic operating conditions, according to calculations made here. These miscellaneous resistances can form 20% or more of total resistance, and there is a greater opportunity to reduce them than conventional bare hull residuary and frictional resistances.

- Length is a major factor in choice of general hull form and optimum proportions, and it is usually driven by complex factors external to the hydrodynamic design process. Selection of hull form characteristics, while ignoring these external factors (such as hull weight, vessel costs), can lead to erroneous conclusions as to the optimum vessel design.

- Optimum hydrodynamic performance curves are shallow. As found by other investigators, performance penalties for having a hull that is “off-design” or non-optimal are small for modest deviations from optimum hull proportions. The multiple forms of resistance affecting ships, and the fact that most vessels operate at several speeds, tends to reduce the total hydrodynamic performance differences between hull designs.

- Hull form optimization is concerned with small improvements, at the level of “ignorance” of the naval architect. The difference in average operating resistance between optimized displacement hulls, of widely different form and residuary resistance properties, is modest. The range is from approximately 0-11%, depending upon ship operating speeds. Therefore, the realistic performance difference between “good” and “bad” hull forms is not large, and is generally smaller than the 95% resistance confidence intervals. This finding makes it clear why there has been little historical progress in hull form resistance performance: even major advances in performance in one area translate into small total performance improvements. The hull form will therefore lack a compelling advantage over prior designs, and may even be worse

if the new design is suboptimal in another one of the complex areas of hull form resistance and design. Without a well-funded research effort and a long-term technical mentor who “champions” design approaches, there is little chance of sustained evolutionary improvements.

- The hull assessment program has been used to evaluate a realistic design for a single rowing shell. Optimized length agrees well with actual shell designs, confirming the general validity of the analysis methods used in this study.

RECOMMENDATIONS FOR FUTURE WORK

Three major recommendations can be made for areas of focus for future work:

- The hull assessment program can be improved by incorporating the suggested improvements listed in Chapter 2. A variety of studies could be usefully performed using the improved program.
- An investigation should be made into ways to reduce miscellaneous forms of resistance. The present study indicated that greater resistance reductions could probably be realized through changes in miscellaneous resistance than through changes to the traditional bare hull frictional and residuary resistances.

- A much bolder vision of the hull assessment program could be realized. In such a more all-encompassing program, the hull assessment program would merely manipulate data and would not perform many calculation tasks. Instead, legacy software or computationally more efficient new software would be run by the hull assessment program, which would serve to transfer data between the programs and guide the overall optimization process. The naval architecture community’s efforts to produce software packages are being far outstripped by commercial efforts to produce flexible software products. New commercially available software

allows pre-existing programs to be linked in operation. The power of these new programs to link virtually all pre-existing computer codes is immense, because it suggests that fully automated optimized design of engineering systems, accounting for all major design considerations, is no longer dependent upon the development of new technology but is now only dependent upon the availability of capital.

Bibliography

Ackers, et al, "An Investigation of the Resistance Characteristics of Powered Trimaran Side-Hull Configurations," *Trans. SNAME*, Vol. 105, 1997.

Bales, Nathan K., "Optimizing the Seakeeping Performance of Destroyer-Type Hulls," 13th Symposium on Naval Hydrodynamics (DTNSRDC Rpt.), Tokyo, Japan, Oct. 1980.

Bales, Nathan K., and Cieslowski, Daniel S., "A Guide to Generic Seakeeping Performance Assessment," *ASNE Naval Engineers Jrnl.*, April, 1981.

Bales, Susan L., "Designing Ships to the Natural Environment," *ASNE Naval Engineers Jrnl.*, March, 1983.

Beck, Robert F., "The Added Resistance of Ships in Waves," MIT Dept. of Naval Architecture and Marine Engineering, Rpt. No. 67-9, June, 1967.

Bridges, Thomas F., Hilliard, Bryant A., and McMullen, John J., "The Influence of Bilge Keels and Rolling in Waves on Sea Speed and Horsepower," *SNAME Trans.*, Vol. 72 1964, pp.203-230.

Bhattacharyya, Rameswar, *Dynamics of Marine Vehicles*, Wiley-Interscience, 1978.

Carlton, J.S., *Marine Propellers and Propulsion*, Butterworth-Heinemann, 1994.

Cebulski, Donald R., "New Initiatives in Ship General Arrangements," *SNAME Ship Technology and Research (STAR) Symposium*, Philadelphia, PA, May 27-30, 1987.

Chen, Xue-Nong, and Sharma, Som Deo, "A Slender Ship Moving at a Near-Critical Speed in a Shallow Channel," *Jrnl. of Fluid Mechanics*, Vol. 291, 1994.

Chen, Xue-Nong, and Sharma, Som Deo, "Zero Wave Resistance for Ships moving in Shallow Channels at Supercritical Speeds," *Jrnl. of Fluid Mechanics*, Vol. 335, 1997.

Cimino, Dominick, and Redmond, Mark, "Naval Ships' Weight Moment of Inertia – A Comparative Analysis," SAWE Paper No. 2013, Category No. 13, 50th Annual Conf. of SAWE, 20-22 May, 1991.

Day, Alexander H., and Doctors, Lawrence J., "Resistance Optimization of Displacement Vessels on the Basis of Principal Parameters," *Jrnl. of Ship Research*, Vol. 41, No. 4, Dec., 1997.

Eggert, Capt. E. F., "Further Form Resistance Experiments," *Trans. SNAME*, Vol. 47, 1939, pp.303-330.

Evans, J. Harvey, "Basic Design Concepts," *Naval Engineers Jrnl.*, Nov., 1959.

Faltinsen, O.M., *Sea Loads on Ships and Offshore Structures*, Cambridge Univ. Press, 1990.

Fung, Siu C., "Resistance Predictions and Parametric Studies for High-Speed Displacement Hulls," *ANSE Jrnl*, Mar. 1987.

Fung, Siu C., "Resistance and Powering Prediction for Transom Stern Hull Forms During Early Stage Ship Design," *Trans. SNAME*, 1991.

Fung, Siu C., and Leibman, Larry, "Statistically-Based Speed-Dependent Powering Predictions for High-Speed Transom Stern Hull Forms," *SNAME Chesapeake Section*, Oct. 12, 1993.

Fung, Siu C., and Leibman, Larry, "Revised Speed-Dependent Powering Predictions for High-Speed Transom Stern Hull Forms," FAST 1998, Germany.

- Garzke, William H., and Kerr, George, "Major Factors in Frigate Design," *SNAME Trans.*, Vol. 89, 1981.
- Gerritsma, Ir. J., "Shipmotions in Longitudinal Waves," *International Shipbuilding Progress*, Vol. 7, No. 66, Feb. 1960, pp.49-71. (Also Publ. no. 14 of the Shipbuilding Lab., Tech. Univ., Delft.)
- Graff, W., Kracht, A., and Weinblum, G., "Some Extensions of D. W. Taylor's Standard Series," *SNAME Trans.*, Vol. 72, 1964, pp.374-403.
- Grigson, 1993, "An Accurate Smooth Friction Line for Use in Power Prediction," *R.I.N.A.*, 1993.
- Grim, O., "A Method for a More Precise Computation of Heaving and Pitching Motions Both in Smooth Water and in Waves," 3rd. Symposium on Naval Hydrodynamics, Sept. 19-22, 1960, Scheveningen, Netherlands.
- Goertler, Morton, "A Reanalysis of the Original Test Data for the Taylor Standard Series," DTMB Rpt. No. 806, 1954 original, SNAME 2nd. Printing 1998.
- Hadler, J., Lecture Notes, Naval Architecture III, Resistance and Propulsion, Webb Institute of Naval Architecture, Fall, 1995.
- Hadler, J.B., et al, "Model Resistance Testing in the Robinson Towing Tank at Webb Institute," 26th American Towing Tank Conference, Glen Cove, NY, July 23-24, 2001.
- Harper, Justin and Scher, Robert M., "Improvements in the Prediction of Maneuvering Characteristics of Ships Using Regression Analysis," 26th American Towing Tank Conference, July 23-24, 2001, Glen Cove, New York.
- Harvald, *Resistance and Propulsion of Ships*, Krieger, 1991.
- Havelock, T.H., "The Effect of Shallow Water on Wave Resistance," *Proceedings of the Royal Society of London. Series A, Containing Papers of a Mathematical and Physical Character*, Vol. 100, Issue 706, Feb. 1, 1922, pp. 499-505.
- Henschke, W., *Schiffbautechnisches Handbuch* Vol. 1, 2, 1957.
- Hoerner, S.F., *Fluid-Dynamic Drag*, 1965.
- Hofman, Milan, and Kozarski, Vladan, "Shallow Water Resistance Charts for Preliminary Vessel Design," *International Shipbuilding Progress*, 47 no. 449, 2000, pp.61-76.
- Hollister, Stephen M., "Automatic Hull Variation and Optimization," SNAME New England Section Mtng., Feb. 28, 1996.
- Holtrop, J., "A Statistical Resistance Prediction Method with a Speed Dependent Form Factor," Presented at SMSSH '88, Varna, Oct. 1988.
- Hughes, Owen and Caldwell, J.B., *Marine Structures- Selected Topics, Examples and Problems – Volume I-Plate Bending – Supplement to Chapter 9 – Plate Bending of "Ship Structural Design"*, SNAME, 1991.
- Isherwood, R.M., "Wind Resistance of Merchant Ships," *RINA Trans.* 1972, pp.327-338.
- Jacobs, W.R., "Estimation of Stability Derivatives and Indices of Various Ship Forms, and Comparison With Experimental Results," *Jrnl. of Ship Research*, Vol. 10, No. 3, Sept. 1966.
- Jiang, Changben, et al, "Ship Hull and Machinery Optimization Using Physics-Based Design Software," *Marine Technology*, Vol. 39, No. 2, April, 2002.
- Kim, Y. and Sclavounos, P.D., "A Finite-Depth Unified Theory for the Linear and Second-Order Problems of Slender Ships," *Jrnl. of Ship Research*, Vol. 42, No. 4, Dec. 1998.
- Kirkman, Karl L., and Kloetzli, John W., "Scaling Problems of Model Appendages," 19th ATTC, Vol. I., Ed. by Stuart Cohen, Ann Arbor, MI, July 9-11, 1980.

- Kirkman, Karl L., and Pedrick, David R., "Scale Effects in Sailing Yacht Hydrodynamic Testing," *Trans. SNAME*, 1974.
- Kirsch, Maria, "Shallow Water and Channel Effects on Wave Resistance," *Jrnl. of Ship Research*, Sept. 1966.
- Korvin-Kroukovzky, *Theory of Seakeeping*, SNAME, 1961.
- Kuiper, G., "Preliminary Design of Ship Lines by Mathematical Methods," *Jrnl. of Ship Research*, March 1970.
- Lackenby, H., "On the Systematic Geometrical Variation of Ship Forms," *RINA Trans.*, Vol. 92, 1950.
- Lamar, John E., "A Vortex Lattice Method for the Mean Camber Shapes of Trimmed Noncoplanar Planforms With Minimum Vortex Drag," NASA TN D-8090, 1976.
- Landauer, Thomas K., *The Trouble with Computers: Usefulness, Usability, and Productivity*, MIT Press, 1995.
- Lavis, David R., and Forstell, Brian G., "The Cost-Benefit of Emerging Technologies Using Physics-Based Ship-Design Synthesis," *FAST 99*, Seattle, WA, Sept. 1999.
- Leibman, Lawrence, Fung, Siu, and Slager, John, "An Engineering Approach to Prediction of Added Resistance in Waves During Early Stages of Ship Design," Chesapeake Section SNAME, Oct. 23, 1990.
- Leopold, Reuven, "Mathematical Optimization Methods Applied to Ship Design," MIT Dept. of Naval Arch. and Marine Eng., Rpt. No. 65-8, Oct., 1965.
- Lewis, Edward V., ed., *Principles of Naval Architecture*, 3rd. ed., SNAME, 1989.
- Lloyd, A R J M, *Seakeeping, Ship Behavior in Rough Weather*, ARJM Lloyd, 26 Spithead Ave., Gosport, Hampshire, UK, 1998.
- Loukakis, Theodore A., Chryssostomidis, Ch., "Seakeeping Standard Series for Cruiser-Stern Ships," *SNAME Trans.*, Vol. 83 1975.
- Mandel, Philip, and Leopold, Reuven, "Optimization Methods Applied to Ship Design," *SNAME Trans.*, Vol.74, 1966.
- Manning, George C., "The Theory and Technique of Ship Design," MIT Press and John Wiley and Sons, Inc., 1959.
- McCormick, Barnes W., *Aerodynamics Aeronautics and Flight Mechanics*, 2nd. ed., John Wiley and Sons, 1995.
- Memorandum, U.S. Navy SEA from: 55W3, "Still Air Drag Estimation Technique," 23 Apr. 1984.
- Michell, J.H., "The Wave-Resistance of a Ship," *Philosophical Magazine*, Vol. 45, 1898, pp. 106-123.
- Millward, A., "The Effect of Water Depth on A Yacht's Performance," *International Shipbuilding Progress*, Vol. 35, No. 404, 1988.
- Millward, A., 'A Review of the Prediction of Squat in Shallow Water,' *Jrnl. of Navigation*, Jan. 1996.
- Moor, D.I., and Murdey, D.C., "Motions and Propulsion of Single Screw Models in Head Seas, Part II," *RINA Trans.* Vol. 112, 1970, pp.121-164.
- Newman, J.N., *Marine Hydrodynamics*, MIT Press, 1977.
- Munro-Smith, R., *Elements of Ship Design*, The Inst. of Marine Eng., 1975.
- Paduda, Joe, *The Art of Sculling*, McGraw Hill Ragged Mountain Press, Camden, ME, 1992.

- Parissis, Gregory G., "The Effect of Hull Shape Non-Linearities on the Calculation of Heave and Pitch of a Ship," MIT Dept. of Naval Arch. and Marine Eng. Rpt. no. 64-6, June, 1964.
- Parsons, J., "The Optimum Shaping of Axisymmetric Bodies for Minimum Drag in Incompressible Flow," Purdue Univ., Ph.D. thesis, June, 1972.
- Parsons, Michael G., "Optimization Methods For Use in Computer Aided Ship Design," SNAME *Ship Technology and Research (STAR) Symposium*, Washington, D.C., Aug. 26-29, 1975.
- Parsons, Michael G., Singer, David J., and Sauter, John A., "A Hybrid Agent Approach For Set-Based Conceptual Ship Design," *Intl. Conference on Computer Applications in Shipbuilding*, Cambridge, MA, June 7-11, 1999.
- Pershin, V.I., and Voznessensky, "Study of Ship Speed Decrease in Irregular Waves," *Proceedings*, Symposium on the Behaviour of Ships in A Seaway, Sept. 7-10, 1957.
- Phillips-Birt, D., *Ship Model Testing*, Int'l. Textbook Co. Ltd., London, 1970.
- Prohaska, C.W., "The Vertical Vibration of Ships," *The Shipbuilder and Marine Engine-BUILDER*, Oct., 1947.
- Rao, S., *Mechanical Vibrations*, 3rd ed., Addison-Wesley, 1995.
- Ratcliffe, Toby J., and Wilson, Michael B., "Uncertainty in the Measurement of Ship Model Wave Profiles and Wave Pattern Resistance," 22nd ATTC, St. John's NF, Aug. 8-11, 1989.
- Rawson, K.J., and Tupper, E.C., *Basic Ship Theory*, Longman, 1994.
- Salvesen, Nils, et al, "Ship Motions and Sea Loads," SNAME *Trans.*, Vol. 78, 1970.
- Salvesen, Nils, "Added Resistance of Ships in Waves," *J. Hydronautics*, Vol. 12, No. 1, January 1978.
- Saunders, Harold E., *Hydrodynamics in Ship Design*, SNAME, 1957.
- Schneekluth, H., and Bertram, V., *Ship Design for Efficiency and Economy*, 2nd ed., Butterworth-Heinemann, 1998.
- Sclavounos, P.D., "The Diffraction of Free-Surface Waves by a Slender Ship," *Jrnl. of Ship Research*, Vol. 28, No. 1, Mar. 1984.
- Sclavounos, P.D., and Nakos, D.E., "Seakeeping and Added Resistance of IACC Yachts by a Three-Dimensional Panel Method," 11th Chesapeake Sailing Yacht Symposium, Annapolis, MD, Jan. 1993.
- Sclavounos, P.D., 13.022 "Surface Waves and Their Interaction with Floating Bodies," lectures, 2002.
- Scott, J. R., "On Blockage Correction and Extrapolation to Smooth Ship Resistance," SNAME *Trans.*, Vol. 78, 1970.
- Scragg, Carl A., and Nelson, Bruce D., "The Design of an Eight-Oared Rowing Shell," *Marine Technology*, Vol. 30, No. 2, April 1993.
- Shintani, A., and Inoue, R., "Influence of Hull Form Characteristics on Propulsive Performance in Waves," SMWP. Dec. 1984.
- Society of Naval Architects of Japan, 60th Anniversary Series, Vol. 8, 1963.
- SNAME Resistance and Data Sheets.
- SNAME *Trans.*, 1954 p.632.
- Strom-Tejsen, Jorgen, Yeh, Hugh Y. H., and Moran, David D., "Added Resistance in Waves," SNAME *Trans.*, 1973, pp.109-143.

- Taylor, D.W., *The Speed and Power of Ships*, 3rd ed., 1943. (Has expanded resistance charts in some cases compared with the 1st ed.)
- Thews, J.G., and Landweber, L., "The Influence of Shallow Water on The Resistance of a Cruiser Model," United States Experimental Model Basin Rpt. No. 408, Oct. 1935.
- Thews, J.G., and Landweber, L., "A Thirty Inch Model of the S.S. Clairton in Shallow Water," United States Experimental Model Basin Rpt. No. 414, Jan. 1936.
- Todd, F. H., and Forest, F. X., "A Proposed New Basis for the Design of Single-Screw Merchant Ship Forms and Standard Series Lines," *SNAME Trans.*, Vol. 59, 1951.
- Todd, F.H., "Series 60 Methodical Experiments with Models of Single Screw Merchant Ships," DTMB Rpt. 1712, July, 1963.
- Townsin, R.L., et al, "Estimating the Technical and Economic Penalties of Hull and Propeller Roughness," *SNAME Trans.*, Vol. 89, 1981.
- Tuck, E.O., "Shallow-water flows past slender bodies," *Jrnl. of Fluid Mechanics*, vol. 26, part 1, 1966.
- U.S. Navy, Memorandum from SEA 55W3: Still Air Drag Estimation, Apr. 23, 1984.
- Vossers, Ir. G., "Fundamentals of the Behaviour of Ships in Waves," *International Shipbuilding Progress*, (Publication no. 151a of the N.S.M.B.), Vol. 6, No.63, Nov. 1959, No. 64, Dec. 1959, Vol. 7., No. 65, Jan. 1960, No. 66, Feb. 1960, No. 67, March 1960, No. 68, April 1960, No. 69, May 1960, No. 70, June 1960.
- Walden, D.A., "Extension of the Bales Seakeeping Rank Factor Concept," DTMB DTNSRDC – 83/085, Presented at 20th ATTC, Stevens Inst., Oct. 1983.
- Walden, David A., and Grundman, Peter, "Seakeeping Optimization," DTNSRDC Rpt. no. SPD-1144-01, May, 1985.
- Watson, David, *Practical Ship Design*, Elsevier Ocean Engineering Book Series Vol. 1, Elsevier, 1998.
- Wehausen, John V., "The Wave Resistance of Ships," *Advances in Applied Mechanics*," Vol. 13, ed. by Chia-Shun Yih, 1973.

Appendix A - Correlation and Limitations of Analysis

3.1/3.2 TAYLOR SERIES GEOMETRY AND RESIDUARY RESISTANCE CHECK

A sample input file was used to compare the reported Taylor Standard Series geometry and residuary resistance to that calculated by the hull assessment program. The start of the input file is shown below:

```

1      2      3      4      5      6      7      8      9      10
2      "TSS Cm, FFG-7 Dims, Frigate Environment Resistance Optimization"
3      Starting inputs and limits on variation:
4      "Displacement, m^3"      Low      High      Vary? Yes or no.
5      1000      0.02      0.03      0
6      Cv      Low      High
7      1.02E-03      0.00101      0.004      1
8      B/T      Low      High
9      2.26      2.251      3.749      0
10     Cp      Low      High
11     0.62      0.581      0.659      0
12     LCB      Low      High
13     0      -0.01      0.015      0
14     Cm      Low      High
15     0.915      0.7      0.99      0

```

The first hull iteration properties, which should match those in the first column above, were calculated as follows:

HYDROSTATIC DATA			
	Total	FWD	AFT
Rho, water	999.00	kg/m ³	
Molded Vol.	1004.84	m ³	
Displ.	1003.84	mt	
Displ.	987.97	LT	
LCB	-0.270	m fwd of midships	
LCB	-0.0027	frac. of LWL fwd of midships	
VCB	1.587	m ABL	
Cs	2.563	w/o obliquity	
Csobl	2.567	w/ obliquity	
WSgirth	809.795	m ² w/o obliquity	
WSobl	810.887	m ² w/ obliquity	

Cb	0.570			
Cm	0.916			
Cpl	0.622	Cpf 0.618	Cpa 0.627	
B/T	2.260			
Cv	0.00102			
DLR	29.284			
LCF	-4.596	m fwd. midships		
KMt	2.709	m		
KMl	238.769	m		
Cwp	0.720	Cwvf 0.627	Cwpa 0.814	
Cvp	0.393	Cvpf 0.902	Cvpa 0.706	
LWL	99.342			
B	6.333			
T	2.802			

The wetted surface charts in Goertler, 1954 give a 2.5425 C_s actual value, vs. 2.567 C_s calculated in the program with obliquity calculation, which is a +0.9% error in C_s . An error of this magnitude is reasonable, especially since: (a) the stern cutaway profile is only crudely accounted for using the current system of waterlines in the hull assessment program, and (b) the sectional area shifting method of Lackenby, 1950, which is used to achieve desired values of C_p , is not identical to the sectional area shifts of the Taylor Standard Series.

The residuary resistance of the Taylor Series calculated using linear data interpolation in the hull assessment program is compared below to the resistance given in published references. Note that the speeds are given in speed-length ratio, and the value η_r is the traditional lb/long ton residuary resistance.

```
EDU>> finalplot
speeds =
  0.44312967086318
  0.49852087972108
  0.60930329743687
  0.72008571515267
  0.83086813286846
  0.94165055058426
  1.05243296830005
  1.16321538601585
  1.27399780373164
  1.38478022144744
  1.49556263916323
  1.66173626573693
  1.71712747459482
  1.77251868345272
  1.82790989231062
```

```

crs =
0.00023243151893      Goertler, 1954:
0.00023243151893      ~0.00023
0.00023243151893      ~0.00023
0.00023199212022      ~0.00024
0.00023770507771      ~0.00024
0.00030684220559      ~0.00026
0.00048447528542      ~0.00046
0.00060696004836      ~0.00056
0.00071616752237      ~0.00065
0.00100805058144      ~0.00096
0.00135252619443      ~0.00132
0.00158121776569      ~0.00155
0.00170308664443      ~0.00167
0.00171380810267      ~0.00168
0.00169489767240      ~0.00166
0.00166996166122      ~0.00165
etar =
0.36273874587397      Taylor, Speed and Power of Ships
0.45921519506330
0.68447622546918
0.97962611276610
1.68367700874389
3.41468386628218      ~3.5
5.34397013955281
7.70162229152497
13.00422517440158
20.61516759175974
28.11207408969263      ~28
37.38009667360883
40.16289030089124      ~38.5
42.32677317335255
44.34915141906856      ~44.89

```

Considering that the wetted surface calculation has a small error which shows up in the C_R values, that the R_R or eta_r values have been determined from the Goertler reanalysis and not the original Taylor analysis, that the error in reading values from the Goertler charts can be large, and that the interpolation is linear, these results are generally satisfactory.

At low values of volumetric coefficient, C_V the program has been adjusted to produce residuary resistance values, eta_r , that are linearly proportional to C_V below 1.0×10^{-3} , as a gross approximation. This feature is confirmed as working in the output below, which is identical to the example case run above, except that it is run at half the volumetric coefficient.

```

EDU>> finalplot
speeds =

```



```

0.44310517520477
0.49849332210537
0.60926961590656
0.72004590970776
0.83082220350895
0.94159849731014
1.05237479111134
1.16315108491253
1.27392737871372
1.38470367251492
1.49547996631611
1.66164440701790
1.71703255391850
1.77242070081909
1.82780884771969
crB =
1.0e-003 *
0.08441309169245
0.08441309169245
0.08423950794876
0.08625301888414
0.11139271244555
0.17482138277083
0.21737172351003
0.25741022660465
0.36188030271147
0.48461135853275
0.56316385922428
0.60736101694105
0.60979213035106
0.60362356379623
0.59501509963114
etar =
0.18618492478353
0.23560628636617
0.35126819504560
0.50237753060597
0.86363720962901
1.74106081463549
2.70430135798667
3.91226328264750
6.59681749130256
10.43772314566356
14.14848936614747
18.83786235308628
20.19433726067997
21.30202423717617
22.33024582473756

```

Also the extension to high speed based upon Graff, et al, 1964 is validated to correctly

scale high speed residuary resistance:

```

EDU>> finalplot
speeds =
1.09994592455354
1.19994100882817
1.29993609310280

```

1.39993117688395
 1.49992626115859
 1.59992134493974
 1.69991642921437
 1.79991151348900
 1.89990659727015
 1.99990168154478
 2.09989676532593
 2.29988693387519
 2.39988201765635
 2.49987710193098
 2.99985252231717

crs =

1.0e-003 *
 0.22628102109337
 0.27323788632992
 0.38856406482785
 0.49876515979448
 0.56552208096352
 0.59773254585555
 0.61128190229067
 0.60018961065372
 0.58093714493898
 0.54839653511892
 0.52449924555623
 0.48330072151372
 0.46472671245915
 0.44739379590062
 0.37397651046476

etar =

3.07546498585301
 4.41931994751373
 7.37530536413692
 10.98054905094257
 14.29170753191183
 17.18626654557904
 19.84301933391682
 21.84165379526538
 23.55687197856203
 24.63886041696803
 25.97978140594644
 28.71687830305927
 30.06575783613592
 31.40828559886957
 37.80409707264553

Export file for percent increase in residuary resistance of TSS above $F_n = 0.60$

F_n

0.6 0.65 0.7 0.75 0.8 0.85 0.9

% of $F_n = 0.60$ Rr

1 1.091644621 1.183950617 1.274801587 1.365784832 1.44627425 1.535714286

The limits of applicability of the Taylor Series data depend not only upon the limits of the Taylor Series data and extensions, but also upon the number of data files that have been used in

the current version of the hull assessment program. The user is referred to the Calm Water Resistance chapter for the latest description of the data included.

3.2 FUNG RESIDUARY RESISTANCE REGRESSION

The residuary resistance regression equations of Fung and Leibman, 1998, that were used in one of the modules of the hull assessment program were correlated against the sample given in that paper. A hard-coded version of the program (correlationfung98.m) was used with variables equal to those used in the paper. The resulting values of C_R matched those given in the paper exactly, confirming that the roughly 774 regression coefficients and terms were entered correctly:

```
EDU>> correlationfung98
input_speed_kts =
    10
    12
    14
    16
    18
    20
current_lwl =
    3.2644000000000000e+002
WSobl =
    16146
rho =
    1.9905000000000000
g =
    32.1740000000000000
Ta_ratio =
    0.1320000000000000
Cp_current =
    0.6330000000000000
Bt_ratio =
    1
B_over_T =
    3.2760000000000000
ie =
    12.9000000000000000
Cv_current =
    0.0029709400000000
Cx =
    0.8050000000000000
Fung constants file can be read.
Opening file:
1998 Fung Regression Coefficients
```

```

Cr =
0.00083522384179
0.00110821281314
0.00132685990155
0.00171054347356
0.00219124441921
0.00233944585942

```

EDU>>

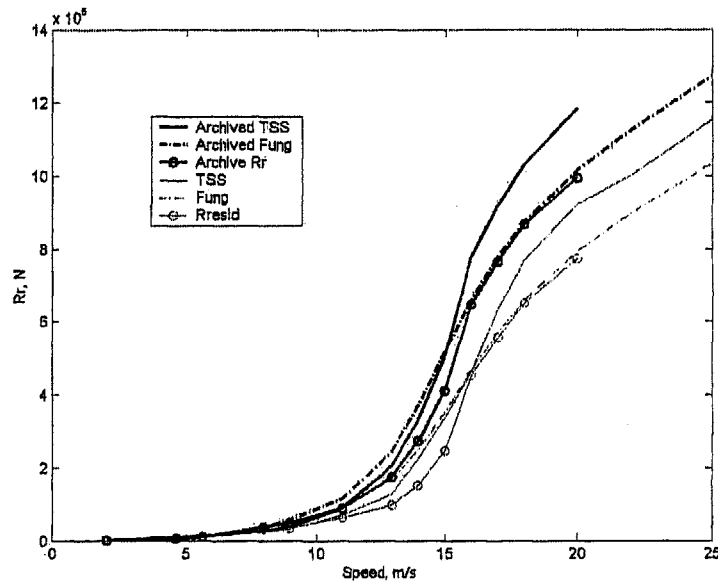


Fig. 3.2-1 A comparison (for two different hull proportions) of the residuary resistance estimates of the: Taylor Standard Series; the Fung regression; and the parent hull worm curve factor times the Taylor Series estimate. As reported by Fung, that regression is accurate at higher speeds, but not as accurate at low speeds. The mathematical wave resistance function used in the regression tends to smooth the resistance curve at low speed.

The limits of the data used to create the Fung regression equations are given in Table 1 of the Fung and Leibman, 1998 paper. For reliable power prediction the paper suggests that the characteristics of a hull form evaluated with the regression equations lie within one standard deviation of the mean value of the characteristics of the original data set.

Table A-1 Database used to develop Fung and Leibman, 1998, residuary resistance regression.

Hull Form Parameter	Number of Observations	Minimum Value	Maximum Value	Mean Value	Standard Deviation
$\Delta/(L_{WL}/100)^3$	739	16.239	359.180	76.871	52.828
FB/L _{WL}	730	0.481	0.591	0.525	0.021
C _{WS}	721	14.324	23.673	16.073	1.051
I _E (deg)	739	2.600	31.730	11.140	4.301
L _{WL} /B _x	739	2.520	17.935	8.018	2.114
B _x /T _x	739	1.696	10.204	3.530	0.856
C _p	739	0.526	0.774	0.625	0.039
A ₂₀ /A _x	739	0.000	0.740	0.158	0.160
C _x	739	0.556	0.994	0.763	0.090
B ₂₀ /B _x	685	0.000	1.000	0.577	0.261
C _{WP}	510	0.662	0.841	0.762	0.036
T ₂₀ /T _x	683	0.000	0.770	0.212	0.146

Note that the term given in the table, FB/L_{WL}, is the LCB/L_{WL} from the forward perpendicular.

3.3 SHALLOW WATER RESISTANCE

Extensive comparisons were made using Excel between the reported shallow water resistance data given in Graff, et al, 1964 and the digitized values used in the present study, and the agreement was found to be satisfactory.

When using the Graff, et al 1964 data it is important to remember the limits are for a minimum water depth of 5% of length, and the maximum water depth for which data is available is 33.3% of length. Extrapolations are made in the hull assessment program to allow estimation of shallow water wavemaking resistance at greater water depths. The user is referred to the chapter on Shallow Water Resistance for further information on the current limits and configuration of the program.

Thin-ship theory was also used to estimate shallow-water wavemaking resistance. To validate that the thin-ship theory calculation routine was functioning properly, a sample case matching one provided in Kirsch, 1966 was run for the wavemaking resistance of a wall-sided wigley hull, for both a deep and shallow water. The results are shown in the Figure A-1. The ratio between shallow water and deep water wavemaking resistance matched exactly to the 111% value provided in the paper. The absolute magnitudes were somewhat smaller than the values provided in the paper. There are several explanations for this value being smaller than that calculated in the original paper, generally stemming from the fact that the final answer is sensitive to integration step size and termination value. It was found that the larger the step size used in the numerical integration of wavemaking resistance, the larger the final resistance value became. Since the original paper was written in the mid-1960's the fine level of step size used in the current study was probably not achieved, and therefore the answer in the original paper could be expected to be slightly larger. Also the current study terminated the integration probably 1-2% short of the total "infinite" integral solution.

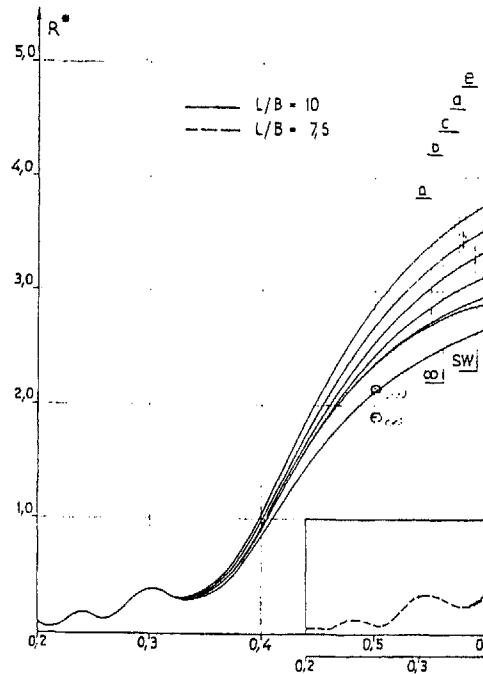


Figure A-1 Comparison of deep and shallow water wavemaking resistance for a wall-sided Wigley hull form as plotted by Kirsch, 1966, (Fig. 5(a)), and as calculated for two points (drawn in) in the present study. The ratios between the resistances are identical to those given in the paper, though the magnitudes are smaller for a variety of reasons.

Overall, these discrepancies do not cause any concern since the resistance ratio is what is used in the program, and this agrees quite well with the published results. Also, a comparison between the thin-ship shallow water wavemaking resistance and the data from Graff, et al, 1964 shows qualitative agreement, though the thin-ship values are somewhat larger. It should be reemphasized that thin-ship theory assumes that vessels are wall-sided, and thus it should be expected that thin-ship theory may exaggerate wave resistance effects.

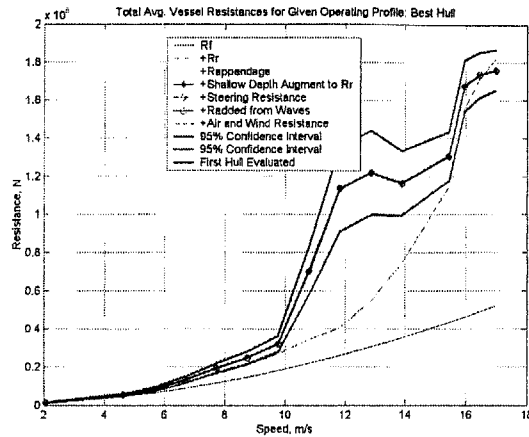


Figure A-2 Shallow water resistance of a vessel with similar proportions to those used in Graff, et al, 1964, calculated using data from that paper.

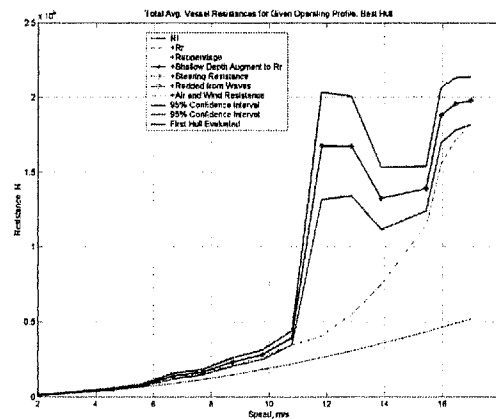


Figure A-3 Similar to Figure A-3 above, but using thin-ship theory shallow water resistance.

3.4/3.5 AIR AND STEERING RESISTANCE

The implementation of the air and steering resistance calculation routines was straightforward and required no major correlation efforts.

3.6 DIRECTIONAL STABILITY

Comparison was made between the directional stability results given for a Taylor Series hull form in Jacobs, 1966, and the results calculated using the same method in the hull assessment program. Unfortunately all of the assumptions and techniques Jacobs used are not fully explained in the paper, especially the details of changing skegs on the standard hull forms

used, and also how the LCG (and therefore the LCB) of a Taylor Series hull form can vary in position as much as 4% of the length, when it should be located nearly at midships.

Evaluating a Taylor Series hull form, number 842, in the bare condition, even without removing the deadwood as done in Fig. 6 of Jacobs, 1966, the stability derivatives and indices are close to those calculated by Jacobs and listed in Table 1 and Fig. 8 of that paper.

HYDROSTATIC DATA

	Total	FWD	AFT
Rho, water	999.00	kg/m ³	
Molded Vol.	0.02	m ³	
Displ.	0.02	mt	
Displ.	0.02	LT	
LCB	0.001	m fwd of midships	
LCB	0.0008	frac. of LWL fwd of midships	
VCB	0.052	m ABL	
Cs	2.564	w/o obliquity	
Csobl	2.579	w/ obliquity	
WSgirth	0.514	m ² w/o obliquity	
WSobl	0.517	m ² w/ obliquity	
Cb	0.494		
Cm	0.915		
Cpl	0.539	Cpf 0.539	Cpa 0.539
B/T	2.920		
Cv	0.00359		
DLR	102.477		
LCF	-0.090	m fwd. midships	
KMt	0.111	m	
KMl	2.347	m	
Cwp	0.649	Cwvf 0.551	Cwpa 0.746
Cvp	0.380	Cvpf 0.895	Cvpa 0.662
LWL	1.829		
B	0.266		
T	0.091		

Hydrostatics program completed running.

Ran loadtss.m

Graff High Speed TSSeries Data file being read.

Opening file:

Export file for percent increase in residuary resistance of TSS above Fn = 0.60

Ran loadspeed.m

Fung constants file can be read.

Opening file:

1998 Fung Regression Coefficients

Operating profile file was read.

Opening file:

1 "Taylor Model Shallow Water Data per Graff, et al."

Operating profile file was read.

Opening file:

1 "B5 Model Shallow Water Data per Graff, et al."

```
archive_sigmal =  
  -100  
tolerance =  
  -1  
rudder_area =  
  1.0000000000000000e-006  
Do =  
  0.01563958341386  
xp_over_lwl =  
  0.02037291752673  
moprime =  
  0.14379334786952  
k1 =  
  0.02495898308238  
k2 =  
  0.95009877422414  
kprime =  
  0.87535854441416  
m1prime =  
  0.00358893573683  
xprime_over_lwl =  
  0.04384848054610  
m2prime =  
  0.14364546575703  
mzprime =  
  0.13234548788830  
total_static_force_rate =  
  0.17237831010359  
total_static_moment_rate =  
  0.14324280339266  
total_rotary_force_rate =  
  -0.15056855697883  
total_rotary_moment_rate =  
  -0.01720259035993  
total_Yrprime =  
  -0.00318627337247  
nzprime =  
  0.01818520326811  
sigmal =  
  1.26581867291999  
sigmal_regression =  
  -0.70149628508781  
sigmal =  
  1.26581867291999
```

However the previous test did not include the option to evaluate a skeg, and did not use the hull form with cutaway deadwood aft that Jacobs used.

Including the skeg in the calculation of stability derivatives, as done in Jacobs, 1966 with the skeg assumed to reach the DWL and the center of pressure assumed to be at the trailing edge,

the results also match those in Fig. 8 of Jacobs, 1966 well, even though the hull form used is not exactly the same as the modified version used by Jacobs:

```
EDU>> direction
archive_sigmal =
  -100
tolerance =
  -1
rudder_area =
  1.0000000000000000e-006
hf =
  0.09125786206491
xf_over_lwl =
  -0.50078890819941
Do =
  0.01563958341386
xp_over_lwl =
  0.02037291752673
moprime =
  0.14379334786952
k1 =
  0.02495898308238
k2 =
  0.95009877422414
kprime =
  0.87535854441416
m1prime =
  0.00358893573683
xprime_over_lwl =
  0.04384848054610
m2prime =
  0.14364546575703
mzprime =
  0.13234548788830
total_static_force_rate =
  0.32910228224565
total_static_moment_rate =
  0.06475717649497
total_rotary_force_rate =
  -0.07208293008113
total_rotary_moment_rate =
  -0.05650732176337
total_Yrprime =
  0.07529935352522
nzprime =
  0.01818520326811
sigmal =
  -0.76387961168213
sigmal_regression =
  -0.70149628508781
sigmal =
  -0.76387961168213
archive_sigmal =
  -0.76387961168213
EDU>>
```

Using a bare hull scaled from the Jacobs, 1966 paper:

```
archive_signal =
  -100
tolerance =
  -1
rudder_area =
  1.0000000000000000e-006
Do =
  0.01523157365007
xp_over_lwl =
  0.04401427977523
moprime =
  0.14383114240608
k1 =
  0.02495898308238
k2 =
  0.95009877422414
kprime =
  0.87535854441416
mlprime =
  0.00358987905003
xprime_over_lwl =
  0.07135375953918
m2prime =
  0.13498885414849
mzprime =
  0.12436985509854
total_static_force_rate =
  0.17197030033981
total_static_moment_rate =
  0.13829041836414
total_rotary_force_rate =
  -0.15431246472179
total_rotary_moment_rate =
  -0.02027968866853
total_Yrprime =
  -0.00689144326568
nzprime =
  0.01700620035965
sigma1 =
  1.23624766076241
sigma1_regression =
  -0.75697077207491
sigma1 =
  1.23624766076241
archive_signal =
  1.23624766076241
```

Using a hull scaled from the Jacobs, 1966 paper and the full skeg in that paper for model

842:

```
archive_signal =
  -100
tolerance =
  -1
```

```

rudder_area =
  1.0000000000000000e-006
hf =
  0.09125786206491
xf_over_lwl =
  -0.50067404331520
Do =
  0.01523157365007
xp_over_lwl =
  0.04401427977523
moprime =
  0.14383114240608
k1 =
  0.02495898308238
k2 =
  0.95009877422414
kprime =
  0.87535854441416
m1prime =
  0.00358987905003
xprime_over_lwl =
  0.07135375953918
m2prime =
  0.13498885414849
mzprime =
  0.12436985509854
total_static_force_rate =
  0.32869427248186
total_static_moment_rate =
  0.05982279354736
total_rotary_force_rate =
  -0.07584483990501
total_rotary_moment_rate =
  -0.05956639165489
total_Yrprime =
  0.07157618155110
nzprime =
  0.01700620035965
sigma1 =
  -0.82192215106852
sigma1_regression =
  -0.75697077207491
sigma1 =
  -0.82192215106852
archive_sigma1 =
  -0.82192215106852

```

The comparisons between the current study's results and Jacobs, 1966 for model 842 are given in Table A-2.

Table A-2 Comparison between directional stability characteristics calculated for a Taylor Series model and characteristics given in Jacobs, 1966. Basic hulls identical except for LCB/LCG characteristics noted below.

	Jacobs Bare	HAP Bare Jacobs Hull	Jacobs w/ Skeg	HAP Jacobs Hull w/ Skeg
LCG/LWL from bow	.52	.50	-	-
k1	.020	.025	-	-
k2	.960	.950	-	-
kprime	.885	.875	-	-
mopprime	.145	.144	-	-
m1prime	.003	.0036	-	-
m2prime	.129	.135	-	-
mzprime	.119	.124	-	-
nzprime	.0165	.017	-	-
xprime/LWL	.110	.0714	-	-
xp/LWL	.091	.044	-	-
Do	.014	.015	-	-
Sigma 1	~1.21	1.24	~- .829	-.822
Ybeta prime	~.169	.172	~.32	.329
Nbeta prime	~.142	.138	~.063	.0598
Yr prime	~-.017	-.007	~.063	.0716
Nr prime	~-.026	-.0203	~-.063	-.0596

Sigma 1 is the item of primary importance, the indicator of directional stability (directionally stable if this value is negative) or not. Some values from the original paper were read from small graphs, and therefore the comparison is by necessity approximate. Nevertheless, the agreement between the characteristics given in the paper and those calculated using the present paper is good, considering the necessary interpolations, integrations, and especially considering that the LCG/LCB placement of the hull used in the original paper is uncertain (since if these were truly shifted, as suggested by the paper, then these hull forms would no longer be standard series hulls).

The limits of use for the directional stability evaluation method of Jacobs, 1966 is for deep water and for speeds where wavemaking does not become a significant contributor to the hull forces. Figure 1. of Harper and Scher, 2001, shows that maneuvering is strongly affected by speeds above Fn 0.3-0.4 for a wide variety of ships. Therefore this directional stability evaluation is probably valid up to similar Froude numbers.

3.7 SEAKEEPING AND ADDED RESISTANCE

To summarize the seakeeping and added resistance correlation study, the following conclusions were drawn:

- The Bhattacharyya, 1978 seakeeping motions method worked most reliably and was used for the final program. Comparisons of seakeeping calculations published in Bhattacharyya matched well.
- This approach also provided the best input data to the added resistance method used, Salvesen, 1978. However, the Bhattacharyya method has a 90° phase shift compared to the typically used seakeeping methods as described in Lewis, 1988 or Salvesen, et al, 1970, because it assumes a sine versus the standard cosine wave. Therefore when using the Salvesen, 1978 added resistance method, the imaginary part of the final resistance equation was used to account for the phase shift instead of using the usual real part of the expression.
- Bhattacharyya, 1978 uses a coordinate system at the LCG, while Lewis, 1988 uses a coordinate system located at midships. Lewis, 1988 also uses a more modern formulation of the seakeeping excitation force equation that drops some of the slender-body theory terms. The Lewis, 1988 method never gave a satisfactory added resistance, probably because of phase angle issues and the section calculation issues mentioned below.
- The use of Lewis-form two-dimensional sectional added mass and damping data from Bhattacharyya, 1978 and Grim, 1960 as opposed to a more time-consuming but precise Rankine-panel method, is probably causing some deviations from the published results. Added resistance in particular is very sensitive to the type of section calculations and motion calculations used. At frequencies at which added resistance is insignificant, errors in the added mass and damping

probably accounted for the slight negative added resistance observed in some cases. This was zeroed-out in the actual program.

- Seakeeping calculations in general, but especially phase angle, were quite sensitive to the number of stations used to evaluate the hull.

- The phase angle calculation had the worst agreement of any quantity between the calculation methods and published results, including model tests of Gerritsma, 1960. The poor agreement with Vossers, 1959-1960 could be excused because the calculation method used in those papers was quite dated, was based on even earlier section calculation methods than used in the present study, and it was not clear if all of the coupling terms were included in those papers.

- Overall, exact comparisons were very difficult to make because small discrepancies crept into the calculations for various reasons (even the available offsets from Todd, 1963 did not exactly match the station system used in other calculations, as Todd ended his stations at the AP, not the DWL, and there were some strange concavities in the wall-sided sections in some of the published offsets). The current seakeeping and added resistance method provides an approximate engineering estimate for added resistance, but should not be relied upon for detailed seakeeping investigations without further work.

SERIES 60 COMPARISON – BHATTACHARYYA 1978

A comparison calculation was made with the head seas seakeeping calculation presented by Bhattacharyya, 1978, p.191. This case uses a $C_b = 0.80$ Series 60 hull form, with a wavelength of 100% L_{WL} , and a $F_n = 0.193$. A similar case is presented in Gerritsma, 1960, except that the B/T ratio is slightly larger (2.51 vs. 2.266 in Bhattacharyya), the LCF/LCB differ, and the wave amplitude is larger. The Gerritsma, 1960 case and also the Vossers, 1959 and

1960, published results for Series 60 hull forms can be used for additional validation. The $C_b = 0.60$ case appears to be for the same model in Gerritsma, 1960 and Vossers, 1959 and 1960.

The program developed here uses a 21-station calculation routine, while the simplified example presented in Bhattacharyya uses only five stations. Also the current program uses metric values, although the output used for comparison purposes was also converted into English-system units to match the published results.

The basic defining geometry, masses, gyradii, etc. were matched to the published results. Hull offsets provided by Todd, 1963, were used in the current program to determine hydrostatics. Because these more accurate offsets were used in the present calculation, the values did not exactly match those used by Bhattacharyya. This was especially true near the stern, where the real section drafts and beam differ from the simplified 5-station values. Fortunately the current program allowed the LCB position to be shifted to match the value given by Bhattacharyya. An example of the validation output is provided below:

```
EDU>> seas
Cb          0.805
           SEAKEEPING VALIDATION OUTPUT
Lwl         5.852 m          19.199 ft
B           0.790 m          2.591 ft
T           0.348 m          1.143 ft
Displ.      12699.302 N      2855.059 lb
LCG +fwd    0.146 m          0.480 ft
LCB +fwd    0.146 m          0.480 ft
Speed       1.459 m/s        4.787 ft/s
Gyradius    1.393 m          4.569 ft
Ampl.       0.061 m          0.200 ft
Rho         999.000 kg/m^3    1.938 slug/ft^3 or lb
s^2/ft^4
ww          3.245 rad/s
we          4.812 rad/s
Station     Bn,m  Bn,ft  Tn,m  Tn,ft  Sn,m^2  Sn,ft^2
-----
0.000      0.000  0.000  0.000  0.000  0.000  0.000
1.000      0.408  1.338  0.348  1.143  0.124  1.337
2.000      0.651  2.137  0.348  1.143  0.203  2.185
```

3.000	0.759	2.491	0.348	1.143	0.247	2.656
4.000	0.789	2.587	0.348	1.143	0.268	2.882
5.000	0.790	2.591	0.348	1.143	0.274	2.952
6.000	0.790	2.591	0.348	1.143	0.275	2.962
7.000	0.790	2.591	0.348	1.143	0.275	2.962
8.000	0.790	2.591	0.348	1.143	0.275	2.962
9.000	0.790	2.591	0.348	1.143	0.275	2.962
10.000	0.790	2.591	0.348	1.143	0.275	2.962
11.000	0.790	2.591	0.348	1.143	0.275	2.962
12.000	0.790	2.591	0.348	1.143	0.275	2.961
13.000	0.790	2.591	0.348	1.143	0.274	2.948
14.000	0.790	2.591	0.348	1.143	0.268	2.886
15.000	0.781	2.561	0.348	1.143	0.252	2.710
16.000	0.744	2.441	0.348	1.143	0.222	2.391
17.000	0.673	2.209	0.348	1.143	0.179	1.923
18.000	0.564	1.850	0.348	1.143	0.124	1.331
19.000	0.399	1.308	0.348	1.143	0.058	0.626
20.000	0.126	0.415	0.083	0.272	0.005	0.050

The added mass coefficient, C, and amplitude ratio, Abar, were interpolated in the current program from the Bhattacharyya data on pages 41 and 44 (these charts were also checked against the original source of Grim, 1960). The values which were interpolated matched well considering that the sections were slightly different between our calculation and the published results, and that linear interpolation was used:

EDU>> Station	C	Abar	Bhatt C,	Bhatt Abar
0.000	1.999	0.000	0	0
1.000	0.709	0.411		
2.000	0.748	0.592		
3.000	0.827	0.638		
4.000	0.925	0.590		
5.000	0.979	0.552	.98	.57
6.000	0.963	0.563		
7.000	0.986	0.547		
8.000	0.963	0.563		
9.000	0.963	0.563		
10.000	0.963	0.563	.98	.57
11.000	0.963	0.563		
12.000	0.986	0.547		
13.000	0.976	0.554		
14.000	0.925	0.590		

15.000	0.809	0.663	.84	.66
16.000	0.694	0.716		
17.000	0.577	0.738		
18.000	0.516	0.694		
19.000	0.518	0.534		
20.000	1.223	0.232	0	0

The A_{33} term matches the Bhattacharyya results well considering the small number of stations used for the published results.

A33 term:	Bhatt. Method	1023.5 kg	70.1 slug or lb s ² /ft
A33 term:	PNA Method	1023.5 kg	70.1 slug
Bhatt. published:			75.6 lb s ² /ft

The longitudinal coordinates of the various stations differ depending on whether the Bhattacharyya method is used (distance to LCG, assumed to equal the LCB), or the method shown in Lewis, 1988 (PNA) is used, which measures distance from midships. The calculation matches the published values using the Bhattacharyya method.

	Bhatt. Method x m, ft		PNA Method x m, ft	
0.00	2.78	9.12	2.93	9.60
1.00	2.49	8.16	2.63	8.64
2.00	2.19	7.20	2.34	7.68
3.00	1.90	6.24	2.05	6.72
4.00	1.61	5.28	1.76	5.76
5.00	1.32	4.32	1.46	4.80
6.00	1.02	3.36	1.17	3.84
7.00	0.73	2.40	0.88	2.88
8.00	0.44	1.44	0.59	1.92
9.00	0.15	0.48	0.29	0.96
10.00	-0.15	-0.48	0.00	0.00
11.00	-0.44	-1.44	-0.29	-0.96
12.00	-0.73	-2.40	-0.59	-1.92
13.00	-1.02	-3.36	-0.88	-2.88
14.00	-1.32	-4.32	-1.17	-3.84
15.00	-1.61	-5.28	-1.46	-4.80
16.00	-1.90	-6.24	-1.76	-5.76
17.00	-2.19	-7.20	-2.05	-6.72
18.00	-2.49	-8.16	-2.34	-7.68
19.00	-2.78	-9.12	-2.63	-8.64
20.00	-3.07	-10.08	-2.93	-9.60

The (added) mass moment of inertia for pitching, A_{55} , is seriously undercounted in the published Bhattacharyya example, probably because of the lack of stations evaluated near the extreme ends of the hull. This discrepancy could seriously influence the pitch motion results.

Bhatt. Published: 1368.5 lb s² ft
 A55 term: Bhatt. Method 1772.4 kg m² 2403.0 lb s² ft
 A55 term: PNA Method 1891.9 kg m² 2565.0 lb s² ft
 (Note that this comparison is in error because of a conversion problem from metric to English.)

The damping term B_{33} matches well:

Bhatt. published: 106.7 lb sec/ft
 B33 term: Bhatt. Method 1699.0 N sec/m 116.4 lb sec/ft
 B33 term: PNA Method 1699.0 N sec/m 116.4 lb sec/ft

Like the A_{55} term, the B_{55} term does not compare well because of the lack of stations used in the published results (note that Vossers, 1959 and 1960 recommends 20 stations be used for acceptable accuracy):

Bhatt. published: 2105.9 ft lb s/rad
 B55 term: Bhatt. Method 4702.9 N m s/rad 3468.7 ft lb s/rad
 B55 term: PNA Method 4710.3 N m s/rad 3474.2 ft lb s/rad

The B_{53} and B_{35} pitch-heave damping coupling terms agree within reasonable limits:

Bhatt. published: -249.7 lb s²/s
 B53 term: Bhatt. Method -860.7 N s²/s -193.5 lb s²/s
 B53 term: PNA Method -1109.2 N s²/s -249.4 lb s²/s

Bhatt. published: 473.9 lb s²/s
 B35 term: Bhatt. Method 2125.9 N s²/s 477.9 lb s²/s
 B35 term: PNA Method 1877.3 N s²/s 422.0 lb s²/s

The spring constants also match approximately:

Bhatt. published: 2588.5 lb/ft
 C33 term: Bhatt. Method 39673.8 N/m 2718.5 lb/ft
 C33 term: PNA Method 39673.8 N/m 2718.5 lb/ft

Bhatt. published: 49501.6 ft lb/rad

C55 term: Bhatt. Method 92108.9 N m/rad 67936.1 ft lb/rad
 C55 term: PNA Method 93505.0 N m/rad 68965.8 ft lb/rad

The A_{35} and A_{53} terms do not match well, but are of small magnitudes:

Bhatt. published $A_{35}=A_{53}=$			14.27 lb s ²
A35 term: Bhatt. Method	-11.8 N s ²		-2.6 lb s ²
A35 term: PNA Method	-268.6 N s ²		-60.4 lb s ²
A53 term: Bhatt. Method	-11.8 N s ²		-2.6 lb s ²
A53 term: PNA Method	-54.5 N s ²		-12.2 lb s ²

The C_{35} and C_{53} terms do not match well either, but again are small compared with the other spring constant terms (the coordinate systems, as well the different formulations, accounts for the differences between the Bhattacharya and PNA methods):

Bhatt. published:			1753.2 lb [/rad for all]
C35 term: Bhatt. Method	7260.4 N	1632.2 lb	
C35 term: PNA Method	-1005.0 N	-225.9 lb	
Bhatt. published:			1242.5 lb [/rad for all]
C53 term: Bhatt. Method	4781.6 N	1075.0 lb	
C53 term: PNA Method	-1005.0 N	-225.9 lb	

The calculated forces and moments do not agree well with those published in Bhattacharyya, 1978, possibly because of all the accumulated differences listed up to this point. It should be noted that Bhattacharyya, 1978 uses a seaway based upon a sine form, while Lewis, 1988 appears to use a seaway based on a cosine form. The phase angles should therefore be expected to differ by 90-degrees in the results presented below.

Bhatt. published:					
F1 term: Bhatt. Method	-67.3 N	-15.1 lb			
Bhatt. published:			7.157 lb		
F2 term: Bhatt. Method	-159.6 N	-35.9 lb			
Force term: PNA Method	22.3 N	5.0 lb real	46.5 N	10.4	
		lb imag			
Bhatt. published:			372.6 ft lb		
M1 term: Bhatt. Method	616.1 N m	454.4 ft lb			
Bhatt. published:			-231.79 ft lb		

M2 term: Bhatt. Method -147.1 N m -108.5 ft lb
Moment term: PNA Method 189.0 Nm 139.4 ftlb real 1117.9 Nm
824.5 ftlb imag

Bhatt. published: 133.7 deg
Force Phase: Bhatt. Method -112.9 deg
Force Phase: PNA Method 64.4 deg

Bhatt. published: -31.9 deg
Moment Phase: Bhatt. Method -13.4 deg
Moment Phase: PNA Method 80.4 deg

The motion amplitudes determined from the traditional solution equation, which assumes that the origin is located at the LCG, are similar to the published results, despite all the differences noted above. The phase angles do not match well.

Bhatt. published: 3.935e-2 ft
Heave Ampl Bhatt. method: 1.4e-002 m 4.6e-002 ft
Bhatt published: -89.95 deg
Heave Phase Bhatt. method: 4.5e-002 rad 2.6 deg

Bhatt. published: 1.04 deg
Pitch Ampl Bhatt. method: 2.3e-002 rad 1.3e+000 deg
Bhatt. published: 178.42 deg
Pitch Phase Bhatt. method: -2.0e+000 rad -117.1 deg

A solution of the Bhattacharyya, 1978 method, and the Lewis, 1988 method, is presented below:

Matrix Solution to Bhatt. Method:

Bhatt. published: 3.935e-2 ft
Heave Ampl Bhatt. method: 1.4e-002 m 4.6e-002 ft
Bhatt published: -89.95 deg
Heave Phase Bhatt. method: 4.5e-002 rad 2.6 deg

Bhatt. published: 1.04 deg
Pitch Ampl Bhatt. method: 2.3e-002 rad 1.3e+000 deg
Bhatt. published: 178.42 deg

Pitch Phase Bhatt. method: -2.0e+000 rad -117.1 deg

Matrix Solution to PNA Method:

Bhatt. published: 3.935e-2 ft
 Heave Ampl PNA method: 3.5e-002 m 1.1e-001 ft
 Bhatt published: -89.95 deg
 Heave Phase PNA method: 9.2e-001 rad 52.7 deg

Bhatt. published: 1.04 deg
 Pitch Ampl PNA method: 4.6e-002 rad 2.6e+000 deg
 Bhatt. published: 178.42 deg
 Pitch Phase PNA method: -3.1e-001 rad -17.5 deg

A comparison with the results published in Gerritsma, 1960, for a $C_b = 0.60$ ship, $Fn = 0.20$, wavelength/ $L_{WL} = 1$, $A/L_{WL} = 1/48$, shows that the heave amplitude is larger, the pitch amplitude is much larger, and the phase lag of heave after pitch is about twice the published results. (Bhatt. method phase lag = 118.2-deg, PNA = 137.1-deg, published = 63-deg.)

wave_ampl =

0.0508000000000000

Cb 0.614

SEAKEEPING VALIDATION OUTPUT

Lwl 2.437 m 7.996 ft
 B 0.325 m 1.068 ft
 T 0.130 m 0.427 ft
 Displ. 621.159 N 139.649 lb
 LCG +fwd -0.036 m -0.119 ft
 LCB +fwd -0.036 m -0.119 ft
 Speed 0.978 m/s 3.209 ft/s
 Gyradius 0.609 m 1.999 ft
 Ampl. 0.051 m 0.167 ft
 Rho 999.000 kg/m³ 1.938 slug/ft³ or lb
 s²/ft⁴

ww 5.026 rad/s

we 7.545 rad/s

Station Bn,m Bn,ft Tn,m Tn,ft Sn,m² Sn,ft²

Station	Bn,m	Bn,ft	Tn,m	Tn,ft	Sn,m ²	Sn,ft ²
0.000	0.000	0.000	0.000	0.000	0.000	0.000
1.000	0.034	0.110	0.130	0.427	0.004	0.039
2.000	0.075	0.247	0.130	0.427	0.008	0.088
3.000	0.129	0.423	0.130	0.427	0.014	0.148
4.000	0.185	0.606	0.130	0.427	0.020	0.217
5.000	0.235	0.772	0.130	0.427	0.027	0.288
6.000	0.275	0.902	0.130	0.427	0.033	0.352

7.000	0.302	0.991	0.130	0.427	0.037	0.402
8.000	0.319	1.046	0.130	0.427	0.040	0.435
9.000	0.325	1.068	0.130	0.427	0.042	0.451
10.000	0.325	1.068	0.130	0.427	0.042	0.456
11.000	0.325	1.068	0.130	0.427	0.042	0.454
12.000	0.325	1.068	0.130	0.427	0.041	0.446
13.000	0.324	1.062	0.130	0.427	0.040	0.428
14.000	0.318	1.042	0.130	0.427	0.037	0.393
15.000	0.306	1.003	0.130	0.427	0.032	0.342
16.000	0.280	0.920	0.130	0.427	0.026	0.278
17.000	0.238	0.780	0.130	0.427	0.019	0.203
18.000	0.176	0.579	0.130	0.427	0.011	0.124
19.000	0.101	0.333	0.130	0.427	0.005	0.051
20.000	0.027	0.088	0.031	0.102	0.000	0.004

Station C Abar

0.000	1.999	0.000
1.000	1.270	0.127
2.000	0.648	0.553
3.000	0.582	0.381
4.000	0.657	0.484
5.000	0.709	0.570
6.000	0.784	0.629
7.000	0.863	0.625
8.000	0.893	0.626
9.000	0.927	0.614
10.000	0.954	0.595
11.000	0.942	0.604
12.000	0.900	0.633
13.000	0.822	0.684
14.000	0.724	0.738
15.000	0.626	0.800
16.000	0.572	0.810
17.000	0.538	0.746
18.000	0.553	0.611
19.000	0.524	0.363
20.000	1.477	0.116

A33 term: Bhatt. Method 48.5 kg 3.3 slug or lb s²/ft

A33 term: PNA Method 48.5 kg 3.3 slug

Bhatt. Method x m, ft PNA Method x m, ft

0.00	1.25	4.12	1.22	4.00
1.00	1.13	3.72	1.10	3.60
2.00	1.01	3.32	0.97	3.20
3.00	0.89	2.92	0.85	2.80
4.00	0.77	2.52	0.73	2.40
5.00	0.65	2.12	0.61	2.00
6.00	0.52	1.72	0.49	1.60
7.00	0.40	1.32	0.37	1.20
8.00	0.28	0.92	0.24	0.80
9.00	0.16	0.52	0.12	0.40

10.00	0.04	0.12	0.00	0.00
11.00	-0.09	-0.28	-0.12	-0.40
12.00	-0.21	-0.68	-0.24	-0.80
13.00	-0.33	-1.08	-0.37	-1.20
14.00	-0.45	-1.48	-0.49	-1.60
15.00	-0.57	-1.88	-0.61	-2.00
16.00	-0.69	-2.28	-0.73	-2.40
17.00	-0.82	-2.68	-0.85	-2.80
18.00	-0.94	-3.08	-0.97	-3.20
19.00	-1.06	-3.48	-1.10	-3.60
20.00	-1.18	-3.88	-1.22	-4.00
A55 term:	Bhatt. Method	9.3 kg m ²	12.5 lb s ² ft	
A55 term:	PNA Method	10.3 kg m ²	13.9 lb s ² ft	
B33 term:	Bhatt. Method	190.6 N sec/m	13.1 lb sec/ft	
B33 term:	PNA Method	190.6 N sec/m	13.1 lb sec/ft	
B55 term:	Bhatt. Method	65.9 N m s/rad	48.6 ft lb s/rad	
B55 term:	PNA Method	71.3 N m s/rad	52.6 ft lb s/rad	
B53 term:	Bhatt. Method	-20.8 N s ² /s	-4.7 lb s ² /s	
B53 term:	PNA Method	-13.8 N s ² /s	-3.1 lb s ² /s	
B35 term:	Bhatt. Method	74.2 N s ² /s	16.7 lb s ² /s	
B35 term:	PNA Method	81.1 N s ² /s	18.2 lb s ² /s	
C33 term:	Bhatt. Method	5633.6 N/m	386.0 lb/ft	
C33 term:	PNA Method	5633.6 N/m	386.0 lb/ft	
C55 term:	Bhatt. Method	1688.4 N m/rad	1245.3 ft lb/rad	
C55 term:	PNA Method	1815.5 N m/rad	1339.0 ft lb/rad	
A35 term:	Bhatt. Method	1.8 N s ²	0.4 lb s ²	
A35 term:	PNA Method	0.3 N s ²	0.1 lb s ²	
A53 term:	Bhatt. Method	1.8 N s ²	0.4 lb s ²	
A53 term:	PNA Method	6.8 N s ²	1.5 lb s ²	
C35 term:	Bhatt. Method	498.0 N	111.9 lb	
C35 term:	PNA Method	512.2 N	115.1 lb	
C53 term:	Bhatt. Method	311.5 N	70.0 lb	
C53 term:	PNA Method	512.2 N	115.1 lb	
bhatt_force_phase =				
-82.99674928361715				
bhatt_mom_phase =				
-20.55724483716117				
F1 term:	Bhatt. Method	0.3 N	0.1 lb	
F2 term:	Bhatt. Method	-2.6 N	-0.6 lb	
Force term:	PNA Method	27.8 N	6.2 lb real	8.7 N 1.9
lb imag				
M1 term:	Bhatt. Method	46.6 N m	34.4 ft lb	
M2 term:	Bhatt. Method	-17.5 N m	-12.9 ft lb	
Moment term:	PNA Method	3.1 Nm	2.3 ftlb real	63.9 Nm
47.1 ftlb imag				
Force Phase:	Bhatt. Method	-83.0 deg		
Force Phase:	PNA Method	17.3 deg		
Moment Phase:	Bhatt. Method	-20.6 deg		
Moment Phase:	PNA Method	87.2 deg		

Published: 2.6e-2 m
 Heave Ampl Bhatt. method: 3.2e-002 m 1.1e-001 ft
 Heave Phase Bhatt. method: -1.3e-001 rad -7.4 deg

Published: 2.8 deg
 Pitch Ampl Bhatt. method: 8.0e-002 rad 4.6e+000 deg
 Pitch Phase Bhatt. method: -2.2e+000 rad -125.6 deg

Matrix Solution to Bhatt. Method:
 Heave Ampl Bhatt. method: 3.2e-002 m 1.1e-001 ft
 Heave Phase Bhatt. method: -1.3e-001 rad -7.4 deg
 Pitch Ampl Bhatt. method: 8.0e-002 rad 4.6e+000 deg
 Pitch Phase Bhatt. method: -2.2e+000 rad -125.6 deg

Matrix Solution to PNA Method:
 Heave Ampl PNA method: 3.6e-002 m 1.2e-001 ft
 Heave Phase PNA method: 2.2e+000 rad 125.8 deg
 Pitch Ampl PNA method: 1.1e-001 rad 6.5e+000 deg
 Pitch Phase PNA method: -2.0e-001 rad -11.3 deg

This comparison is unsatisfactory, so a comparison will be made with Vossers, 1959 and

1960, below, for $F_n = 0.25$, wavelength/ $L_{WL} = 1.0$.

Cb	0.601					
	SEAKEEPING VALIDATION OUTPUT					
Lwl	2.439 m	8.002 ft				
B	0.325 m	1.067 ft				
T	0.130 m	0.427 ft				
Displ.	608.187 N	136.733 lb				
LCG +fwd	-0.037 m	-0.122 ft				
LCB +fwd	-0.037 m	-0.122 ft				
Speed	1.220 m/s	4.003 ft/s				
Gyradius	0.610 m	2.001 ft				
Ampl.	1.000 m	3.281 ft				
Rho	999.000 kg/m ³	1.938 slug/ft ³ or lb				
s ² /ft ⁴						
ww	5.025 rad/s					
we	8.166 rad/s					
Station	Bn,m	Bn,ft	Tn,m	Tn,ft	Sn,m ²	Sn,ft ²
-----	-----	-----	-----	-----	-----	-----
0.000	0.000	0.000	0.000	0.000	0.000	0.000
1.000	0.032	0.104	0.130	0.427	0.003	0.036
2.000	0.070	0.230	0.130	0.427	0.008	0.082
3.000	0.121	0.397	0.130	0.427	0.013	0.139
4.000	0.176	0.576	0.130	0.427	0.019	0.205

5.000	0.227	0.745	0.130	0.427	0.026	0.276
6.000	0.269	0.882	0.130	0.427	0.032	0.342
7.000	0.299	0.979	0.130	0.427	0.037	0.395
8.000	0.317	1.041	0.130	0.427	0.040	0.432
9.000	0.325	1.067	0.130	0.427	0.042	0.450
10.000	0.325	1.067	0.130	0.427	0.042	0.456
11.000	0.325	1.067	0.130	0.427	0.042	0.453
12.000	0.325	1.067	0.130	0.427	0.041	0.444
13.000	0.323	1.060	0.130	0.427	0.039	0.423
14.000	0.316	1.037	0.130	0.427	0.036	0.386
15.000	0.303	0.993	0.130	0.427	0.031	0.333
16.000	0.275	0.902	0.130	0.427	0.025	0.267
17.000	0.231	0.756	0.130	0.427	0.018	0.192
18.000	0.169	0.555	0.130	0.427	0.011	0.116
19.000	0.097	0.318	0.130	0.427	0.004	0.047
20.000	0.027	0.088	0.031	0.102	0.000	0.004

Station	C	Abar
0.000	1.999	0.000
1.000	1.197	0.140
2.000	0.658	0.572
3.000	0.581	0.369
4.000	0.629	0.501
5.000	0.713	0.591
6.000	0.781	0.646
7.000	0.863	0.640
8.000	0.932	0.611
9.000	0.970	0.594
10.000	0.975	0.591
11.000	0.986	0.584
12.000	0.939	0.617
13.000	0.847	0.686
14.000	0.719	0.793
15.000	0.615	0.869
16.000	0.551	0.866
17.000	0.508	0.799
18.000	0.505	0.645
19.000	0.461	0.384
20.000	1.388	0.136

Published:			37.24 kg	
A33 term:	Bhatt. Method	48.4 kg	3.3 slug	or lb s ² /ft
A33 term:	PNA Method	48.4 kg	3.3 slug	
Bhatt. Method x m, ft		PNA Method x m, ft		
0.00	1.26	4.12	1.22	4.00
1.00	1.13	3.72	1.10	3.60
2.00	1.01	3.32	0.98	3.20
3.00	0.89	2.92	0.85	2.80
4.00	0.77	2.52	0.73	2.40
5.00	0.65	2.12	0.61	2.00

6.00	0.53	1.72	0.49	1.60
7.00	0.40	1.32	0.37	1.20
8.00	0.28	0.92	0.24	0.80
9.00	0.16	0.52	0.12	0.40
10.00	0.04	0.12	0.00	0.00
11.00	-0.08	-0.28	-0.12	-0.40
12.00	-0.21	-0.68	-0.24	-0.80
13.00	-0.33	-1.08	-0.37	-1.20
14.00	-0.45	-1.48	-0.49	-1.60
15.00	-0.57	-1.88	-0.61	-2.00
16.00	-0.69	-2.28	-0.73	-2.40
17.00	-0.82	-2.68	-0.85	-2.80
18.00	-0.94	-3.08	-0.98	-3.20
19.00	-1.06	-3.48	-1.10	-3.60
20.00	-1.18	-3.88	-1.22	-4.00

Publ. 7.25 kg m²
A55 term: Bhatt. Method 8.6 kg m² 11.7 lb s² ft
A55 term: PNA Method 9.9 kg m² 13.4 lb s² ft

Publ. 155.82 N sec/m
B33 term: Bhatt. Method 159.8 N sec/m 11.0 lb sec/ft
B33 term: PNA Method 159.8 N sec/m 11.0 lb sec/ft

Publ. 61.7 N m s/rad
B55 term: Bhatt. Method 57.5 N m s/rad 42.4 ft lb s/rad
B55 term: PNA Method 63.2 N m s/rad 46.6 ft lb s/rad

B53 term: Bhatt. Method -32.8 N s²/s -7.4 lb s²/s
B53 term: PNA Method -26.8 N s²/s -6.0 lb s²/s

B35 term: Bhatt. Method 85.3 N s²/s 19.2 lb s²/s
B35 term: PNA Method 91.2 N s²/s 20.5 lb s²/s
C33 term: Bhatt. Method 5555.3 N/m 380.7 lb/ft
C33 term: PNA Method 5555.3 N/m 380.7 lb/ft
C55 term: Bhatt. Method 1656.0 N m/rad 1221.4 ft lb/rad
C55 term: PNA Method 1769.8 N m/rad 1305.4 ft lb/rad
A35 term: Bhatt. Method 1.6 N s² 0.4 lb s²
A35 term: PNA Method 0.5 N s² 0.1 lb s²
A53 term: Bhatt. Method 1.6 N s² 0.4 lb s²
A53 term: PNA Method 6.4 N s² 1.4 lb s²
C35 term: Bhatt. Method 511.5 N 115.0 lb
C35 term: PNA Method 518.7 N 116.6 lb
C53 term: Bhatt. Method 316.5 N 71.2 lb
C53 term: PNA Method 518.7 N 116.6 lb

bhatt_force_phase =
-94.21147273575444
bhatt_mom_phase =

-21.28474326353453

F1 term: Bhatt. Method -28.7 N -6.4 lb
F2 term: Bhatt. Method -389.1 N -87.5 lb

Publ. 728 N total force vice 517 N PNA
Force term: PNA Method 472.6 N 106.2 lb real 209.9 N 47.2 lb imag
M1 term: Bhatt. Method 810.7 N m 597.9 ft lb
M2 term: Bhatt. Method -315.8 N m -232.9 ft lb

Publ. 931 Nm total vice 1232 Nm PNA
Moment term: PNA Method 20.6 Nm 15.2 ftlb real 1231.8 Nm 908.5 ftlb imag
Force Phase: Bhatt. Method -94.2 deg
Force Phase: PNA Method 23.9 deg
Moment Phase: Bhatt. Method -21.3 deg
Moment Phase: PNA Method 89.0 deg
Heave Ampl Bhatt. method: 3.0e-001 m 9.8e-001 ft
Heave Phase Bhatt. method: -8.7e-001 rad -50.0 deg
Pitch Ampl Bhatt. method: 1.3e+000 rad 7.5e+001 deg
Pitch Phase Bhatt. method: -2.6e+000 rad -148.9 deg
Matrix Solution to Bhatt. Method:
Heave Ampl Bhatt. method: 3.0e-001 m 9.8e-001 ft
Heave Phase Bhatt. method: -8.7e-001 rad -50.0 deg
Pitch Ampl Bhatt. method: 1.3e+000 rad 7.5e+001 deg
Pitch Phase Bhatt. method: -2.6e+000 rad -148.9 deg
Matrix Solution to PNA Method:
Heave Ampl PNA method: 4.8e-001 m 1.6e+000 ft
Heave Phase PNA method: 1.2e+000 rad 67.6 deg
Pitch Ampl PNA method: 1.9e+000 rad 1.1e+002 deg
Pitch Phase PNA method: -6.4e-001 rad -36.8 deg

The results show the following poor comparison to the published results:

Heave amplitude is undersized, with published heave/A = 0.9, Bhatt. = 0.3, PNA = 0.48; Pitch /kA is more accurate, with published = 0.38, Bhatt. = 0.50, PNA = 0.74. Phases have the following comparison:

	Pitch	Heave	Difference
Publ.	-37	-114	-77
Bhatt.	-149	-50	-99
PNA	-36.8	67.6	-104.4

Another comparison will be made with Vossers, 1959 and 1960, below, for $F_n = 0.25$,

wavelength/ $L_{WL} = 2.0$.

Cb 0.601
 SEAKEEPING VALIDATION OUTPUT
 Lwl 2.439 m 8.002 ft
 B 0.325 m 1.067 ft
 T 0.130 m 0.427 ft
 Displ. 608.187 N 136.733 lb
 LCG +fwd -0.037 m -0.122 ft
 LCB +fwd -0.037 m -0.122 ft
 Speed 1.220 m/s 4.003 ft/s
 Gyradius 0.610 m 2.001 ft
 Ampl. 1.000 m 3.281 ft
 Rho 999.000 kg/m³ 1.938 slug/ft³ or lb
 s²/ft⁴

ww 3.553 rad/s

we 5.123 rad/s

Station Bn,m Bn,ft Tn,m Tn,ft Sn,m² Sn,ft²

 0.000 0.000 0.000 0.000 0.000 0.000 0.000
 1.000 0.032 0.104 0.130 0.427 0.003 0.036
 2.000 0.070 0.230 0.130 0.427 0.008 0.082
 3.000 0.121 0.397 0.130 0.427 0.013 0.139
 4.000 0.176 0.576 0.130 0.427 0.019 0.205
 5.000 0.227 0.745 0.130 0.427 0.026 0.276
 6.000 0.269 0.882 0.130 0.427 0.032 0.342
 7.000 0.299 0.979 0.130 0.427 0.037 0.395
 8.000 0.317 1.041 0.130 0.427 0.040 0.432
 9.000 0.325 1.067 0.130 0.427 0.042 0.450
 10.000 0.325 1.067 0.130 0.427 0.042 0.456
 11.000 0.325 1.067 0.130 0.427 0.042 0.453
 12.000 0.325 1.067 0.130 0.427 0.041 0.444
 13.000 0.323 1.060 0.130 0.427 0.039 0.423
 14.000 0.316 1.037 0.130 0.427 0.036 0.386
 15.000 0.303 0.993 0.130 0.427 0.031 0.333
 16.000 0.275 0.902 0.130 0.427 0.025 0.267
 17.000 0.231 0.756 0.130 0.427 0.018 0.192
 18.000 0.169 0.555 0.130 0.427 0.011 0.116
 19.000 0.097 0.318 0.130 0.427 0.004 0.047
 20.000 0.027 0.088 0.031 0.102 0.000 0.004

Station C Abar

 0.000 1.999 0.000
 1.000 1.686 0.055
 2.000 1.331 0.126

3.000	0.951	0.222
4.000	0.837	0.307
5.000	0.822	0.368
6.000	0.810	0.437
7.000	0.869	0.478
8.000	0.910	0.491
9.000	0.914	0.494
10.000	0.915	0.493
11.000	0.915	0.492
12.000	0.909	0.498
13.000	0.893	0.507
14.000	0.842	0.525
15.000	0.747	0.530
16.000	0.766	0.478
17.000	0.805	0.406
18.000	0.864	0.337
19.000	1.077	0.182
20.000	1.759	0.054

Publ. 45.1 kg
A33 term: Bhatt. Method 52.0 kg 3.6 slug or lb s²/ft
A33 term: PNA Method 52.0 kg 3.6 slug

	Bhatt. Method x m, ft		PNA Method x m, ft	
0.00	1.26	4.12	1.22	4.00
1.00	1.13	3.72	1.10	3.60
2.00	1.01	3.32	0.98	3.20
3.00	0.89	2.92	0.85	2.80
4.00	0.77	2.52	0.73	2.40
5.00	0.65	2.12	0.61	2.00
6.00	0.53	1.72	0.49	1.60
7.00	0.40	1.32	0.37	1.20
8.00	0.28	0.92	0.24	0.80
9.00	0.16	0.52	0.12	0.40
10.00	0.04	0.12	0.00	0.00
11.00	-0.08	-0.28	-0.12	-0.40
12.00	-0.21	-0.68	-0.24	-0.80
13.00	-0.33	-1.08	-0.37	-1.20
14.00	-0.45	-1.48	-0.49	-1.60
15.00	-0.57	-1.88	-0.61	-2.00
16.00	-0.69	-2.28	-0.73	-2.40
17.00	-0.82	-2.68	-0.85	-2.80
18.00	-0.94	-3.08	-0.98	-3.20
19.00	-1.06	-3.48	-1.10	-3.60
20.00	-1.18	-3.88	-1.22	-4.00

Publ. 9.1 kg m²
A55 term: Bhatt. Method 11.3 kg m² 15.4 lb s² ft
A55 term: PNA Method 14.6 kg m² 19.8 lb s² ft

Publ. 296 N sec/m

B33 term: Bhatt. Method 286.2 N sec/m 19.6 lb sec/ft
 B33 term: PNA Method 286.2 N sec/m 19.6 lb sec/ft

 Publ. 93.1 N m s/rad
 B55 term: Bhatt. Method 72.4 N m s/rad 53.4 ft lb s/rad
 B55 term: PNA Method 91.2 N m s/rad 67.3 ft lb s/rad

 Publ. 131 N s²/s
 B53 term: Bhatt. Method -33.5 N s²/s -7.5 lb s²/s
 B53 term: PNA Method -22.8 N s²/s -5.1 lb s²/s

 Publ. 19.6 N s²/s
 B35 term: Bhatt. Method 93.4 N s²/s 21.0 lb s²/s
 B35 term: PNA Method 104.0 N s²/s 23.4 lb s²/s
 C33 term: Bhatt. Method 5555.3 N/m 380.7 lb/ft
 C33 term: PNA Method 5555.3 N/m 380.7 lb/ft
 C55 term: Bhatt. Method 1656.9 N m/rad 1222.1 ft lb/rad
 C55 term: PNA Method 1769.8 N m/rad 1305.4 ft lb/rad
 A35 term: Bhatt. Method 3.4 N s² 0.8 lb s²
 A35 term: PNA Method -8.0 N s² -1.8 lb s²
 A53 term: Bhatt. Method 3.4 N s² 0.8 lb s²
 A53 term: PNA Method 18.6 N s² 4.2 lb s²
 C35 term: Bhatt. Method 665.7 N 149.7 lb
 C35 term: PNA Method 518.7 N 116.6 lb
 C53 term: Bhatt. Method 316.5 N 71.2 lb
 C53 term: PNA Method 518.7 N 116.6 lb
 bhatt_force_phase =
 72.26753955853319
 bhatt_mom_phase =
 -18.10080744648123
 F1 term: Bhatt. Method 796.9 N 179.2 lb
 F2 term: Bhatt. Method 2492.1 N 560.3 lb

 Publ. force 3097 N vice 3079 N PNA 2616 Bhatt.
 Force term: PNA Method 3065.4 N 689.1 lb real -289.6 N -65.1
 lb imag
 M1 term: Bhatt. Method 1319.5 N m 973.2 ft lb
 M2 term: Bhatt. Method -431.3 N m -318.1 ft lb

 Publ. moment 1215 N vice 1438 N PNA 1388 Bhatt.
 Moment term: PNA Method 233.4 Nm 172.1 ftlb real 1419.1 Nm
 1046.7 ftlb imag
 Force Phase: Bhatt. Method 72.3 deg
 Force Phase: PNA Method -5.4 deg
 Moment Phase: Bhatt. Method -18.1 deg
 Moment Phase: PNA Method 80.7 deg
 Heave Ampl Bhatt. method: 9.4e-001 m 3.1e+000 ft
 Heave Phase Bhatt. method: 1.1e+000 rad 65.6 deg
 Pitch Ampl Bhatt. method: 1.5e+000 rad 8.3e+001 deg
 Pitch Phase Bhatt. method: -9.3e-001 rad -53.4 deg

Matrix Solution to Bhatt. Method:
Heave Ampl Bhatt. method: 9.4e-001 m 3.1e+000 ft
Heave Phase Bhatt. method: 1.1e+000 rad 65.6 deg
Pitch Ampl Bhatt. method: 1.5e+000 rad 8.3e+001 deg
Pitch Phase Bhatt. method: -9.3e-001 rad -53.4 deg
Matrix Solution to PNA Method:

Publ. Heave/A = 0.95 vice 1.1 PNA
Heave Ampl PNA method: 1.1e+000 m 3.7e+000 ft

Publ. -15 deg
Heave Phase PNA method: -1.0e+000 rad -59.9 deg

Publ. Pitch/kA = 1.1 vice 1.24 PNA
Pitch Ampl PNA method: 1.6e+000 rad 9.4e+001 deg

Publ. 44 deg
Pitch Phase PNA method: 7.9e-001 rad 45.0 deg

Publ. difference = -89 vice -104.9 PNA, -119 Bhatt.

As far as amplitudes and phases are concerned, the comparison made at this longer wavelength/ $L_{WL} = 2.0$ looks good, except for the heave phase angle. The forces and moments also have reasonable comparisons.

Added resistance comparisons using the input file seacor5.txt, to compare with the results given in Salvesen, 1978, and Strom-Tejsen, et al, 1973, for a $C_b = 0.60$ Series 60 hull form, showed reasonable maximum added resistance values but at the wrong frequencies. The phase angles of motion responses appeared to be reasonable. However, the motion amplitude responses looked strange.

An "exact" comparison was also made with the Bhattacharyya calculation method, and it was found that even with the different interpolation of section characteristics, and differences in rounding errors and the precise hull displacement, the results generally matched the values given in Bhattacharyya. The largest discrepancy was probably heave, which was about 20% larger than as published by Bhattacharyya, 1978.

Cb	0.805					
	SEAKEEPING VALIDATION OUTPUT					
Lwl	5.852 m	19.199 ft				
B	0.790 m	2.591 ft				
T	0.349 m	1.144 ft				
Displ.	12699.302 N	2855.059 lb				
LCG +fwd	0.146 m	0.480 ft				
LCB +fwd	0.146 m	0.480 ft				
Speed	1.459 m/s	4.788 ft/s				
Gyradius	1.369 m	4.493 ft				
Ampl.	0.061 m	0.200 ft				
Rho	999.000 kg/m ³	1.938 slug/ft ³ or lb				
s ² /ft ⁴						
ww	3.245 rad/s					
we	4.812 rad/s					
Station	Bn,m	Bn,ft	Tn,m	Tn,ft	Sn,m ²	Sn,ft ²

0.000	0.000	0.000	0.349	1.144	0.000	0.000
1.000	0.790	2.592	0.349	1.144	0.274	2.944
2.000	0.790	2.592	0.349	1.144	0.274	2.944
3.000	0.790	2.592	0.349	1.144	0.256	2.752
4.000	0.000	0.000	0.349	1.144	0.000	0.000
Station	C	Abar	Bhatt			

0.000	1.999	0.000	0	0		
1.000	0.970	0.559	0.98	0.57		
2.000	0.970	0.559	0.98	0.57		
3.000	0.814	0.667	0.84	0.66		
4.000	1.999	0.000	0	0		

Bhatt. published: 75.6 lb s² /ft
A33 term: Bhatt. Method 1083.2 kg 74.2 slug or lb s²/ft
A33 term: PNA Method 1083.2 kg 74.2 slug

Bhatt. Method x	m,	ft	PNA Method x	m,	ft
0.00	2.78	9.12	2.93	9.60	
1.00	1.32	4.32	1.46	4.80	

2.00	-0.15	-0.48	0.00	0.00
3.00	-1.61	-5.28	-1.46	-4.80
4.00	-3.07	-10.08	-2.93	-9.60

Bhatt. Published: 1368.5 lb s² ft
A55 term: Bhatt. Method 1814.0 kg m² 1338.0 lb s² ft
A55 term: PNA Method 1922.4 kg m² 1417.9 lb s² ft

Bhatt. published: 106.7 lb sec/ft
B33 term: Bhatt. Method 1534.6 N sec/m 105.2 lb sec/ft
B33 term: PNA Method 1534.6 N sec/m 105.2 lb sec/ft

Bhatt. published: 2105.9 ft lb s/rad
B55 term: Bhatt. Method 2850.6 N m s/rad 2102.5 ft lb s/rad
B55 term: PNA Method 2863.8 N m s/rad 2112.2 ft lb s/rad

Bhatt. published: -249.7 lb s²/s
B53 term: Bhatt. Method -1031.0 N s²/s -231.8 lb s²/s
B53 term: PNA Method -1255.6 N s²/s -282.3 lb s²/s

Bhatt. published: 473.9 lb s²/s
B35 term: Bhatt. Method 2130.6 N s²/s 479.0 lb s²/s
B35 term: PNA Method 1906.0 N s²/s 428.5 lb s²/s

Bhatt. published: 2588.5 lb/ft
C33 term: Bhatt. Method 39673.8 N/m 2718.5 lb/ft
C33 term: PNA Method 39673.8 N/m 2718.5 lb/ft

Bhatt. published: 49501.6 ft lb/rad
C55 term: Bhatt. Method 66936.9 N m/rad 49370.1 ft lb/rad
C55 term: PNA Method 93505.0 N m/rad 68965.8 ft lb/rad

Bhatt. published A35=A53= 14.27 lb s²
A35 term: Bhatt. Method 49.5 N s² 11.1 lb s²
A35 term: PNA Method -205.7 N s² -46.2 lb s²
A53 term: Bhatt. Method 49.5 N s² 11.1 lb s²
A53 term: PNA Method -12.3 N s² -2.8 lb s²

Bhatt. published: 1753.2 lb [/rad for all]
C35 term: Bhatt. Method 7762.3 N 1745.0 lb
C35 term: PNA Method 0.0 N 0.0 lb

Bhatt. published: 1242.5 lb [/rad for all]
C53 term: Bhatt. Method 5522.7 N 1241.6 lb
C53 term: PNA Method 0.0 N 0.0 lb

Publ. Bhatt. force phase = 133.7 deg
bhatt_force_phase =
1.362041670455612e+002

Publ. Bhatt. moment phase = -31.9 deg
bhatt_mom_phase =
-30.09595607063016

Bhatt. published: -6.85 lb
F1 term: Bhatt. Method -41.7 N -9.4 lb

Bhatt. published: 7.157 lb
F2 term: Bhatt. Method 40.0 N 9.0 lb
Force term: PNA Method 198.1 N 44.5 lb real 22.4 N 5.0
lb imag

Bhatt. published: 372.6 ft lb
M1 term: Bhatt. Method 530.8 N m 391.5 ft lb

Bhatt. published: -231.79 ft lb
M2 term: Bhatt. Method -307.6 N m -226.9 ft lb
Moment term: PNA Method 259.6 Nm 191.5 ftlb real 1088.8 Nm
803.0 ftlb imag

Force Phase: Bhatt. Method 136.2 deg
Force Phase: PNA Method 6.5 deg
Moment Phase: Bhatt. Method -30.1 deg
Moment Phase: PNA Method 76.6 deg

Bhatt. published: 3.935e-2 ft
Heave Ampl Bhatt. method: 1.4e-002 m 4.8e-002 ft

Bhatt published: -89.95 deg
Heave Phase Bhatt. method: -1.4e+000 rad -82.0 deg

Bhatt. published: 1.04 deg
Pitch Ampl Bhatt. method: 1.9e-002 rad 1.1e+000 deg

Bhatt. published: 178.42 deg
Pitch Phase Bhatt. method: -3.1e+000 rad -177.9 deg
(A 3.68-deg difference).

Matrix Solution to Bhatt. Method:
Heave Ampl Bhatt. method: 1.4e-002 m 4.8e-002 ft
Heave Phase Bhatt. method: -1.4e+000 rad -82.0 deg
Pitch Ampl Bhatt. method: 1.9e-002 rad 1.1e+000 deg
Pitch Phase Bhatt. method: -3.1e+000 rad -177.9 deg
Matrix Solution to PNA Method:
Heave Ampl PNA method: 4.3e-002 m 1.4e-001 ft
Heave Phase PNA method: 8.8e-001 rad 50.3 deg
Pitch Ampl PNA method: 7.1e-002 rad 4.1e+000 deg
Pitch Phase PNA method: -4.2e-001 rad -24.3 deg

ADDED RESISTANCE

In general the added resistance correlation was good when comparing the results of the present study to those of published papers. This is especially so considering the difficulty that was had in matching published motion phases in the seakeeping motions calculations. It should be noted that the added resistance results tended to bottom-out at added resistances that were slightly negative, and that these negative results were zeroed-out in the final program. The slight negative values were probably a result of the approximate nature of the sectional added mass and damping calculations. It should also be noted that ray-theory or diffraction resistance effects for very short wavelength waves also produce an added resistance that was added onto the final calculated added resistance, for the higher frequencies, as discussed in the added resistance section of this thesis.

Two added resistance calculation comparisons were made with published results. One was for a Series 60 hull form for which offsets were available. The peak frequency and values calculated in this case were quite reasonable, falling between experimental and calculated results published in Salvesen, 1978. In fact the peak value fell closer to experimental results in this case than the Salvesen paper results, probably because the seakeeping motion calculations were so different.

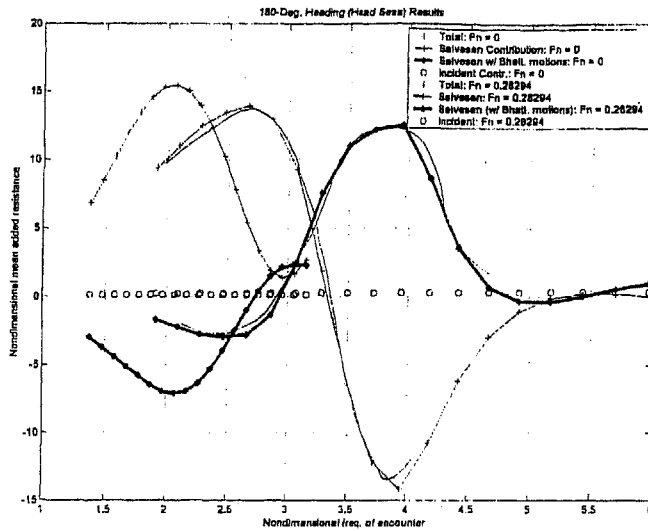


Figure A-4 Calculated Series 60 $C_B = 0.60$ added resistance in head waves at $F_N = 0.283$ (heavy blue line being Bhattacharyya, 1978 method used).

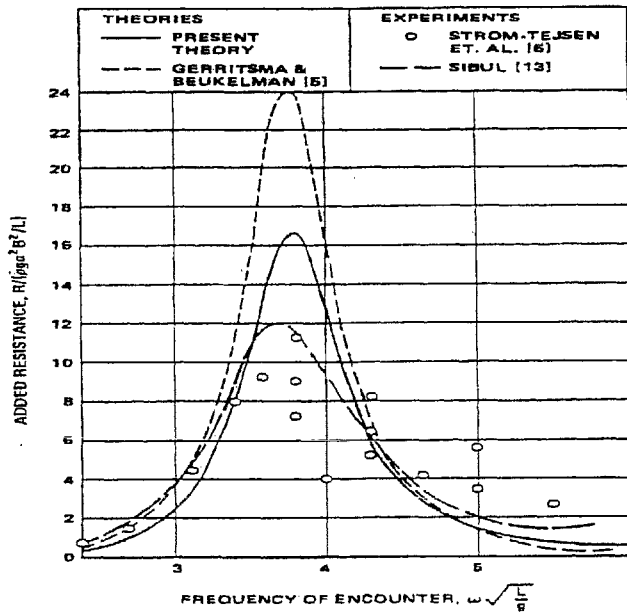


Figure A-5 Published Series 60 $C_B = 0.60$ added resistance in head waves at $F_N = 0.283$ (Salvesen, 1978).

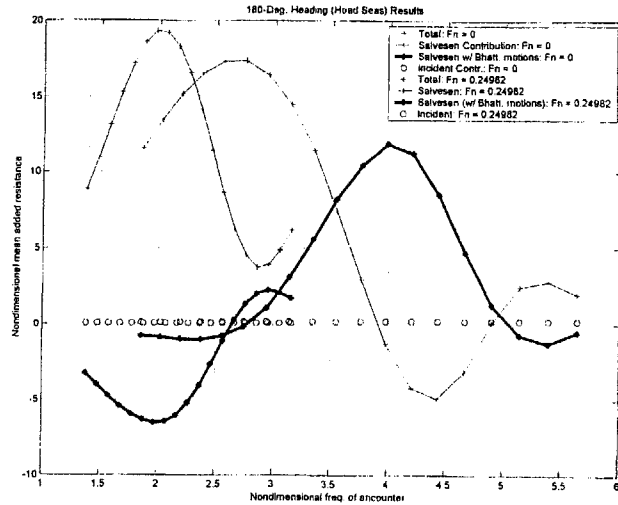


Figure A-6 Calculated destroyer added resistance in head waves at $F_N = 0.25$ (heavy blue line being Bhattacharyya, 1978 method used).

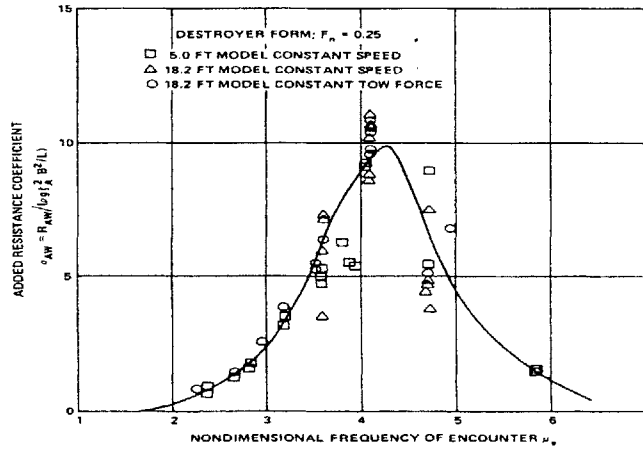


Figure A-7 Published destroyer added resistance in head waves at $F_N = 0.25$ (Strom-Tejsen, et al, 1973).

The other comparison was made for a destroyer form, which was approximately matched in proportions but for which no offsets were available. An FFG-7 hull form was used in place of the actual offsets in this case. Despite the approximate nature of this comparison, the agreement was good, with the peak value and frequency range matching the experimental data. Also captured was the fact that the added resistance “hump” was wider in terms of frequency of encounter for this example than for that of the Series 60 comparison.

Considering all of the intermediate calculations involved in making these added resistance calculations, the results are quite satisfactory.

3.8-3.11 MISCELLANEOUS ITEMS

The validity of other analyses made during this study were validated during the writing of the hull assessment program, and were straightforward.

Appendix B – Sample Input Files

BATCH FILE

An example batch file, batch.txt, that is used to run the HAP program is shown below.

This batch file is necessary if the batch file option is chosen at the beginning of the program.

Normally a batch file is used to run the program, though several options exist to also run the program in various other ways, generally for manual debugging or detailed investigations. The batch file batch.txt describes what run options to use (generally automatic optimizer), what operating profile file to use, what parent hull form and also worm curve factor file to use, how many iterations of the hull form should be run, and if the Fung, 1998 high-speed transom stern resistance regression can be used to make resistance estimates instead of only relying upon the worm curve factor.

```
Automatic Optimizer Batch File for HAP:
manual =
0
iteration options=
1
profile =
profile3.txt
offsets =
phelps2.txt
wcf =
ffg7wcf.txt
iterations=
10
Use Fung 1998 regression?
1
```

A profile file is necessary for every run of the program. The example profile file shown below, prof14.txt, describes many things for the program, including which dimensions may be varied and by how much, what limits on hydrostatic and directional stability exist, what the

expected operating conditions are going to be, expected air drag coefficients, and limits on propeller sizing for the efficiency calculations and the like.

```

1      2      3      4      5      6      7      8      9      10
2      FFG-7 Dims, Frigate Environment, One Speed Comprehensive Resistance
Optimization, Changing Cv
3      Starting inputs and limits on variation:

4      Displacement, m^3 Low High Vary? Yes or no.
5      3342.47      3000 4000 0
6      Cv Low High
7      0.0016      0.00025      1.70E-03      1
8      B/T Low High
9      3.148 2.251 3.25 0
10     Cp Low High
11     0.6 0.581 0.659 0
12     LCB Low High
13     -0.0032      -0.01 0.015 0
14     Cm Low High
15     0.744 0.7 0.8 0
16     Weighting Factors:
17     Resistance
18     1
19     Payload Per Displacement
20     0
21     SPI-1 Mision Effectiveness Use Bales?
22     0 0
23     Yearly Cost per Payload
24     0
25     Limits
26     GM/B Low HighGMprd. vcg Depth/Draft Evaluate?
27     0 0.04 8 6.3 2.211 0
28     Tactical Diameter Low High Evaluate? Fix Dir'n Stability?
29     0 0 0 0 1
30     Conditional Frequency Distribution - Speed Profile

31     Speed kts m/s %Time
32     4 2.058 0
33     9 4.630 0
34     11 5.658 0
35     13 6.687 0
36     15 7.716 0
37     17 8.745 0
38     19 9.774 0
39     21 10.802 0
40     23 11.831 0
41     25 12.860 0
42     26 13.374 0
43     27 13.889 0
44     28 14.403 0
45     29 14.918 0
46     30 15.432 1
47     sum 1.000
48     Evaluate?
49     1
50     Conditional Frequency Distribution - Water Depth Profile

51     Depth, m %Time
52     7 0.01

```



```

102  Rudder/Fin Data
103  rudders      Cp pos'n, in 40 sta units      chord, m      span, m      t
mean, m      ao      sweep ,deg taper ratio end plate factor      e      Cdo      Clmax
Eval?
104  1      38      2.72  3      0.41  0.1  0      0.45  2      0.9  0.009  1.53
105  1
105  Other Appendage Drag vs. Hull
106  Perc. Other appendage drag      Eval?
107  0.1  1
108  Skeg
109  Skeg? Start STA      End STA of 40      Top ht % DWL
110  0      28      40      0.9

```

Some of the lines above do not fit within the width of the paper and are shown here wrapped around to the next line. In the actual profile text file each numbered line would use only one line.

The rows and columns have been numbered in Excel, where the text file was created, to simplify error-checking operations. The title line is purely informational and is displayed on some of the output. The dimensional variations are controlled on the next several lines. The first value on each of the dimension lines will be the value used for the first hull evaluated in the optimization. Upper and lower limiting values are also described, and these should bracket the first value used. A one is used to signify that the dimension is to be changed during optimization. If a zero is used to signify that the value is to remain fixed, then the first hull dimensional value will be used for that dimensions for all hulls. Midships coefficient variation is not yet available.

Weighting factors can be entered to determine the relative weighting of several factors in the optimization process. Ship Performance Index 1 in this case is actually a center of gravity heave acceleration criterion for the vessel. An option also exists to use the Bales rank-factor method instead of detailed seakeeping calculations, if desired.

Stability limits are dealt with in the next lines. The first value of GM/B is a placeholder that is not currently used. The next value represents the minimum value of GM/B allowed if the stability evaluation option is being used. The next value represents the shortest roll period in seconds that is allowable in combination with the highest GM/B value. The next value represents the VCG or KG of the original parent hull. Note that this relates to the parent hull offsets file dimensions, and so this value must be used in conjunction with a well-chosen parent hull offsets file. Hull depth versus draft is given next, again as related to the original parent hull data. Depth is fixed in all variations run in the current version of the program. Note that this depth, used for structural and stability evaluations can differ from the freeboard values used later in the file to determine air drag. This allows accounting to be made of minor bulwarks and breakwaters which may cause significant air drag but not significantly affect the stability of structural weight of the vessel. The next value asks if the stability limit is to be evaluated or not.

The line below starts with a placeholder and a low and high value of TD/LWL, and also asks if tactical diameter should be evaluated. This option is currently not available. The last value on this line is set to one if directional stability is to be held constant for the vessel (1), or if it is not (0).

The next line provides the speed-time operating profile of the ship. The m/s values are the ones actually used by the program. The knot values are merely information. Speeds should be in ascending order. The probabilities must sum to one. There is a line that asks if this should be evaluated, but in reality this option is not active because the speed-time operating profile (or conditional frequency distribution) is always active.

The next section describes the water depth operating profile versus time. To set a water depth to being equivalent to infinitely deep water, use a depth about five times the expected ship

length. If no water depth evaluations are to be made then select 0 for the “evaluate?” option for water depth. An option also exists to use thin-ship theory to estimate shallow water resistance, and another option exists to use thin-ship theory to estimate residuary resistance. Both thin-ship theory options take a very long time to calculate compared with the other available methods used in the program.

The next section describes heading distributions but is not yet active.

The next section describes wave and wind strengths for use in the head seas calculations. An evaluate option must be set to 1 if the seakeeping evaluations are desired.

Air and wind drag inputs are entered in the next section. Superstructure frontal projected area in m^2 , drag coefficients for superstructure and hull, freeboard versus draft, and whether or not to evaluate air/wind drag are listed in this line. Also listed is whether or not steering resistance is to be evaluated.

Propulsion characteristics are presented in the next line, including whether or not a fixed PC is used, the value of the fixed PC, the number of propellers, the percent of beam inset from the maximum beam within which the propeller must be located for safety, the percent of draft below the waterline the propeller disk must be below for safety and air drawing, is the vertical dimension to follow relative or not, the max draft or the height above baseline of the propeller depending upon if the prior line states that this dimension is absolute or not (then it is relative). This information allows the propeller disk area to be automatically resized for each hull, if desired.

The next line describes fixed constants, average hull roughness, and whether the hull roughness will be evaluated as part of the overall frictional resistance.

Weight group information is provided next for the parent hull offsets file dimensions.

Speeds are used to ratio machinery and cruising fuel weights. A full load displacement is given which states the parent hull displacement this data is drawn from, allowing a set of ratios to be made to the current displacement. The percentage hull weight that is volume-driven is given, and it is indicated whether or not hull weights are to be evaluated.

Basic rudder or fixed stabilizing fin information is provided. Taper ratio is not yet used in the program, nor is the efficiency factor e , or C_{do} or CL_{max} . For rudder resistance to be used the option to evaluate must be set to one, as well as the option on the next line to evaluate appendage drag. On the appendage line there is also an option to add a lump percentage of bare hull resistance to represent other appendage resistances.

A final line asks whether there is a skeg, what station out of 40 total stations the skeg starts and ends at, and the height of the skeg termination in terms of percent of draft.

The offsets file describes parent hull geometry, an example of which is shown below:

1	2	3	4	5	6	7
LWL,m	Beam	Draft	Cs			
124.3584		13.767816		4.37388 0		
Max Station at AP						
20						
No. of rows		No. of cols.				
22	11					
Sta	CL	Height as % DWL				
0	0.000	0.139372822	0.278745645	0.557491289	0.836236934	1
0	0.000	0	0	0	0	
1	0.000	0.033210332	0.054889299	0.089944649	0.121309963	0.144833948
2	0.026	0.115774908	0.160516605	0.213099631	0.25599631	0.283210332
3	0.026	0.183579336	0.255073801	0.336715867	0.389760148	0.420202952
4	0.026	0.235239852	0.336715867	0.451568266	0.512453875	0.546125461
5	0.026	0.278136531	0.410516605	0.548431734	0.620848708	0.660055351
6	0.026	0.31595941	0.477859779	0.63699262	0.722324723	0.761531365
7	0.026	0.350553506	0.540590406	0.723247232	0.8099631	0.845479705
8	0.026	0.377767528	0.593173432	0.799354244	0.881918819	0.911439114
9	0.026	0.397601476	0.627306273	0.852398524	0.936346863	0.960332103
10	0.026	0.400830258	0.641143911	0.881457565	0.968634686	0.990774908
11	0.026	0.380073801	0.61900369	0.879151292	0.975553506	1
12	0.026	0.341328413	0.568726937	0.85101476	0.964483395	0.993542435
13	0.026	0.28597786	0.49400369	0.797509225	0.937269373	0.974630996
14	0.000	0.164667897	0.385147601	0.72001845	0.896678967	0.942804428
15	0.000	0	0.205719557	0.622232472	0.843634686	0.897601476
16	0.000	0	0.492619926	0.776752768	0.838099631	
17	0.000	0	0.22601476	0.692804428	0.768450185	
18	0.000	0	0	0.582564576	0.694649446	
19	0.000	0	0	0.30904059	0.610701107	
20	0.000	0	0	0	0.513210332	

The worm curve factor file describes the parent hull worm curve factor of residuary resistance versus the equivalent Taylor Series hull, as shown below for the example file ffg7wcf.txt.

"Worm Curve Factor file for FFG-7 per Fung, 2002"

Data points:

15

v/sqrt(L)	WCF
0	0.71
0.5	0.71
0.6	0.96
0.7	1.4
0.8	1.38
0.9	1.23
1	1.07
1.1	0.94
1.2	0.86
1.3	0.84
1.4	0.81
1.5	0.83
1.6	0.83
1.7	0.84
3.5	0.84

Appendix C – Sample Output

Sample program output is given below for test 32. This test demonstrates the calculation of many forms of miscellaneous resistance, as well as the 95% confidence interval. Only one hull was evaluated in this test.

 BEST RESULTING HULL

For profile file:
 2 "FFG-7 Dims, Frigate Environment, One Speed Comprehensive Resistance
 Optimization, Changing Cv"

ITERATIONS OF HULL FORM:

Iterations tried = 1
 Of all iterations, counting down to the last:
 Best iteration = 1
 Number of limits this design exceeds = 0

DIMENSIONS:

Cv 0.00174
 Cpl 0.600
 BoverT 3.148
 LCB -0.0032 frac. of LWL fwd of midships
 Cm 0.744
 Molded Vol. 3342.463 m³
 Csobl 2.663
 WSobl 1716.554 m²
 Lwl 124.310 m
 Beam 13.770 m
 Draft 4.374 m
 Depth 0.000 m
 GMT 0.000 m
 GMT / B 0.000
 GMTmax allow 0.000 m

RESISTANCE:

Avg. Profile Resistance 1024350.89 N
 Ratio of best profile resistance to original hull 1.000
 Avg. Profile Resistance error 0.113 fraction of
 total
 Avg. Profile power 22935.10 kW
 Ratio of best profile power to original hull 1.000
 Avg. Profile power error 0.113 fraction of
 total

Speed	Rt	+/-95 perc. Resist vs. P.C.	Pb
kt m/s	N	Confidence 1st Hull	kW
4.00 2.06	3.18e+004	0.20 1.00	0.67 9.74e+001
9.00 4.63	8.20e+004	0.17 1.00	0.69 5.48e+002
11.00 5.66	1.12e+005	0.17 1.00	0.69 9.11e+002
13.00 6.69	1.51e+005	0.16 1.00	0.69 1.45e+003
15.00 7.72	2.04e+005	0.15 1.00	0.69 2.27e+003

17.00	8.74	2.54e+005	0.15	1.00	0.69	3.20e+003
19.00	9.77	3.12e+005	0.15	1.00	0.69	4.39e+003
21.00	10.80	3.84e+005	0.14	1.00	0.69	5.97e+003
23.00	11.83	4.50e+005	0.14	1.00	0.70	7.65e+003
25.00	12.86	5.75e+005	0.14	1.00	0.69	1.07e+004
26.00	13.37	6.45e+005	0.13	1.00	0.69	1.24e+004
27.00	13.89	7.38e+005	0.13	1.00	0.69	1.48e+004
28.00	14.40	8.06e+005	0.12	1.00	0.69	1.68e+004
29.00	14.92	9.44e+005	0.12	1.00	0.69	2.04e+004
30.00	15.43	1.02e+006	0.11	1.00	0.69	2.29e+004

Rf Rr Rappg RrShallow Rsteer Rair Radded
- all in percent of Rt -

0.258	0.04	0.03	0.00	0.01	0.27	0.40
0.462	0.07	0.06	0.00	0.01	0.15	0.24
0.496	0.09	0.07	0.00	0.01	0.13	0.20
0.504	0.13	0.08	0.00	0.01	0.10	0.17
0.489	0.17	0.08	0.03	0.01	0.09	0.13
0.497	0.18	0.08	0.04	0.01	0.08	0.11
0.500	0.20	0.08	0.04	0.01	0.07	0.10
0.492	0.22	0.08	0.05	0.01	0.06	0.08
0.499	0.23	0.08	0.05	0.02	0.06	0.07
0.458	0.29	0.09	0.05	0.01	0.05	0.06
0.439	0.32	0.09	0.05	0.01	0.05	0.05
0.412	0.36	0.09	0.04	0.01	0.04	0.04
0.404	0.38	0.09	0.03	0.01	0.04	0.04
0.369	0.43	0.09	0.03	0.01	0.04	0.03
0.363	0.44	0.09	0.03	0.01	0.04	0.03

SEAKEEPING:

Bales R-factor of "best" hull: 1.937
Bales R-factor of initial hull: 1.937
Avg. profile heave accel. of "best" hull: 1.118 m/s^2
Avg. profile heave accel. of initial hull: 1.118 m/s^2

WEIGHTS:

Payload/Displ. of "best" hull: 0
Payload/Displ. of initial hull: 0

COSTS:

Payload/Annual Cost of "best" hull/first: 0

Sample output for test 35 is shown below. The test evaluated 320 hulls to minimize resistance at one speed. The resistance improvement over the first hull evaluated is listed in the output.

BEST RESULTING HULL

For profile file:
2 "FFG-7 Dims, Frigate Environment, One Speed Basic Resistance
Optimization, Changing all Dims."

ITERATIONS OF HULL FORM:

Iterations tried = 320
Of all iterations, counting down to the last:

Best iteration = 12
 Number of limits this design exceeds = 0

DIMENSIONS:

Cv 0.00035
 Cpl 0.600
 BoverT 2.266
 LCB -0.0032 frac. of LWL fwd of midships
 Cm 0.744
 Molded Vol. 3342.472 m³
 Csobl 2.599
 WSobl 2191.946 m²
 Lwl 212.838 m
 Beam 8.930 m
 Draft 3.940 m
 Depth 0.000 m
 GMt 0.000 m
 GMt / B 0.000
 GMtmax allow 0.000 m

RESISTANCE:

Avg. Profile Resistance 389919.89 N
 Ratio of best profile resistance to original hull 0.540
 Avg. Profile Resistance error 0.063 fraction of total
 Avg. Profile power 8596.06 kW
 Ratio of best profile power to original hull 0.540
 Avg. Profile power error 0.063 fraction of total

Speed kt	Speed m/s	Rt N	+/-95 perc. Confidence	Resist vs. 1st Hull	P.C.	Pb kW
4.00	2.06	8.44e+003	0.06	1.03	0.70	2.51e+001
9.00	4.63	3.86e+004	0.06	1.02	0.70	2.58e+002
11.00	5.66	5.62e+004	0.06	0.99	0.70	4.59e+002
13.00	6.69	7.69e+004	0.06	0.94	0.70	7.42e+002
15.00	7.72	1.01e+005	0.06	0.87	0.70	1.13e+003
17.00	8.74	1.29e+005	0.06	0.87	0.70	1.63e+003
19.00	9.77	1.61e+005	0.06	0.85	0.70	2.27e+003
21.00	10.80	1.94e+005	0.06	0.82	0.70	3.03e+003
23.00	11.83	2.32e+005	0.06	0.82	0.70	3.96e+003
25.00	12.86	2.74e+005	0.06	0.75	0.70	5.08e+003
26.00	13.37	2.96e+005	0.06	0.70	0.70	5.71e+003
27.00	13.89	3.18e+005	0.06	0.65	0.70	6.37e+003
28.00	14.40	3.40e+005	0.06	0.62	0.70	7.08e+003
29.00	14.92	3.63e+005	0.06	0.55	0.70	7.83e+003
30.00	15.43	3.90e+005	0.06	0.54	0.70	8.69e+003

Rf Rr Rappg RrShallow Rsteer Rair Radded
 - all in percent of Rt -

0.981	0.02	0.00	0.00	0.00	0.00	0.00
0.979	0.02	0.00	0.00	0.00	0.00	0.00
0.979	0.02	0.00	0.00	0.00	0.00	0.00
0.978	0.02	0.00	0.00	0.00	0.00	0.00
0.973	0.03	0.00	0.00	0.00	0.00	0.00
0.964	0.04	0.00	0.00	0.00	0.00	0.00

0.956	0.04	0.00	0.00	0.00	0.00	0.00
0.953	0.05	0.00	0.00	0.00	0.00	0.00
0.947	0.05	0.00	0.00	0.00	0.00	0.00
0.939	0.06	0.00	0.00	0.00	0.00	0.00
0.936	0.06	0.00	0.00	0.00	0.00	0.00
0.935	0.06	0.00	0.00	0.00	0.00	0.00
0.936	0.06	0.00	0.00	0.00	0.00	0.00
0.936	0.06	0.00	0.00	0.00	0.00	0.00
0.930	0.07	0.00	0.00	0.00	0.00	0.00

SEAKEEPING:

Bales R-factor of "best" hull:	0.000
Bales R-factor of initial hull:	0.000
Avg. profile heave accel. of "best" hull:	0.000 m/s ²
Avg. profile heave accel. of initial hull:	0.000 m/s ²

WEIGHTS:

Payload/Displ. of "best" hull:	0
Payload/Displ. of initial hull:	0

COSTS:

Payload/Annual Cost of "best" hull/first:	0
---	---